UNIVERSITY OF OKLAHOMA

GRADUATE COLLEGE

POWER CONTROL AND MANAGEMENT OF THE GRID CONTAINING LARGE-SCALE WIND POWER SYSTEMS

A DISSERTATION

SUBMITTED TO THE GRADUATE FACULTY

in partial fulfillment of the requirements for the

Degree of

DOCTOR OF PHILOSOPHY

By

FADHIL TOUFICK AULA
Norman, Oklahoma
2013

POWER CONTROL AND MANAGEMENT OF THE GRID CONTAINING LARGE-SCALE WIND POWER SYSTEMS

A DISSERTATION APPROVED FOR THE
SCHOOL OF ELECTRICAL AND COMPUTER ENGINEERING

BY

_____
Dr. Samuel C. Lee, Chair

_____
Dr. Djebbar Tiab

_____
Dr. John (Ning) Jiang

_____
Dr. Ronald Barnes

_____
Dr. Monte P. Tull

© Copyright by FADHIL TOUFICK AULA 2013
All Rights Reserved.

In memory of my Father

To my beloved mother, my wonderful wife, and my lovely children

Acknowledgements

I would like to gratefully and sincerely thank my great advisor Professor Samuel C. Lee for his guidance, assistance, encouragement and patience while I pursued this research and entire my Ph.D. study at the University of Oklahoma. It has been a very enlightening and fruitful experience to work with him.

I would also like to thank Dr. Djebbar Tiab, Dr. John (Ning) Jiang, Dr. Ronald Barns, and Dr. Monte Tull for their willingness serving as members of my doctoral committee. The insights and suggestions that they have provided me have greatly strengthened the content of this work.

I am also grateful for the invaluable helps granted to me by the faculties and staff of School of Electrical and Computer Engineering at OU, particularly Dr. Joseph Havlicek, Ms. Lisa Wilkins, and Ms. Lynn Hall for their unforgettable assistances.

I cannot go without acknowledging both Ministries of Higher Education and Scientific Research in Baghdad and Erbil/ Iraq and Iraqi Cultural Office in Washington DC, USA for their supporting and supervising my Ph.D. study.

My sincere appreciations are extended to my wife, Bayan, my brother, Fariq, and all my friends at University of Salahaddin-Hawler/ Kurdistan Regional-Iraq, especially Dr. Ibrahim I. Hamarash, Mr. Hilmi Fadhil and Mr. Jalil Aziz who have assisted and supported me in different ways during my study in the U.S.A.

Finally, I wish to give my heartfelt thanks to everyone who offered me invaluable help and assistance. This dissertation would not have been possible without the support of them.

Table of Contents

List of Tables

List of Figures

Abstract

The ever increasing demand for electricity has driven many countries toward the installation of new generation facilities. However, concerns such as environmental pollution and global warming issues, clean energy sources, high costs associated with installation of new conventional power plants, and fossil fuels depletion have created many interests in finding alternatives to conventional fossil fuels for generating electricity. Wind energy is one of the most rapidly growing renewable power sources and wind power generations have been increasingly demanded as an alternative to the conventional fossil fuels. However, wind power fluctuates due to variation of wind speed. Therefore, large-scale integration of wind energy conversion systems is a threat to the stability and reliability of utility grids containing these systems. They disturb the balance between power generation and consumption, affect the quality of the electricity, and complicate load sharing and load distribution managing and planning. Overall, wind power systems do not help in providing any services such as operating and regulating reserves to the power grid.

In order to resolve these issues, research has been conducted in utilizing weather forecasting data to improve the performance of the wind power system, reduce the influence of the fluctuations, and plan power management of the grid containing large-scale wind power systems which consist of doubly-fed induction generator based energy conversion system. The aims of this research, my dissertation, are to provide new methods for: smoothing the output power of the wind power systems and reducing the influence of their fluctuations, power managing and planning of a grid containing these systems and other conventional power plants, and providing a new structure of

implementing of latest microprocessor technology for controlling and managing the operation of the wind power system.

In this research, in order to reduce and smooth the fluctuations, two methods are presented. The first method is based on a de-loaded technique while the other method is based on utilizing multiple storage facilities. The de-loaded technique is based on characteristics of the power of a wind turbine and estimation of the generated power according to weather forecasting data. The technique provides a reference power by which the wind power system will operate and generate a smooth power. In contrast, utilizing storage facilities will allow the wind power system to operate at its maximum tracking power points' strategy. Two types of energy storages are considered in this research, battery energy storage system (BESS) and pumped-hydropower storage system (PHSS), to suppress the output fluctuations and to support the wind power system to follow the system load demands. Furthermore, this method provides the ability to store energy when there is a surplus of the generated power and to reuse it when there is a shortage of power generation from wind power systems. Both methods are new in terms of utilizing of the techniques and wind speed data.

A microprocessor embedded system using an Intel® Atom™ processor is presented for controlling the wind power system and for providing the remote communication for enhancing the operation of the individual wind power system in a wind farm. The embedded system helps the wind power system to respond and to follow the commands of the central control of the power system. Moreover, it enhances the performance of the wind power system through self-managing, self-functioning, and self-correcting.

Finally, a method of system power management and planning is modeled and studied for a grid containing large-scale wind power systems. The method is based on a new technique through constructing a new load demand curve (NLDC) from merging the estimation of generated power from wind power systems and forecasting of the load.

To summarize, the methods and their results presented in this dissertation, enhance the operation of the large-scale wind power systems and reduce their drawbacks on the operation of the power grid.

Chapter 1: Introduction

This chapter introduces the general concepts of the motivation behind this dissertation. Backgrounds and literature reviews are discussed with the consideration of a power system contains large-scale wind power systems.

1.1 Motivation

The economic issues and environmental impact of conventional power systems using fossil and nuclear fuels do not encourage the addition of more of these systems to the grid to ease the increasing demand of electricity. The global direction is to use renewable power sources, not just for the increasing demand of electricity, but also to eliminate the usage of the conventional power plants.

Currently, the most dominate renewable energy source used for generating electricity is wind energy. This is because wind currently leads the way as the most developed energy source [1]. However, the generated power from wind energy is not constant, which is considered the main drawback of this type of energy. The output power of the wind energy conversion systems (WECS) fluctuates due to variation of wind speeds. Integrating large-scale wind power systems into the grid poses challenges like maintaining parallel operations of conventional power plants, load frequency deviations, power generation and load balancing, and stability of the grid. Therefore, wind power developers should follow the strict condition for output power regulation and smoothing when significant penetrations of wind power generations are installed in a power system [2].

1.2 Overview of the Contributions of Renewable Power Systems

The world electrical energy consumption is in a rising rate and there is a steady demand to increase the power capacity from each year. It is expected that the demand on electricity will double within twenty years [3]. The growth in world electricity generation and its projection up to 2035 is shown in Figure 1-1[4].

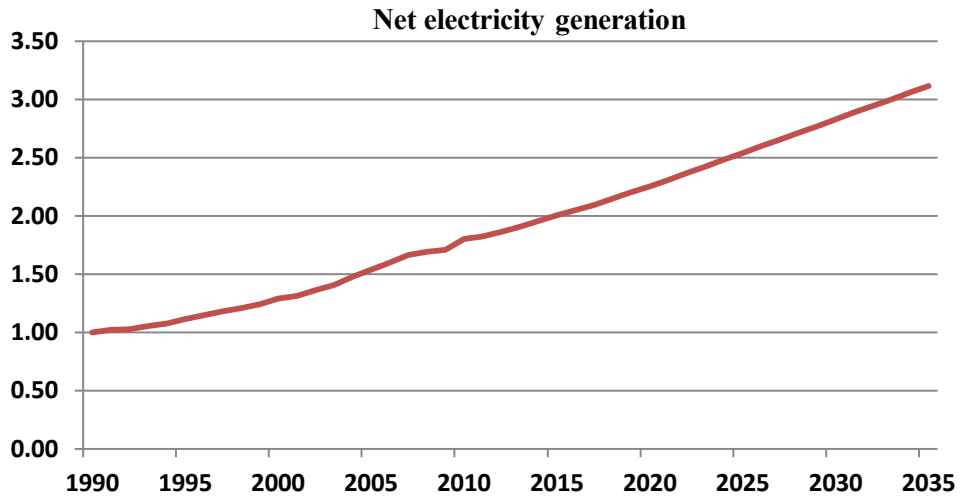

Source: U.S. Energy Information Administration, International Energy Outlook, DOE/EIA-0484, 2011

Figure 1-1. Growth in world electric power generation 1990-2035 [4]

Deregulation of energy has lowered the investment in larger power plants, which means the need for new electrical power sources may be very high in the near future. However, since some of these sources are potentially exhausted, uneconomical, or have negative impacts on the environment it not practical to depend only on conventional energy sources to meet the demand on electrical power. On the other hand, increasing the number of nuclear power plants to increase grid capacity may not be the best way either, since these types of power plants produce hazardous radioactive waste materials and increase safety problems. Furthermore, these types of power plants do not provide automatic governor controls to regulate system frequency. Therefore, increasing the

number of nuclear power generation units the bulk power system's response to frequency will be declined and the power system vulnerable to collapse [5]. In contrast to the traditional fossil fuel and nuclear energies, the renewable energies are popular and have received much attention in recent years. Many countries plan to depend on renewable energies more than ever before to generate power for many reasons. Economic issues, environment friendly, availability and inexhaustibility of these sources are among the most important reasons that made these countries to go with these types of energies.

The global direction is to use the renewable power sources for generating the power not just for covering the increasing demand on the electrical power, but also to eliminate the usage and substitute the conventional fossil power plants. The vision of the power grid will be changed through the increasing use of renewable energies such as wind, solar, tide, water waves, etc., to produce electrical power and increase their contribution to the grid. The U.S. projections for electricity generation by fuel types from 2008 to 2035 and the growth of the contribution of renewable energies to electricity generation from 2008 up to 2035 are shown in Tables 1-1 and 1-2, respectively [6].

Table 1-1. U.S. total electricity generation by fuel type projection [6]

Energy Sources	2008	2015	2020	2025	2030	2035	Annual Growth
Coal	1995	2037	2093	2147	2210	2305	0.5%
Petroleum	45	46	47	48	48	49	0.3%
Natural Gas	879	690	767	871	1015	1093	0.8%
Nuclear Power	806	834	883	886	886	898	0.4%
Renewable Sources [1]	373	649	713	795	852	891	3.3%
Other[2]	17	23	23	23	23	23	1.2%
Total Electricity Generation (Billion kWh)	4116	4280	4525	4769	5034	5259	0.9%

Source: U.S. Energy Information Administration, Annual Energy Outlook with Projection to 2035, DOE/EIA-0383, 2011

Table 1-2. U.S. renewable energy capacity and generation projection [6]

Energy Sources	2008	2015	2020	2025	2030	2035	Annual Growth
Conventional Hydropower	273	297	302	307	309	312	0.80%
Geothermal	15	19	24	32	40	47	4.50%
Municipal Waste	18	17	17	17	17	17	-0.30%
Wood and Other Biomass	36	55	91	116	133	145	5.60%
Solar	3	20	23	25	28	44	9.60%
Wind	74	154	154	165	174	194	2.90%
Total Electricity Generation (Billion kWh)	**419**	**562**	**611**	**662**	**701**	**759**	**2.30%**

Source: U.S. Energy Information Administration, Annual Energy Outlook with Projection to 2035, DOE/EIA-0383, 2011

[1] Include conventional hydroelectric, geothermal, municipal waste, wood and other biomass, solar, and wind power

[2] Includes pumped storage, non-biogenetic municipal waste, refinery gas, batteries, chemical, hydrogen, sulfur, and miscellaneous

Wind energy is considered the main source of renewable energy and gets more attention than other energy sources. This attention makes wind power systems to be more attractive to many countries and companies who increased their investments in building wind farms to generate electrical power through both grid connected and stand-alone systems. The U.S. Department of Energy reports that total electrical power from wind power generation will reach up to 300 GW or 20% of the whole nation of electrical power generated by 2030 [7]. Globally, it is expected that 34% of the world electrical power may come from wind power systems by 2050 [8].

Solar energy is another important renewable energy source which can be used for producing electrical power. In general, there are two types of solar power systems: photovoltaic and concentrating power plants. In the first, the most popular solar power system, sunlight is directly converted to electricity, while in the second heat produced from the solar thermal is collected to boil water which produces sufficient steam for generating electrical power. Global photovoltaic production has been doubling approximately every two years, which make it the world's fastest growing energy technology [9]. It is expected that the electrical power which is generated from photovoltaic cells may grow from 0.1% of the total current global electrical power to 5% by 2030, and rise up to 11% by 2050 [10].

Since wind power gained more focus by the electricity sector investment, the wind power systems will be considered throughout this dissertation and referred as to renewable energy whenever they are used. Also, wind power systems may be referred to as wind farm or wind energy conversion systems (WECSs) and vice versa throughout this dissertation.

1.3 Wind Energy Conversion System (WECS)

The doubly-fed induction generator (DFIG) is currently the system of choice for multi-MW wind turbines [11]. The aerodynamic system must be capable for operating over a wide wind range of speeds in order to achieve an optimum aerodynamic efficiency by tracking the optimum tip-speed ratio. Therefore, the generator's rotor must be able to operate at variable rotational speed. The DFIG system operates in both sub-and super-synchronous modes with a rotor speed range around the synchronous speed.

1.3.1 Principle of the DFIG's Operation

In DFIG-based WECS, the stator circuit is directly connected to the grid while the rotor winding is connected via slip-rings to a three-phase converter. The WECS basically consists of DFIG, wind turbine with drive train, AC-DC-AC converter controlled through back-to-back pulse width modulation (PWM) and includes rotor-side and grid-side controllers, DC-link capacitor, pitch controller, coupling transformer, and protection system. The schematic diagram of DFIG-based WECS is depicted in Figure 1-2.

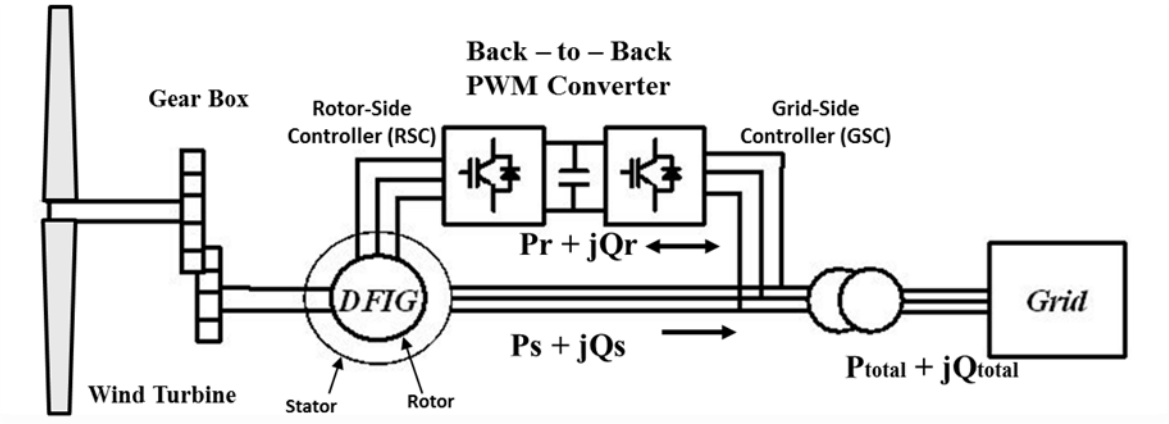

Figure 1-2. Schematic diagram of a grid connected DFIG-based WECS

The slip power can flow both directions, i.e. to the rotor from the grid and from the grid to the rotor, hence the speed of the machine can be controlled from either rotor-side or grid-side converter in both super- or sub –synchronous operating modes. Below the synchronous speed in motoring mode and above the synchronous speed in the generating mode the rotor-side converter operates as a rectifier and the grid-side converter operates as inverter, while slip power is returned to the stator. Below the synchronous speed in the generating mode and above the synchronous speed in the motoring mode, rotor-side converter operates as inverter and grid-side operates as a rectifier, while slip power is supplied to the rotor. At the synchronous speed, slip power is taken from the supply to excite the rotor windings and in this case the machine behaves as a synchronous machine. The relation between motoring and generating modes are shown in Figure 1-3.

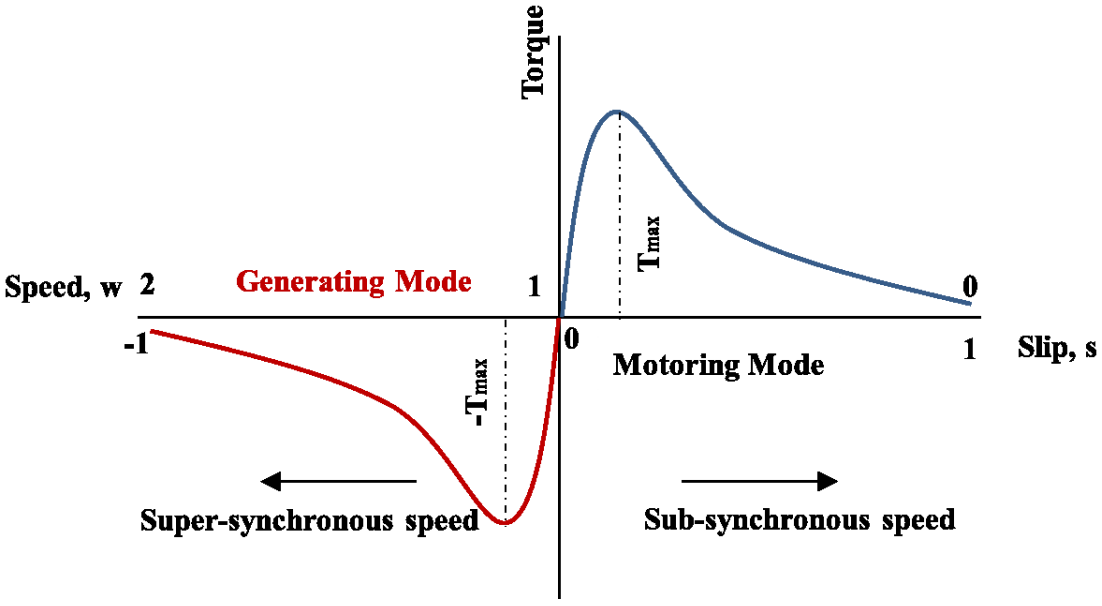

Figure 1-3. Motoring and generating modes of induction machine

In [12][13], *Luna et al. and Endusa el al., © 2011 & 2009 IEEE*, gave the active and reactive stator and rotor powers after neglecting the power losses in stator and rotor resistances as the following:

$$P_s = v_{ds} i_{ds} + v_{qs} i_{qs} \tag{1.1}$$

$$Q_s = v_{ds} i_{ds} - v_{qs} i_{qs} \tag{1.2}$$

$$P_r = v_{qr} i_{qr} + v_{dr} i_{dr} \tag{1.3}$$

$$Q_r = v_{qr} i_{qr} - v_{dr} i_{dr} \tag{1.4}$$

where v_{qs}, v_{ds}, v_{qr}, and v_{dr} are the q-axis and d-axis stator and rotor voltages, respectively, i_{qs}, i_{ds}, i_{qr}, and i_{dr} are the q-axis and d-axis stator and rotor current, respectively, P_s, and P_r are active powers of stator and rotor, respectively, Q_s and Q_r are reactive powers of stator and rotor, respectively.

The total active and reactive power that generated from DFIG is:

$$P_{total} = P_s + P_r \tag{1.5}$$

$$Q_{total} = Q_s + Q_r \tag{1.6}$$

If P_{total} and/or Q_{total} is positive, this means that the DFIG is supplying power to the grid, otherwise it is drawing power from the grid

1.3.2 Characteristics of the Wind Turbine

The aerodynamic system in a wind turbine converts the kinetic energy from wind flow to mechanical power. The extracted power depends on the incoming wind, turbine rotor swept area, the air density, and the blade pitch angle. However, physically it is not

possible to extract the whole kinetic energy of the wind, since the wind will not stand still directly behind the wind turbine. The wind speed is reduced by blades of the wind turbine, which extracts only a fraction of the power in the wind energy. Betz proved that the maximum power extractable by an ideal wind turbine with infinite blades from wind under ideal conditions is around 59% of the total available power in the wind. This limit is known as Betz limit, and it is represented by wind turbine power coefficient C_p. In practice, wind turbines are designed with two or three blades due to economic considerations, a combinational of structure, and the weight, therefore, the amount power they can extract will be around 50% only of the available wind power [14]. In general, C_p is a measure of the wind turbine rotor efficiency, and it is defined as the ratio between total extracted power and the total wind power:

$$C_p = \frac{Total\ Extaracted\ Power\ by\ the\ Wind\ Turbine}{Total\ Wind\ Power\ Avalibale} \tag{1.7}$$

The power coefficient, C_p, depends on the tip-speed ratio,λ, which, if maintained for all wind speeds, will result in optimal C_p curve and optimal power extraction from the wind. Variable-speed wind turbines are equipped with a blade pitch angel controller to adjust the blades and obtain the best power coefficient. *Barakati et al, © 2009 IEEE*, [15] provided the expressions for calculating the tip-speed ratio,λ, and power coefficient, C_p , as follows:

$$\lambda = \frac{w_T R}{V_w} \tag{1.8}$$

$$C_p(\lambda,\beta) = 0.5176\left(\frac{116}{\lambda_t} - 0.4\beta - 5\right)e^{-\frac{21}{-223\lambda_t}} + 0.0068\lambda \qquad (1.9)$$

where $\lambda_t = \frac{1}{\frac{1}{\lambda+0.08\beta} - \frac{0.035}{\beta^3+1}}$

where w_T is the turbine rotor speed in rad/s, R is the blade length in m, V_w is the wind speed in m/s, and β is the pitch angle.

The power coefficient of a wind turbine is not constant but varies with wind speed, rotational speed of the turbine, angle of blade pitch. Figure 1-4 shows the relation between C_p and tip-speed ratio, λ, for different blade pitch angle.

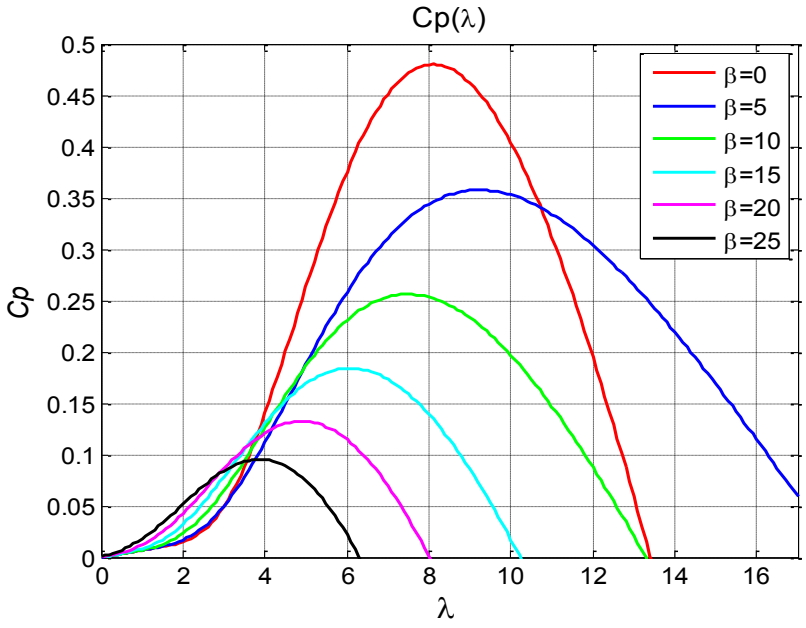

Figure 1-4. Wind turbine coefficient for different pitch angles

The expression of the mechanical power of a wind turbine, which is given by *Barakati et al, © 2009 IEEE*, [15], is as follows:

$$P_m = \frac{1}{2}\rho\pi R^2 V_w^3 C_p(\lambda, \beta) \tag{1.10}$$

and, the torque of the wind turbine as:

$$T_m = \frac{P_m}{w_T} \tag{1.11}$$

where P_m is the wind turbine mechanical power in *watt*, ρ is the air density in kg/m^3 ($\rho = 1.225\ kg/m^3$), and T_m is the torque of the wind turbine in $N{\cdot}m{\cdot}s$.

The characteristics of wind turbine torque and power versus rotor speed are shown in Figures 1-5 and 1-6, respectively. In both relationships, the wind turbine blade length was chosen to be 35 m.

When wind speed increases beyond the rated value, the electromagnetic torque is no longer sufficient to control rotor speed since this leads to an overload on the generator and the converter. To prevent rotor speed from becoming too high, the extracted power from incoming wind must be limited. This can be done by reducing the coefficient of the performance of the turbine or the C_p value. Altering the pitch angle β means slightly rotating the turbine blades along the axis. The blades are considerably heavy in a large turbine. Therefore, the rotation must be facilitated by either hydraulic or electric drivers.

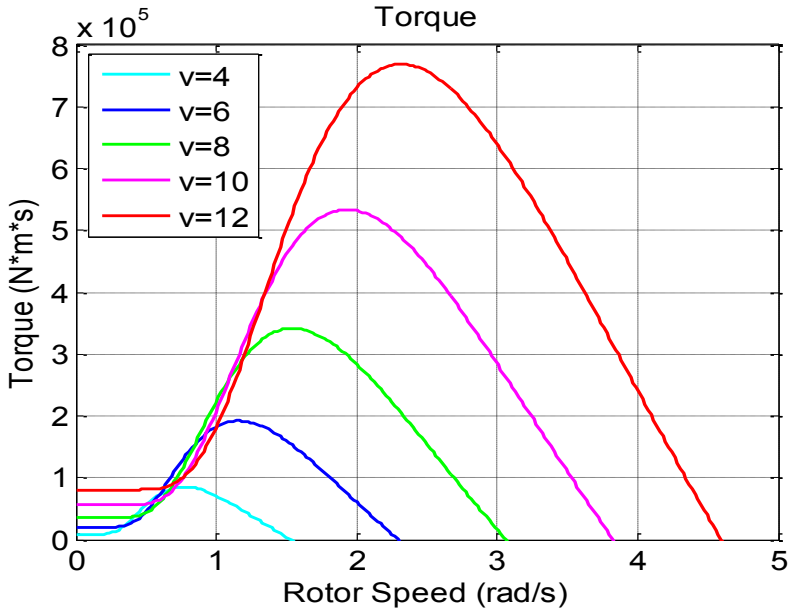

Figure 1-5. Wind turbine torque versus rotor speed

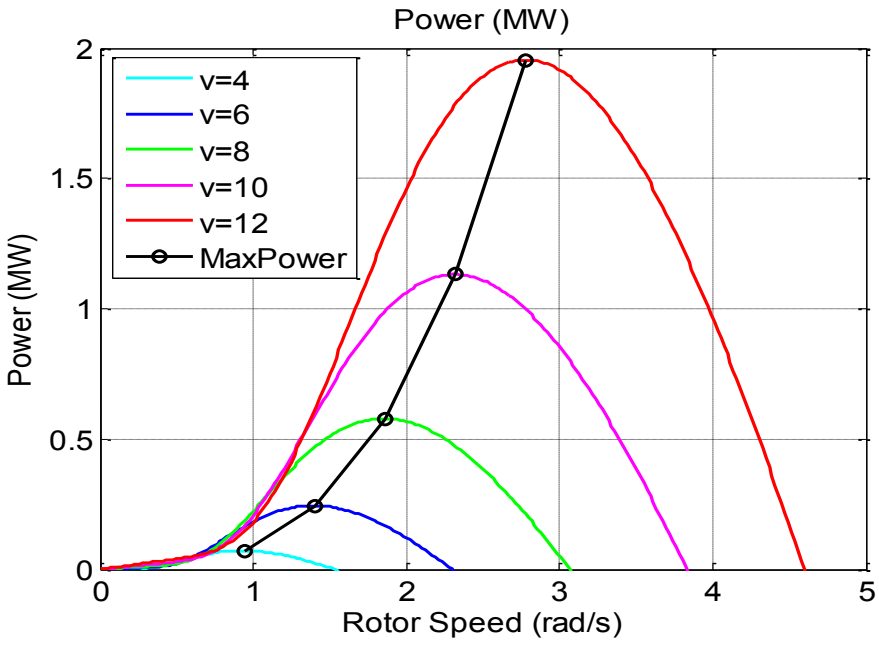

Figure 1-6. Wind turbine power versus rotor speed

1.4 Grid integration of Wind Power Systems

In the past a power grid fed only from conventional power sources. In general, conventional sources are considered to supply sustainable energies to the power plants to generate power when and where they are needed. The nature of these energies is predictable long term which leads to flexible and controllable generating power systems. Furthermore, the availability of these energies makes it possible to build large power systems such as nuclear power plants, natural gas power plants, coal power plants, large hydro power plants, etc. These traditional power plants are providing the majority of power needed on a grid.

Currently, the vision of the power grid has been changed through the increased usage of wind energies and their increased power contribution to the gird. Figure 1-7 shows a typical current power grid.

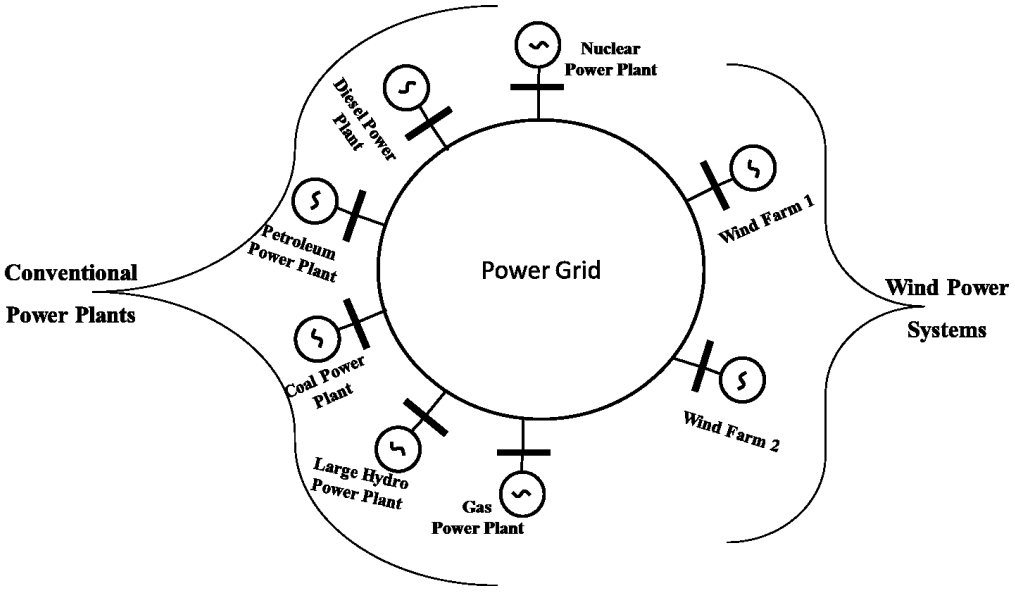

Figure 1-7. Conventional power plants and wind power systems on the grid

In contrast to the conventional power energies, the nature of wind energy, which depends on the weather, is uncertain. The availability of wind energy is unknown and varies from time to time, and from place to place. Therefore, wind power system is considered an intermittent, uncontrollable, and an uncertain source of power generation. These drawbacks of wind energy create different problems to the power grid.

However, when the contribution of the wind power systems to the grid is low, these drawbacks will not affect the power grid. These effects will be absorbed by the large power plants on the grid [16]. On the other hand, with the increased penetration of the generated power from wind energy to the grid, these problems will affect the grid and disturb the operation and performance of other power plants. The majority of these problems are:

1. Disturbance of the parallel operations of the power plants on the grid.
2. Disturbance of the load sharing between the power plants.
3. Increase the frequency deviation.
4. Make the power system vulnerable to collapse.
5. Decrease the overall power system efficiency and reliability.
6. Complication of the Load transition from fossil fuel to wind energy.

1.5 Wind Energy and Wind Speed Data

1.5.1 Impact of the Weather on Wind Energy

Wind energy depends directly on the prevailing weather and weather is chaotic and difficult to predict with a lot of turbulent variability over both short and long durations. Although it is possible to get average or mean values for potential wind energy for some geographic locations and to predict on average what the potential energy yields will be

for a given site, it is pretty much impossible to predict or guarantee what the energy profile for a site (or region) will be in any given future instant. The accuracy of weather predictions decreases rapidly the further out in time that they are projected; so it is difficult to predict what a sites energy production will be in say, a week.

Wind energy varies over a short duration, in addition to the longer more predictable seasonal and diurnal fluctuations. Wind gusts and swirls; wind is a chaotic laminar flow on the boundary of the earth/water to atmosphere interface. While preferred wind sites are selected in part because the wind blows steadily and does not gust and shift directions, all sites experience short duration peaks and troughs of power output in addition to longer duration swings between periods of stable weather patterns.

1.5.2 Short-Term Wind Forecasting Methods

Wind forecast for wind energy applications rely most on wind speed and direction at 50 meters to 100 meters from ground level, at the top of the atmosphere surface layer, and only marginally on the forecast of air density. In general, there are two models for short-term wind forecast, Rapid Update Cycle (RUC) and North American Mesoscale (NAM). The RUC is designed to provide numerical guidance for a very short term forecast to users [17]. The features of RUC are as follow:

1. Maximum forecast length is 12 hr. (it's expanded to 18 hr. in 2010).
2. The forecast is issued every hour starting at 00, 03, 06, 09, 12, 15, 18 and 21 Coordinated Universal Time (UTC).
3. Provide very high frequency updates of current conditions and short-range forecasts.

The NAM model is designed to provide short term weather forecast numerical guidance, day-ahead [18]. The general features for this model are:

1. Maximum forecast length of 84 hrs
2. A day-ahead forecast
3. Forecast values updated every 3 hrs.

1.5.3 Wind Speed Model

Wind is very difficult to model because of its highly-variable behavior both in location and time. Wind speed has persistent variations over a long-term scale. However, surface conditions such as buildings, trees, and areas of water affect the short term behavior of wind and introduce fluctuations in the flow, i.e. wind speed turbulence.

In [13], Endusa el al., © *2009 IEEE*, implemented a mathematical model for wind speed signal generated by autoregressive moving average (ARMA). The wind speed $V_{wind}(t)$ has two constituent part and can be written as:

$$V_{wind}(t) = V_{w\_mean} + V_t(t) \tag{1.12}$$

where V_{w_mean} is the mean wind speed at hub height and $V_t(t)$ is the instantaneous turbulent part, whose linear model is composed by the first order filter excited by Gaussian noise.

$$\dot{V}_t(t) = -\frac{1}{T_w} V_t(t) + \alpha_t \tag{1.13}$$

where T_w is the time constant and α_t is the white noise process with zero mean. The white noise is smoothed by a signal low pass filter, thereby transforming it to colored noise V_t. The instantaneous turbulence component of wind speed is obtained from the following expression:

$$V_t(t) = \sigma_t V_t \tag{1.14}$$

where σ_t is the standard deviation and V_t is the ARMA time series model which is given by:

$$V_t = a_1 V_{t-1} - a_2 V_{t-2} \ldots + a_n V_{t-n} + \alpha_t - b_1 \alpha_{t-1} \ldots + b_m \alpha_{t-m} \tag{1.15}$$

where a_i $(i = 1,2,\ldots,n)$ and b_j $(j = 1,2,\ldots,m)$ are the autoregressive parameters and moving average parameters, respectively. Neglecting higher order terms, the following coefficients constitute the significant terms in the moving average methodology in (1.15) for recursive estimation of parameters: $a_1 = 1.7091$, $a_2 = 0.9087$, $a_3 = 0.0948$, $b_1 = 1.0929$, and $b_2 = 1.7091$. The ARMA simulink model and its simulated wind speed using MATLAB/Simulink are shown in Figures 1-8.

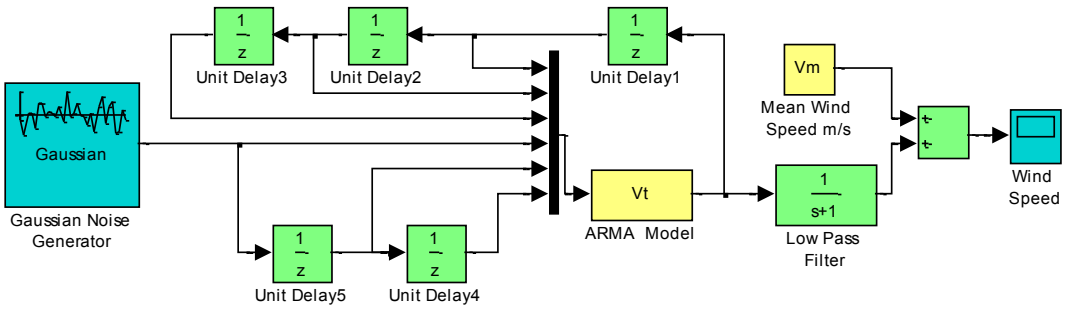

Figure 1-8. Wind speed Model by ARMA model in MATLAB Simulink [13]
(© 2009 IEEE, reused by permission)

1.5.4 Wind Forecasting Data

There are many online resources which provide weather forecasting including wind speed data [19] [20]. However, most of this data is limited for hour based forecasting data and 15-30 minutes actual recording data time frames and do not include seconds which are important for indicating the wind turbines performance all the time. Appendixes A and B include the wind data both predicted and actual wind speed data. For restoring these data in shorter intervals, the ARMA model which was presented in the previous section is used. Figure 1-9 shows the reconstructed wind forecasting data for a day ahead. The day ahead forecasting data is used for planning the power system power management which requires knowing the situation of all power plants on the grid. Figure 1-10 shows the reconstructed actual wind data for the same time frame of wind forecasted data.

It should note that due to wind turbine and generator rotor inertias, wind power system may absorb some changes in the wind speed variations, and the high wind speed variations (in milliseconds) may not make consequence changes in the output power of the wind power system.

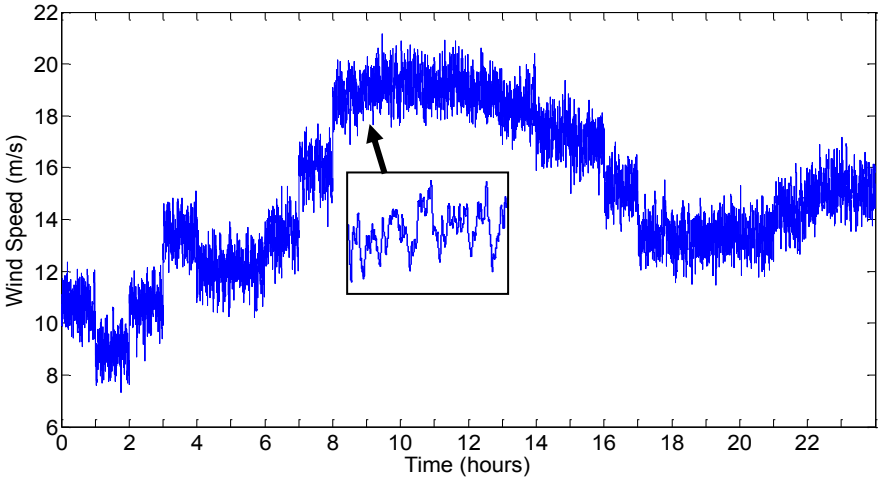

Figure 1-9. Reconstructed a day ahead wind speed forecasting data

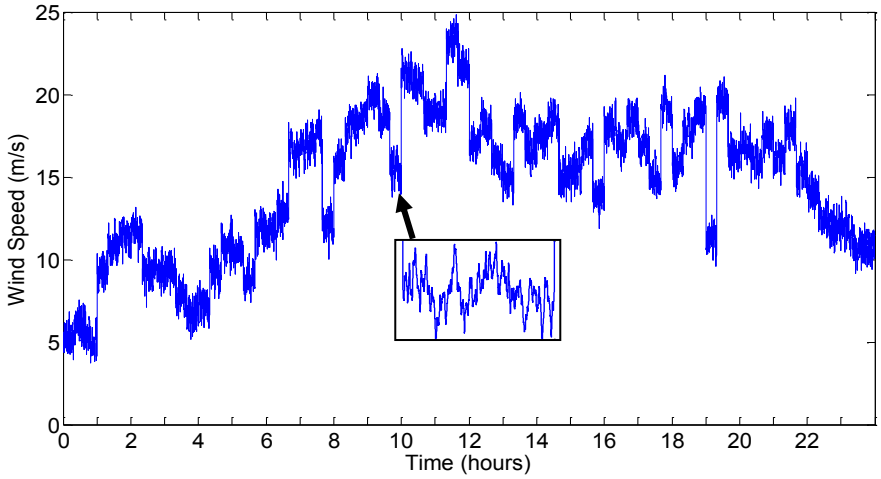

Figure 1-10. Reconstructed actual wind speed data

1.5.5 Wake Effect and Wind Speed Time Delay

In a large wind farm, the time aspect of wind transport is an important consideration. For example, a wind farm with 8 rows wind turbines and 80 meters of rotor diameter for each wind turbine, and 7 rotor diameters of distance each adjacent row has a length of nearly 4 km. At a wind speed of 12 m/s, it takes more than 5 minutes for the wind to travel across the wind farm. At a wind speed of 8 m/s, the travel time for the wind can be more than 8 minutes. Any changes in upstream wind speed will have effects on a downstream turbine after a certain time delay due to the wind speed traveling. The delay depends on distance and wind speed. In [21], *Magnusson and Smedman, © 1999 Elsevier*, defined the traveling time of wind speed passing between two successive turbine rows as follows:

$$t_{delay} = \frac{l}{\bar{V}_w} \tag{1.16}$$

where l is the distance between the two successive turbine rows and $\bar{V}_w$ is the average wind speed passing the first wind turbine.

Power extraction on wind flow passing a turbine creates a wind speed deficit in the area behind the turbine. This phenomenon is commonly called wake effect. As a consequence, wind turbines that are located to downstream obtain less wind speed than those which are upstream. The deficit in wind velocity due to the wake effect depends on several factors, such as the distance behind the turbine, turbine efficiency and turbine rotor size. In [22], *Moskalenko et al., © 2010 IEEE*, calculated wind speed in the wake at a distance d behind the turbine rotor using the following expression:

$$V_w(d) = V_o[\,1 - \left(\frac{R}{k_w d + R}\right)^2 \left(1 - \sqrt{1 - C_T}\,\right)] \tag{1.17}$$

where V_o is the incoming free-stream wind speed, C_T is the turbine thrust coefficient, in which is equal $7/V_w$, k_w is the wake decay constant which is 0.075 for onshore wind farms and 0.04 for offshore wind farms, and R is the turbine rotor radius.

1.6 Literature review

1.6.1 Constant Voltage and Frequency Strategy of the Wind Power System

Most doubly-fed induction generators (DFIG) in the industry today are used to generate electrical power in large wind turbines. This is primarily due to the many advantages that DFIGs offer over the types of generators in applications where the mechanical power provided by the prime mover during the generator varies greatly such as in wind blowing at variable speeds on the bladed rotor of a wind turbine. The DFIG allows the generator output voltage and frequency to be maintained at constant values, no matter the generator rotor speed (and thus, no matter the wind speed) [23]. This is achieved by feeding AC currents of variable frequency and amplitude into the generator rotor windings. By adjusting the amplitude and frequency of the AC currents fed into the generator rotor windings, it is possible to keep the amplitude and frequency of the stator voltages produced by the generator constant, despite variations in the wind turbine rotor speed (and, consequently, in the generator rotation speed) caused by fluctuations in wind speed. By doing so, this also allows operation without sudden torque variations at the wind turbine rotor, thereby decreasing the stress imposed on the mechanical components of the wind turbine and smoothing variations in amount of electric power produced by the generator. Using the same means, it is also possible to adjust the amount of reactive power exchanged between the generator and the AC power network. This allows the power factor of the system to be controlled. Moreover, using a DFIG in

variable-speed wind turbines allows electrical power generation at lower wind speed than with fixed-speed wind turbines using asynchronous generator [24].

1.6.2 WECS Developments

Recently, there have been many development applied to the wind turbine to increase their efficiency and performance. Applying the matrix converter method for controlling power of the wind turbine systems is studied in [25]-[27]. A matrix converter, which is an electronic power converter, interfaces the wind power generating system with the grid power system. Thus, the matrix converter provides direct AC/DC power conversion in such a way that no DC link necessary, and provides bidirectional power flow at unity power factor.

Stability analysis and load sharing of wind power systems is studied in [28]-[30], in which the behavior of wind power systems is monitored under different load conditions. A wind generation model based on metrological data is presented in [31][32], the anticipatory concept is applied for modeling the wind turbine in order to optimize the predictive control system. Other analyses are studied as well. Error evaluation and performance assessment of the simulation model in [33], DFIG harmonic analysis in [34], the proposal of applying z-source inverter for tracking maximum power in [35], the proposal scheme that uses reactive power vector control and speed control is presented in [36], a methodology assessment for the optimal behavior of non-dispatch able wind generating units under an increment loss allocation policy is discussed in [37]. Different strategies for optimizations are presented in the papers [38]-[40]. These papers dealt with techniques that produce a reliable and cost-efficient wind power system that connects to high-voltage transmission systems. The economic planning of

wind power systems is presented in [41]-[43]. These papers discussed different methodologies for best financial estimation and cost effectiveness for building wind power farms.

1.6.3 Aggregation of Large-Scale Wind Farm Modeling

The impacts of power system transient stability and power quality should be carefully studied when large wind farms are integrated into the power grid. It is necessary to establish an accurate dynamic model for wind farms. Large wind farms contain hundreds of WECSs, for example, Roscoe Wind Farm, Texas, one of the largest wind farms in the world, has installed capacity of 780 MW, and 627 WECSs [44]. If each WECS is presented by detailed model, it will aggravate the computational errors. It is very difficult to know each subsystem's parameters and working conditions. Furthermore, the structure of WECS is more complicated than the conventional generator. However, when studying the dynamic behavior for a power system, including wind farms the voltage, the active and reactive powers at the point of common coupling to the grid (PCC) are often the main objects while the detailed characteristics in the wind farm may be neglected. Therefore, the wind farm can be aggregated if the impacts on the power grid at the PCC points are completely maintained. It will reduce the system complicated order and significantly increase the computational speed. It also emphasizes the total impacts of the wind farm on the power grid.

A proper aggregation model can be easily obtained for a wind farm consists of fixed-speed WECSs where a one-to-one correspondence between wind speed and active power output exists. In this case, aggregation is done by adding mechanical power of each wind turbine and by using an equivalent induction generator which receives the

total mechanical power. Parameters of the equivalent generator are the same as those of the individual generators [45][46].

In case of a wind farm consists of DFIG-based WECSs, it has been seen that mutual interaction exits between turbines. If it is negligible, then aggregation is possible and the wind farm can be represented by a single turbine generator. However, to investigate the mutual interaction (especially interaction of back-to-back converters), single machine representation may not adequate and may lead to loss of the accuracy. Converting blocking protection may be altered and torsional oscillations may be incorrectly predicted when an inappropriate aggregation is performed for modeling such type of the wind farm [47].

Generally, there are two connection ways in wind farms. One way is that, all step-up transformers are directly connected to the PCC point. This structure is relatively simple and when the connection lines are short these resistances may be omitted. Nevertheless, for large-scale wind farms the second way as showed in Figure 1-11 (from [48], © *2011 IEEE, used by permission*) is often used. It uses an internal network for transmitting the wind power to the PCC.

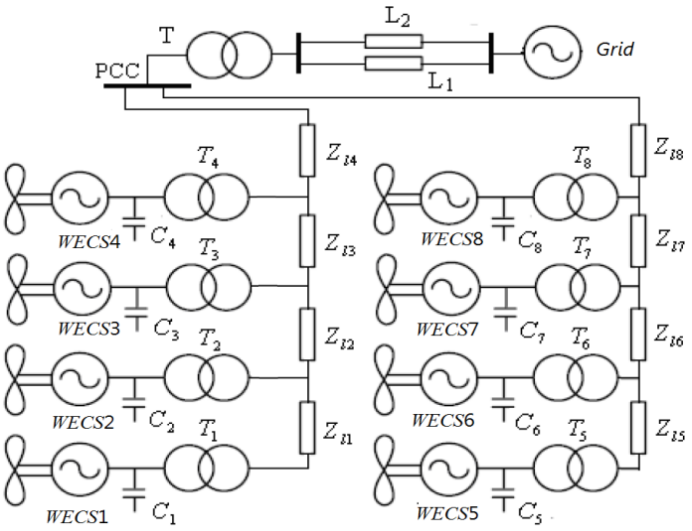

Figure 1-11. Schematic diagram of Wind Farm [48]
(© 2011 IEEE, reused by permission)

A reduced model of a wind farm can be obtained by the aggregation of DFIG WECSs into an equivalent wind turbine operating in an equivalent network of aggregated wind turbines. From [49], (*Yongbo et al, © 2011 IEEE, used by permission*), the coherent theory for aggregating the induction generator is used. They provide the dynamic equations of the induction in the third-order model based on a space vector as follows:

$$\begin{bmatrix}\dot{E}'_d\\ \dot{E}'_q\end{bmatrix} = \begin{bmatrix}-\frac{1}{T'_0} & w_s s\\ -w_s s & -\frac{1}{T'_0}\end{bmatrix}\begin{bmatrix}E'_d\\ E'_q\end{bmatrix} +$$

$$\begin{bmatrix}0 & -(X_s - X'_s)/T'_0\\ (X_s - X'_s)/T'_0 & 0\end{bmatrix}\begin{bmatrix}I_{ds}\\ I_{qs}\end{bmatrix} + \begin{bmatrix}0 & -w_s X_m/X_r\\ w_s X_m/X_r & 0\end{bmatrix}\begin{bmatrix}E_{fd}\\ E_{fq}\end{bmatrix} \tag{1.18}$$

$$\begin{bmatrix}E_d\\ E_q\end{bmatrix} = \begin{bmatrix}E'_d\\ E'_q\end{bmatrix} + \begin{bmatrix}0 & -(X_s - X'_s)\\ (X_s - X'_s) & 0\end{bmatrix}\begin{bmatrix}I_{ds}\\ I_{qs}\end{bmatrix} \tag{1.19}$$

$$\begin{bmatrix} V_d \\ V_q \end{bmatrix} = \begin{bmatrix} E'_d \\ E'_q \end{bmatrix} - \begin{bmatrix} R_s & -X'_s \\ X'_s & R_s \end{bmatrix} \begin{bmatrix} I_{ds} \\ I_{qs} \end{bmatrix} \tag{1.20}$$

where *s* and *r* refer to stator and rotor, E_d and E'_d are the internal voltage components of the induction generator, w_s is the synchronous speed, T'_o is the transient open circuit time constant, X_s and X'_s are the stator reactance, R_s is the stator resistance, and V_d and V_q are direct and quadrature terminal voltages.

The dynamic voltage equation (1.18) can be simplified to the following expression [49]:

$$\dot{E}'_{dqk} = M_k E'_{dqk} + F_k I_{dqk} + G_k E_{fdqk} \tag{1.21}$$

The d-q axis components of the terminal voltages in the simplified form of (1.20) can be given as the following [49]:

$$V_{dqk} = E'_{dqk} - A'^{-1}_k I_{dqk} \tag{1.22}$$

The relation between d-q axis components of the internal electromotive force and transient electromotive force of the induction generator stator winding can be simplified from (1.19) to the following from [49]:

$$E_{dqk} = E'_{dqk} + X'_k I_{dqk} \tag{1.23}$$

From (1.22), the machine current can be given by the following expression [49]:

$$I_{dqk} = A_k V_{dqk} - A_k E_{dqk} = A'_k V_{dqk} - A'_k E'_{dqk} \tag{1.24}$$

where *k* in (1.21)-(1.24) is the k^{th} DFIG in the wind farm.

Assuming all the induction generators' buses are the same, then terminal voltage for all unites will be the same as the terminal voltage of the wind farm, thus, the equivalent

terminal voltage is: $V_{dqe} = V_{dqk}$. According to coherent, the equivalent current will be the sum for current in each induction generator as the following [49]:

$$I_{dqe} = \sum_{k=1}^{n} I_{dqk} = \sum_{k=1}^{n} A_k V_{dqe} - \sum_{k=1}^{n} A_k E_{dqk} = \sum_{k=1}^{n} A'_k V_{dqe} - \sum_{k=1}^{n} A'_k E'_{dqk} \tag{1.25}$$

where *n* is the number of DFIGs in the farm.

The equivalent synchronous reactance and transient reactance can be obtained under the assumption that equation of the equivalent generator and the coherent generator has the same form. *Yongbo et al* in [50] concluded that from (1.25), the equivalent reactance and transient reactance are as the following:

$$X_{es} = 1/\sum_{k=1}^{n} A_k \quad \text{and} \quad X'_{es} = 1/\sum_{k=1}^{n} A'_k \tag{1.26}$$

The equivalent transient time constant, T'_e, can be given from the average transient tine constant of the DFIGs:

$$T'_e = \frac{1}{n} \sum_{k=1}^{n} T'_k \tag{1.27}$$

From (1.23),

$$I_{ae} = I_{de} \sin(wt) + I_{qe} \cos(wt) + I_{oe}$$

$$I_{be} = I_{de} \sin(wt - 2\pi/3) + I_{qe} \cos(wt - 2\pi/3) + I_{oe}$$

$$I_{ce} = I_{de} \sin(wt + 2\pi/3) + I_{qe} \cos(wt + 2\pi/3) + I_{oe} \tag{1.28}$$

The equivalent active power is giving by:

$$P_{eagg} = 3\, V_e I_e cos\, \emptyset \tag{1.29}$$

where V_e is the terminal phase voltage (from V_{dqe}), I_e is the total phase current, and $cos\ \emptyset$ is the power factor of the wind farm.

In [51], Fernandez et al. stated that the equivalent reactive power of the DFIG is equal to the sum of the reactive power of each DFIG.

In [52], ZhenHua at el presented another method for aggregating DFIG-based WECSs wind farm. The method is based on two steps: first, the transient power response of every generator is measured, which is used as characteristic parameters to cluster DFIGs into groups, second step is calculating the equivalent generator parameters by the weighted method.

The following steps summarize this procedure [52]:

1. Normalization of characteristic parameters; assuming that i^{th} sample in the same group is the set $P_i=\{P_{i1}, P_{i2}, ..., P_{ik}\}$ and $Q_i=\{Q_{i1}, Q_{i2}, ..., Q_{ik}\}$, where k is a sample point. The apparent power of this sample is:

$$S_{in} = \sqrt{P_{in}^2 + Q_{in}^2} \tag{1.30}$$

where S_{in} means the n^{th} $(n=1, 2, ..., k)$ sample points of the i^{th} sample and then the i^{th} sample's apparent is $S_i=\{S_{i1}, S_{i2}, ..., Sik\}$. Furthermore, the normalization value of apparent power can be via $S'_i=\{S_{i1}, S_{i2}, ..., S_{ik}\}/max^k_{j=1}(Sij)$.

2. Calculation of weight of every sample in the same group; the classical sample can be founded through using fuzzy C-means clustering method [53] and the distance between the i^{th} sample from this group and the classical sample could be given by:

$$D_i = \sum_{m=1}^{k}(S'_{im} - S_{Cm})^2 \tag{1.31}$$

If there are N samples in this class, the weight of every sample can be given by:

$$\gamma_i = \frac{1}{D_i}\sum_{i=1}^{N}\left(\frac{1}{D_i}\right) \tag{1.32}$$

3. Aggregation parameters: if steps 1 and 2 are prepared, the equivalent parameters of the equivalent DFIG of every group can be detected conveniently though weighting that combining γ_i and every parameter of i^{th} DFIG in the same group.

Compared with the aggregation of DFIGs, external characteristic modeling focuses on the external description of DFIG and must be studied based on the known equivalent structure. According to the superposition theorem, the external characteristic equivalent of the DFIG can be obtained from the standpoint of the stator of DFIG, the equivalent DFIG steady state diagram is shown in Figure 1-12 [52], *© 2011 IEEE, used by permission*.

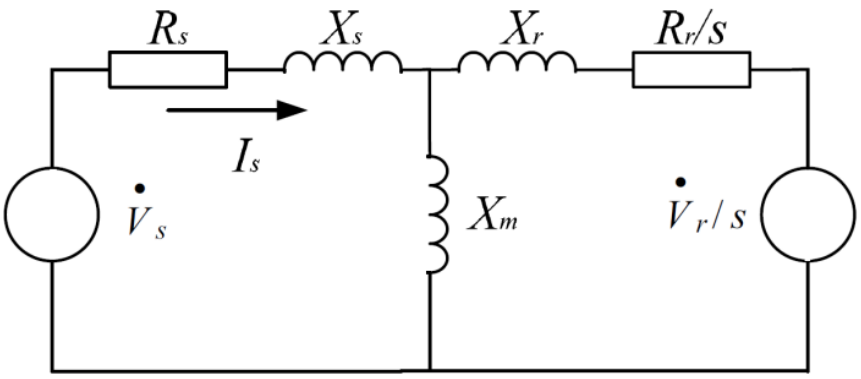

Figure 1-12. Steady-state DFIG equivalents model [52]
(© 2011 IEEE, reused by permission)

The steady-state relationship between V_s and V_r is given by the following expression [52];

$$\frac{\dot{V}_s}{\dot{V}_r} = \frac{V_s\,(\cos\theta_s + j\sin\theta_s)}{V_r(\cos\theta_r + j\sin\theta_r)} \tag{1.33}$$

Due to the relation between the total output power of DFIG with the direct and quadratic axis value of rotor voltage V_r, therefore, the output power can be adjusted to the rotor voltage as the following [52]:

$$V_{dr} = -P + k_1 + k * k_3 \tag{1.34}$$

$$V_{qr} = Q + k_2 + k * k_4 \tag{1.35}$$

where k_1, k_2, k_3, and k_4 are constant values, and they are derived through a large number of samples analysis, and they may have the following values 0.679, 0.122, -0.063, and -0.101, respectively [52], k is the switch number, when the fault is on, $k = 1$, and when the fault is off, $k=0$.

Stator current I_s, in Figure 1-13, can be calculated by the following expression with neglecting the value of R_r since it is very small in comparison with X_r [52]:

$$\dot{I}_s = \left[\dot{V}_s - \dot{V}_s \left(\frac{X_m}{X_m + X_r}\right)\frac{V_r}{V_s}\right] / j\left(\frac{X_m X_r}{X_m + X_r} + X_s\right) \tag{1.36}$$

Hence, the wind farm can be represented by an equivalent DFIG, and then the total active and reactive powers of the wind farm are [52]

$$P_{agg} = P_{s,resp} + kP_{s,resp} \tag{1.37}$$

$$Q_{agg} = Q_{s,resp} \tag{1.38}$$

where $P_{s,resp}$ is the stator active power response of DFIG, $kP_{s,resp}$ is active power of the grid-side equivalent DFIG, k is a coefficient belong to the set of independence parameters, and $Q_{s,resp}$ is the reactive power response of a stator of the equivalent DFIG, and the reactive power of the grid-side of equivalent DFIG is neglected.

$P_{s,resp}$ and $Q_{s,resp}$ can be calculated from the following [52]:

$$P_{s,resp} = Re[\dot{V}_s(\dot{I}_s)^*] \tag{1.39}$$

$$Q_{s,resp} = Im[\dot{V}_s(\dot{I}_s)^*] \tag{1.40}$$

The different depth of voltage sags can be determined from the differences between detailed model, which is represented by P_i and Q_i, and equivalent aggregation (external characteristic) model, which is represented by P_{agg} and Q_{agg} as the following [52]:

$$E = \sum_{i=1}^{k}[(P_i - P_{agg,i})^2 + (Q_i - Q_{agg,i})]^{1/2} \tag{1.41}$$

The depth of voltage sag in (1.41) helps for defining the group turbines in each cluster. For example, 12 DFIG-based WECSs in a wind farm is depicted in Figure 1-13(from [52], © *2011 IEEE, used by permission)*, and for 20% for depth of voltage sag, there will be three clusters 1, 2, and 3. In which cluster 1 has a group turbines 3 and 4, cluster 2 has a group of 5-12, and cluster 3 has grouped of turbines 1 and 2.

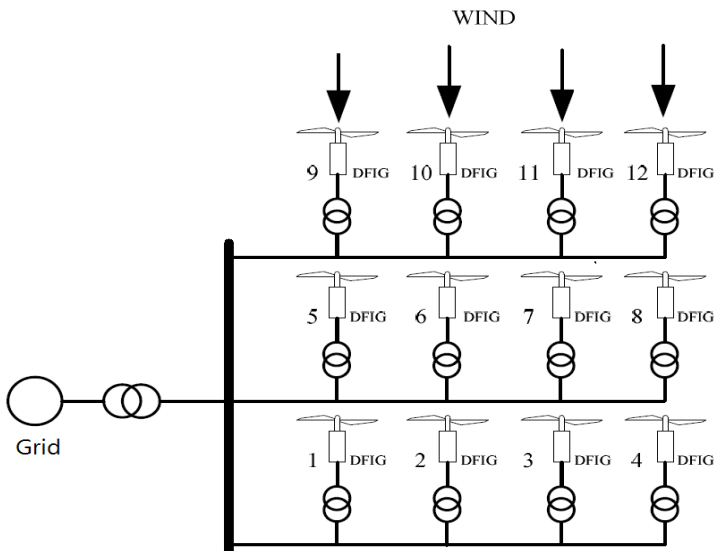

Figure 1-13. DFIG-based WECS wind farm [52]
(© 2011 IEEE, reused by permission)

Overall, the equivalent of DFIG is still in the stage of early study. In comparison with other generators such as synchronous and squirrel-cage induction generators that are used in WECSs, DFIG has the following significant problems:

1. DFIG can work in a wide range of rotor speed while others work in approximately fixed rotor speeds.
2. In DFIG-based WECS the power coefficient C_p is adjusted continuously by controlling both the tip speed ratio λ and pitch angle β which provide the ability of maximum energy capturing from the wind. This causes a large excursion of working points of DFIG.
3. The stator electromagnetic force (emf) is affected by not only the slip frequency but also by the rotor voltage V_{dr} and V_{qr}. In squirrel-cage induction generator, the rotor windings are short-circuited. Therefore, the dynamic of emf in DFIG is more complex than other machines.

4. The issues of a low voltage ride through of DFIG deserve special attentions due to the limited capacity of PWM converters. It should be affirmed that the equivalent DFIG has similar reactive power responses as the DFIGs.
5. The active and reactive power controller DFIG is more complex than synchronous and squirrel-cage induction generators, therefore, the equivalent single-machine dynamic parameters are more challenging in DFIG than other wind farm generators.

For the above reasons, many researchers are interesting to simplify the calculation of the active power of the aggregation DFIG-based WECS as the sum of the active power of the individual unit under the assumption that the active power generated from each unit is calculated according to its incoming wind, and all WECSs have been same rated output voltage and some control strategy [54]-[57].

1.6.4 Others Related Works

The two-stage wind farm network based on weather forecast modeling in Fan et al. [58] proposed a model for increasing the performance of the wind power systems. This is a practical method that applied for a specific wind farm and must be modified when applied to other wind farm power systems. The aim of the European project team work [59] was to develop wide research and advanced solutions for onshore and offshore short-term wind power forecasting. The project provided an advanced technology for wind power forecasting, based on multiple stages of NWPs, applicable on a large scale: at a single wind farm, a regional or national level, and for both interconnected and island systems. However, the project addressed variety contribution of accuracy, robustness, and value oriented models and included both deterministic and probabilistic

forecasting; the characteristics of power managements in interconnected systems were not addressed. That is, the load sharing between different power systems has to be included in the model as a result of forecasting procedure. The weather research and forecasting (WRF) numerical model is presented in [60] for predicting the wind speed for the next day. Although the paper is well organized for implementing the WRF method, but it was not showed the on-grid wind power system performance and their power fluctuations effect on the power grid. Also, it does not address the self-correction procedures when an error occurred during the next day wind prediction.

A considerable amount of research has been published in the area of reducing the output power fluctuations of the wind power systems. In [61], the authors investigated the usage of flux weakening of the induction machine driven by a flywheel, although the results showed improvement of DC-link voltage, but did not show the active power response. Furthermore, the method was implemented on a fractional power wind turbine and did not mention the implementation on the other higher rate turbines. Reference [62] described the usage of turbine inertia for smoothing output of wind turbine power; however, this method usually gave the best results over a short period or in transient cases only, since the turbine inertia cannot handle the output power without controlling the input power. The researchers in [63] discussed the stability issues for smoothing wind power fluctuations by controlling the voltage-source converter. The authors defined different areas of stability and instability of the wind turbine. These areas are essential for knowing the operations of the wind turbines. Reference [64] analyzed the non-linearity feedback/feedforward control method for regulating the rotor voltage and blade pitch angle. However, the method gave the achievement of the reduction of the

fluctuation of active power, but according to the simulation results, the method assumed the consistency of the wind speed over long periods, and in realty, the wind speed is continuously changed over time.

Utilizing energy storage systems for reducing the fluctuations of the output power from the wind power systems are interested in the recent studies. For instance, the ultra-capacitor storage system presented in [65], superconducting magnetic energy storage (SEMS) technology presented in [66], and battery storage facilities are studied in [67]-[69]. All these studies considered only the fluctuation reduction of the output power and not dealing with the actual planning management for supplying the load by the wind power system in the presence of the energy storage facilities in the system.

1.7 Dissertation Objectives and Contributions

1.7.1 Objectives

The main objectives of this dissertation are to make the wind power systems act as conventional power plants in terms of power control, and load supplying and power management planning. The intermittence, uncontrollability, and uncertain nature of wind energy are the main factors that prevent the wind power systems from working as conventional power plants. Furthermore, to accommodate the integration of large-scale wind power systems to the grid, more controllable resources must be employed in order to cope with their drawbacks. By adapting accurate weather forecasting data, the availability of generated power from wind power systems can be estimated. This will help plan the power management of the grid and load sharing process. Reducing the output power fluctuations helps the wind power systems provide regulated power to the grid, and makes them follow the requirements of the grid control management.

1.7.2 Contributions

The contributions of this dissertation are summarized as follows:

1. Utilization of wind forecasting data for estimating the generated power of the WECS (Chapters 2, 3, and 5)
2. Active power control of the DFIG-based WECS using de-loaded method (Chapter 2)
3. Utilization of multiple energy storage systems for smoothing the output power and load supply of WECS (Chapter 3)
4. Power management and load sharing planning of the grid contains large-scale wind power systems and other conventional power plants (Chapter 5)
5. Utilization of latest microprocessor based controller for enhancing the operation of WECS (Chapter 4).

1.8 Organization of Dissertation

The rest of this dissertation is organized as follows: The de-loaded method for smoothing the active output power of the DFIG is presented in Chapter 2. The utilization of multiple energy storage facilities for reducing the output power fluctuations and load supply of the WECS is given in Chapter 3. Chapter 4 deals with the role of microprocessor based controller for enhancing the operation of WECS. The management and planning for the grid contains large-scale wind power systems are presented in Chapter 5. The conclusions of the dissertation and the proposal for future works are given in Chapter 6.

Chapter 2: Smoothing Control of the Wind Power Fluctuations

This chapter discusses different approaches for controlling and regulating the wind active power. The aim for these control and regulations are to smooth the fluctuations of the active power of the wind power generation. In this chapter a new method for smoothing the active power for a DFIG- based WECS is presented.

2.1 Wind Power Fluctuations

The uncertain, unstable, and uncontrollable nature of wind energy makes the fluctuations in the generated power of the wind power system. In general, according to the wind speed, the following regions can be classified for wind power systems:

1. No power generation region:

   No power generation occurs when wind speed is either very low or very high. At very low wind speeds, usually less than 4 meter per second, there will be insufficient torque exerted by the wind on the turbine blades to make them rotate and therefore no power will be generated. As wind speed increases, the force on the turbine structure will continue to rise and, at some point, there is a risk of damage to the rotor and other mechanical parts of the wind power systems. As a result, a braking system is employed to bring the rotor to a standstill and no power will be generated. This is called a cut-off speed and usually occurs when wind speed is above 25 m/s.

2. Variable power generation region:

   The wind turbine starts to rotate and generate power at wind speed which of around 4 m/s. This is known as a cut-in speed. The generated power continuously rises with the increase of wind speed until the wind speed reaches

the rated wind speed which is around 12-14 m/s where the turbine generates constant power.

3. Constant power generation region:

   For the range of wind speed between rated wind speed and cut-off speed, the design of the wind turbine is arranged to limit the power to the maximum possibility of capturing wind energy, which is referred to as the rated power output, and there is no further increase in the output power. This is done by adjusting the blade pitch angles to keep the rotor wind speed generating a constant power regardless of wind speeds as long as they are between rated and cut-off wind speed.

The above regions are shown in Figure 2-1. However, the figure shows the large range for the wind speeds which provide the rated turbine power in comparison to the variable region, but in reality, the wind speed varied between all regions and especially between cut-in and rated wind speeds. Therefore, intermittences and fluctuations of the generated electrical power are related to the wind power systems. They become a behavior of these systems and cannot be avoided.

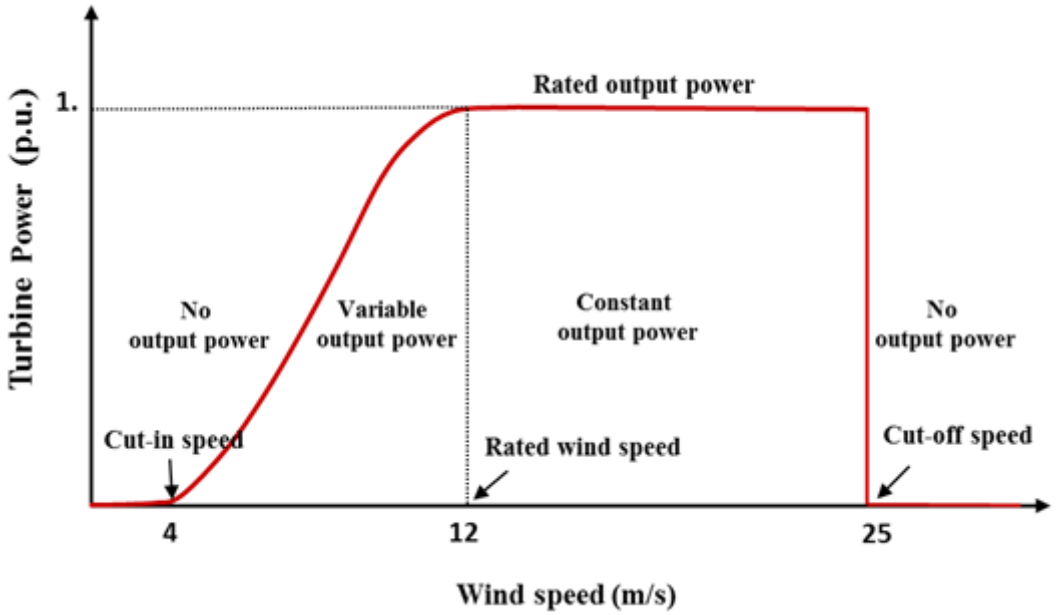

Figure 2-1. Typical wind turbine output power with wind speed

2.2 Smoothing Strategies for Reducing the Active Wind Power Fluctuations

With the rapid increase in the penetration of wind power in the power system, it becomes necessary to require wind farms to behave as much as possible as conventional power plants to support network voltage and frequency and sharing loads. On the other hand, the quick fluctuations of wind power disturb the generation load balance especially when these fluctuations exceed the limitation of the system low frequency control [70]. However, when penetration and load sharing of the wind power system are small, there will be no significant impact of the power fluctuations behavior on the power system. These fluctuations are absorbed by other large conventional power plants [16] or by batteries bank facilities [71]. In contrast, with the integration of large-scale wind power systems and increased power contributions for these systems to the power grid, these fluctuations indeed increase the system instability, disturb the operation of other conventional power plants, and may lead to grid failure. In order to reduce the

impact of these problems, the fluctuations of wind power systems have to be reduced and smoothed. Therefore, it is necessary to modify the operation of current wind power systems which are designed to work at maximum power point to capture as much as wind energy as possible. These modifications, however, may sacrifice some of wind energy but will increase the overall system efficiency.

There are different approaches available for smoothing the fluctuations in the wind active generated power. These approaches work as strategies for increasing the system performance and stability, and for creating more reliable power system by integrating large-scale wind power systems. These approaches can be numerated as the follows:

1. Power smoothing using a flywheel:

   Figure 2-2 shows a schematic diagram of power smoothing of the wind power system using a flywheel system (*from [61], Cardenas el al., © 2004 IEEE, reused by permission*). The principle of this system is as follows: First, the induction machine-flywheel is run by an external power source, in this system a diesel generator is used, to store a large amount of energy in the flywheel. Since the stored energy increases only linearity with its moment of inertia but increases as the square of its rotational speed, the induction machine-flywheel is designed to operate up to twice the rated speed of the induction machine. Then, the stored energy in the flywheel will be used to run the induction machine to generate power to the system, thus the flux weakening or constant power operation is appropriate. The whole system is controlled through a nonlinear DC link voltage control system. While that system is implemented on the fractional wind power system, the system also requires an additional power system to be

associated with the wind power system to run the induction machine-flywheel. Furthermore, this strategy may not work for large-scale wind farms or the cost will be very high since it requires very large induction machine-flywheel systems.

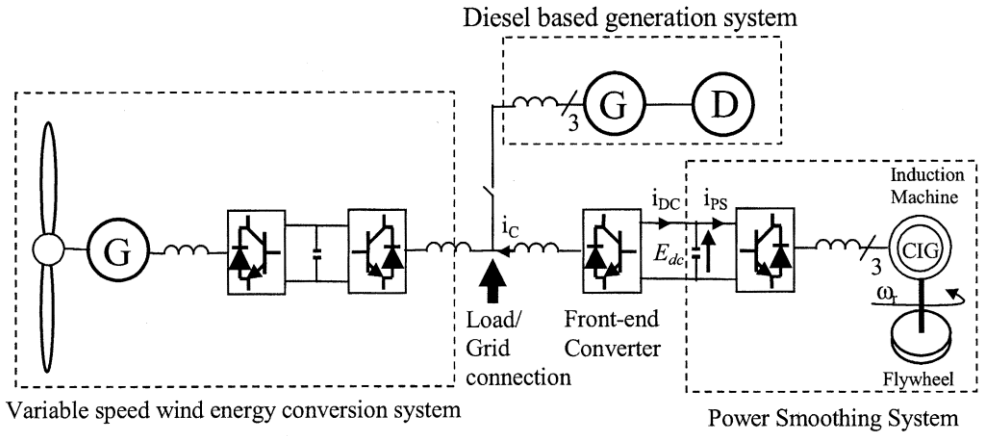

Figure 2-2. Power smoothing using induction machine-flywheel system [61]
(© 2004 IEEE, reused by permission)

2. Smoothing control using superconducting magnetic energy storage (SMES):

   In this approach a SEMS system, which is a large superconducting coil capable of storing electric energy in the magnetic field generated by DC current flowing through it, is used. Due to high response speed, the SEMS is capable of quickly releasing megawatt amount of power. The active power as well as the reactive power can be absorbed by or released from the SMES unit according to the system power requirements. The DC current flowing through a superconducting wire in a large magnet creates the magnetic field [72]. Figure 2-3 shows the control system diagram of the wind power system using SEMS (*from [66], Sheikh el al., © 2009 IEEE, used by permission*). The controller is used to decrease voltage and output power fluctuations of a fixed speed wind generator

during random wind speed variations. However, the SMES is capable of controlling both active and reactive power simultaneously, independently, and quickly, but there is a cost-effectiveness drawback. The cost of an SMES system can be separated into two independent components where one is the cost of energy storage capacity and other is the cost of power handling capability. Therefore, large wind power systems require very large capacity SMES systems which make implementation of SMES impractical.

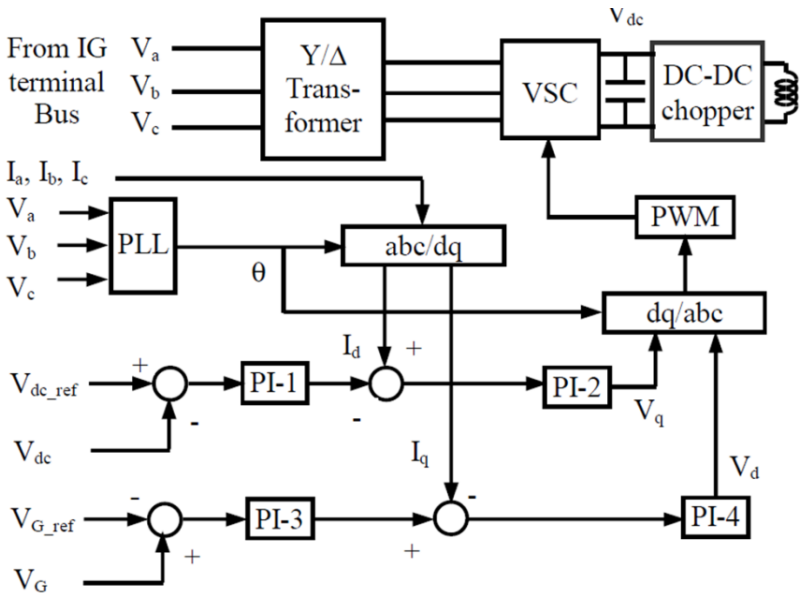

Figure 2-3. Schematic diagram of power regulation using SMES system [66]
(© 2009 IEEE, reused by permission)

3. Power smoothing using turbine inertia:

   This approach implies that the variable turbine energy is to be jointly absorbed through the turbine speed variation and the power delivered into the grid; the degree of sharing depends on the turbine moment of inertial [62]. In order to maintain stability, it is necessary to reduce the output power slightly below the instantaneous maximum wind power available. However, increasing the moment

of inertia in the turbine of wind power system will attenuate the ripple in the rotor speed and hence the output power, but there will be significant loss of the energy as the rotor moment on inertia is increased. Furthermore, this approach is perfect for reduction in power fluctuations for a short time after a disturbance occurs or the variation of the wind speed is around rated wind speed.

4. Power smoothing using energy storage facilities:

   Energy storage can be used to save energy at periods of low demand and release it during periods of high demand, reducing the amount of generation capacity needed to serve the same peak load. Energy storage can also help reduce congestion in a transmission system, deferring investment in a new transmission. For instance, when placed near a load center connected through a congested line, energy can be stored at times when there is no congestion, and released when there is no available capacity in the line. Storage can also reduce the size of a transmission line needed to connect wind farms. In a high wind energy scenario, storage devices can store energy during periods of high wind energy production and release it when needed, reducing conventional generation resources needed to handle wind variations or the amount of wind energy curtailed. The energy storage can be pumped hydro energy storage, compressed air energy storage, or battery energy storage system. Each of these systems works differently but can serve the same purpose; however, they require different types of operation controlling systems [73]. Energy storage has advantages for supporting all types of power systems in different ways. A method for implementing this approach in wind power systems will be presented in the next chapter.

5. Power regulation using blade pitch angle control:

   The pitch control is one of the most widely used control techniques to regulate the output power of a wind turbine generator [74]-[76]. The method relies on the variation in power captured by the turbine as the pitch angle of the blade is changed. Hydraulic actuators are used to vary the pitch angle which gives full control over the mechanical power. At wind speeds below the rated power of the generator, the pitch angle is at its maximum though it can be lower to help the turbine accelerate faster. Above the rated wind speed, pitch angle is controlled to keep the generator power at rated power by reducing the angle of blades. In other words, the blade pitch angle is used to control the rotor speed when the wind speed is higher than rated speed, but it cannot control the rotor speed when the wind speed is below the rated wind speed. Therefore, this approach is limited for smoothing the output power and only effective when the wind speed is higher the rated wind speed.

6. Power smoothing using generator power (P_{ref}) versus rotor speed (w_m):

   The wind power attenuation is implanted by inputting their P_{ref} versus w_m functions into a lookup table. The speed w_m from a speed sensor is used as a pointer to P_{ref} in the lookup table, which then loads this P_{ref} as the active power reference of the decoupled P-Q control. In general the reference power P_{ref} at w_m, a counter-torque $T_e = P_{ref} / w_m$ is produced to impede the wind turbine torque $T_T = P_m / w_T$ associated with wind velocity V_w [63][69]. This approach require controlling the rotor and stator fluxes through the rotor current which is controlled by the P_{ref} , also the blade pitch angle control should be used for

controlling the rotor speed at high wind speeds. Furthermore, the wind speeds must be predicted in order to avoid the instability occurrences of wind power systems.

The approaches described above are capable of reducing the fluctuations of wind power output. They are able to retain the constant level of the wind power in the limited range of the wind variations. Hereafter in this chapter a new approach is proposed for smoothing power fluctuations in wind power systems. This approach is based on implementing different tools such as de-loaded technique, weather forecasting, and controlling the rotor flux.

2.3 Active Power Control

The rotor-side converter (RSC) in DFIG (Figure 1-2) is responsible for controlling the active power of the wind power system. At a certain wind speed a unique turbine shaft speed exists, in which the wind turbine extracts the maximum power from the wind, which is known as the maximum power point tracking (MPPT) [77]. The optimal operating point which gives the maximum power is usually determined from the wind turbine characteristics as was shown in Figure 1-6. The RSC regulates the stator -active power and rotor speed of the DFIG at this optimal point. The active power and speed control in [2] has been modified in order to be applicable for de-loaded technique. This modification is shown in Figure 2-4. The blade pitch controller is activated whenever the wind speed is above the rated wind speed to maintain the turbine output power and the rotor wind speed within their rated values. Figure 2-5 shows the PI controller of blades pitch controller was given by Almeida and Lopes (*from [78], © 2012 IEEE, used by permission*), in which K_p, K_i, and T are 150, 50, and 0.1, respectively.

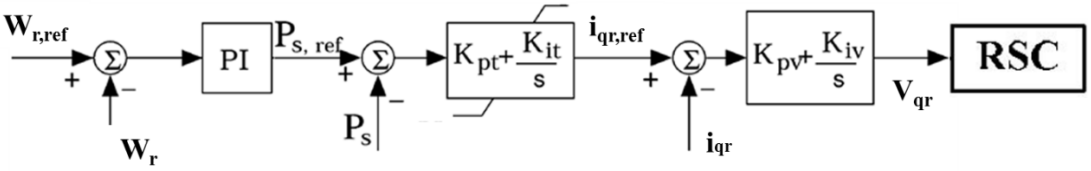

Figure 2-4. Active and speed controllers of DFIG wind turbine

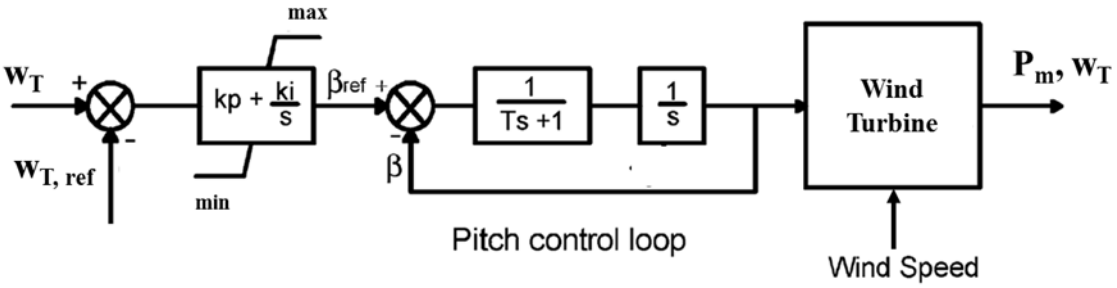

Figure 2-5. Pitch angle controller scheme [78]
(© 2012 IEEE, used by permission)

The stator active power reference $P_{s,ref}$ which is determined by the speed controller (Figure 2-4), is compared with P_s to control the stator active power, and the output is rotor current reference $i_{qr,ref}$. Rotor current i_{qr} is then compared with this $i_{qr,ref}$ to obtain the q-component current control loop. The proportional gain K_p and integral K_i in the active power/speed controller are K_{pv} is 0.3 and K_{iv} is 0.5 for voltage, and K_{pt} is 500 and K_{it} is 250 for torque. The d-q transformation allows the rotor injection voltage v_{qr} to be regulated. By neglecting the stator d-axis flux linkage [2], the decoupled stator active power in (1.1) can be simplified to the following:

$$P_s = v_{qs} i_{qs} \tag{2.1}$$

while the rotor active power, P_r, was given in (1.3).

Note that the stator and rotor reactive power is not shown here, since only active power is of interest in this research. The stator active power P_s is fed directly to the grid, while the rotor active power P_r passes through the power converter.

2.4 De-loaded technique

The strategy of the new approach is based on changing the way that wind power systems work. Knowing that, the current wind power systems are designed to operate in the maximum power production for pursuing the maximum economic benefit. However, this type of operation does not help to preserve the generation margin that is required by system power management and causes many problems for the power plants [79]. Because wind power system is an intermittent motive source which differs from the source applying to the conventional power plants, it is more challenging to attempt wind power control. Moreover, there is an interest of power grid instability when an operator's request is beyond the limit of the available wind power and the wind turbine speed is not able to run in the stable operating region. Therefore, an appropriate coordination between stability and controllability of active power in wind turbine should be further defined [80].

Compared to different types of generators in WECSs, a DFIG has more capabilities for providing control flexibility through the electronic converter and is able to work in the wide range of the wind speeds. These features make the ability of applying the majority of the strategies, which are described in section 2.2, on DFIG. Therefore, the DFIG is used throughout this chapter for implementing the control approach for active power regulating and smoothing.

In order to control the active generated power from the wind energy conversion system, it is necessary for the wind turbine to have sufficient generation margin available at any time. This is not possible if the wind turbine is operated under MPPT strategy which aims to extract the maximum energy from the wind. However, for establishing the

control strategy two important features of the considered wind power system must be taken into account. First, there is no control over the primary source, since it depends on wind which is an uncertain and uncontrollable. Second, the active power which is injected by DFIGs can vary almost instantly. Thus at wind speeds lower than the nominal wind speed the wind turbine is required to not operate at its maximum capturing power and should sacrifice some of its generated power in order to regulate the output power at a certain level.

For the purpose of power controlling, the wind turbine is de-loaded by shifting the operating point towards the left or the right of the maximum power line as shown in Figure 2-6. The de-loaded reference power is varied with the wind speed over the power curve which gives instantaneous reference power in which the wind turbine is operating. This reference power is feedback to control the rotor current which controls the rotor flux.

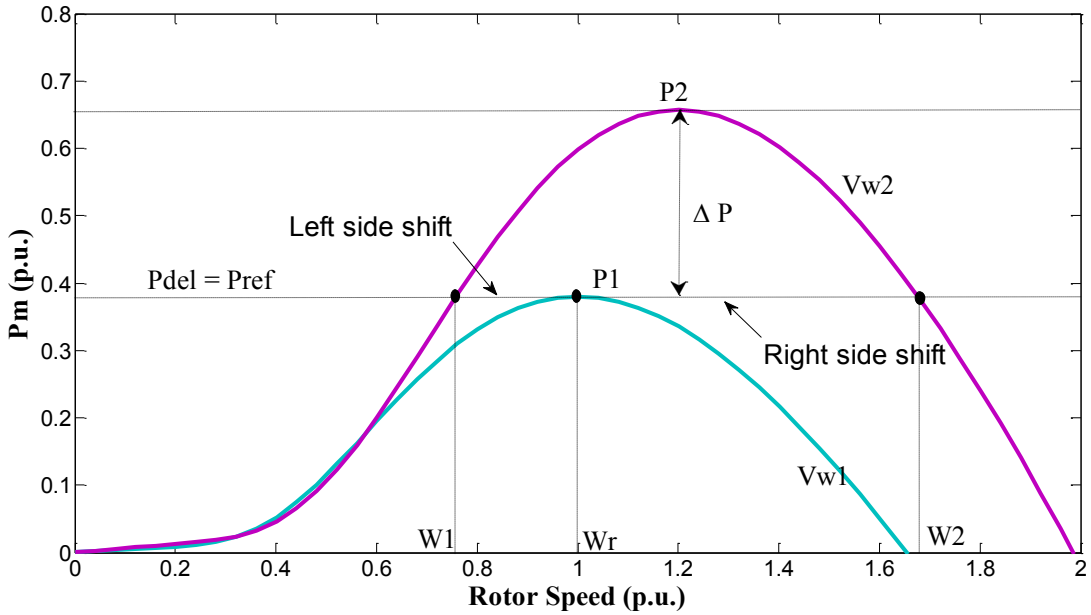

Figure 2-6. De-loaded technique of wind turbine output power

From Figure 2-6, the power margin for the de-loaded process is given by:

$$\Delta P = P2 - P1 \tag{2.2}$$

and,

$$P_{del} = P_{ref} = P1 \tag{2.3}$$

where *P1* and *P2* are the maximum active power at wind speed V_{w1} and V_{w2}, respectively. The *ΔP* gives the ability of the turbine power to follow the increase of the load or any disturbances occur to the power system. Based on the shifting point, the rotor speed w can be either w_1 or w_2 and can be determined from Figure 1-5 and by using the following relation:

$$T_m = \frac{P_{ref}}{w_{T,del}} \tag{2.4}$$

where, $w_1 < w_{T,del} < w_2$.

According to the wind forecasting data, V_{w1} and V_{w2} are predicted to be the maximum and minimum expected wind speeds for the wind forecasting period, and the total wind power margin area (PMA) can be determined by the following expression:

$$PMA = \int_{w1}^{w2} T_{m2}\, dw_T - \int_{w1}^{w2} T_{m1}\, dw_T \tag{2.5}$$

where T_{m1} and T_{m2} are measure turbine torques at V_{w1} and V_{w2} , respectively. It should be noted that, PMA is the maximum power generated from the wind power system which is limited by the maximum occurrences of the wind speed. However, for smoothing the fluctuations in the generated power, the DFIG will be forced to work at reference power ($P_{ref} = P_{del}$) regardless of the rotor speed w_T as long as the rotor speed greater than cut-in speed. Therefore, the power regulation can be done into two ways;

1. With the variation of the turbine rotation in the range $w_1 < w_{T,del} < w_2$
2. With fixed turbine speed

In the first case, the turbine speed is varied over a specific range and no control will be done to regulate it as long as wind speed is below the rated wind speed. In the second case, the turbine speed is regulated through the blade pitch angle control system and the reference is set at w_1. For the optimum operation and to avoid the instability of the wind energy conversion system, the wind speed is regulated based on the reference power which is given by de-loaded process and wind speed forecasting data. This regulation will be done by the control system of the blade pitch. The implementation of the de-loaded technique, which is described in this section and referring to in Figures 2-4, 2-5, and 2-6 is shown in Figure 2-7, where *n* is *100*.

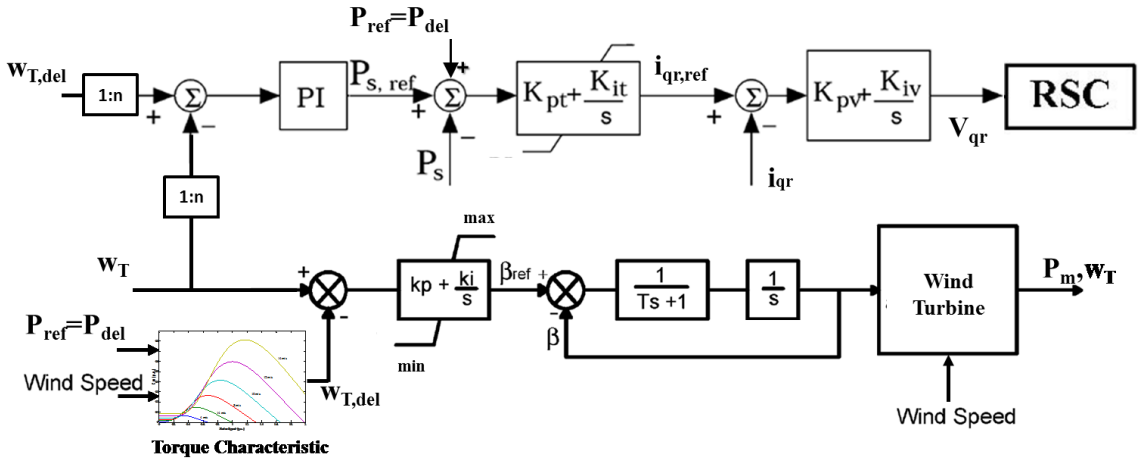

Figure 2-7. Schematic diagram of de-loaded technique of active power control

2.5 Simulations and Results

The de-loaded technique which is presented in section 2-4 is applied to the wind farm consisting of 200 units of 1.5 MW DFIG each. The MATLAB environment resource is used for simulation and the modified controller is applied to the wind power system which is available in MATLAB Simulink Library R2012b. The wind farm is assumed to be integrated with the infinite bus system of constant voltage and frequency. The

simulation is carried out under the consideration that each wind turbine unit in the wind farm gets the same wind speed and wind density at the same time, i.e. minimum effect of the wake. The planning of smoothing and controlling the active generated power from the wind turbine based on wind data in Figure 1-9 can be done in the following cases:

Case 1: One level power regulation

According to the given wind forecasting data, the minimum and the maximum wind speed during 24 hours are 7.8 m/s and 21.2 m/s which are represented by V_{m1} and V_{m2}, respectively. This is indicated in Figure 2-8.a. Referring to the turbine power characters in Figure 1-6 and using (2.4), the de-loaded reference power is related to V_{m1} is 0.153 p.u. The result of this implementation is shown in Figure 2-8.

Case 2: Multiple levels power regulation

In this case, the wind forecasting data is divided into different regions with the minimum and maximum wind speeds indicated in each region separately. These regions are detected based on the mean value of wind speed. Figure 2-9.a shows these regions. For the given wind data, seven regions can be detected and the minimum wind speeds in each of these areas are detected to be 9.2, 7.5, 8.5, 14.4, 13.5, 15.5, and 11.5 m/s, respectively. The corresponding reference powers to these wind speeds are 0.286, 0.1539, 0.22, 0.42, 0.71, 0.8152, and 0.5617 p.u., respectively. Figure 2-9 shows the simulation results for this case.

The results show that the presented approach is capable of producing a constant level of generated power from the wind power systems in the wind farm. The constant level is not affected by wind speed variations, and rotor speed kept at the level that is necessary

for producing the power is set by the reference power. This procedure for controlling the rotor speed is done by the blade pitch angle control system. Figures 2-8.c, 2-8.d, 2-9.c, and 2-9.d show both rotor speed variations and blade angle variations.

2.6 Discussion

In this chapter, the de-loaded technique is used for regulating and smoothing the active power generated by the DFIG wind power system. The wind speed forecasting data helps to detect the available power of the wind farm in the coming time frame. This is very important for managing a power system where different power plants are working together to supply loads. Due to the nature of the energy sources in conventional power plants, the availability of these power plants is known and controllable unlike in wind power systems. Therefore, the de-loaded technique is useful in making wind power systems act as conventional power plants. This increases the stability of the power grid and decreases the problems associated with integration large-scale wind power systems. However, the de-loaded technique requires sacrificing some of the output power from the wind power system, but overall it helps the WECS to retain the stability of the grid rather than disturb it.

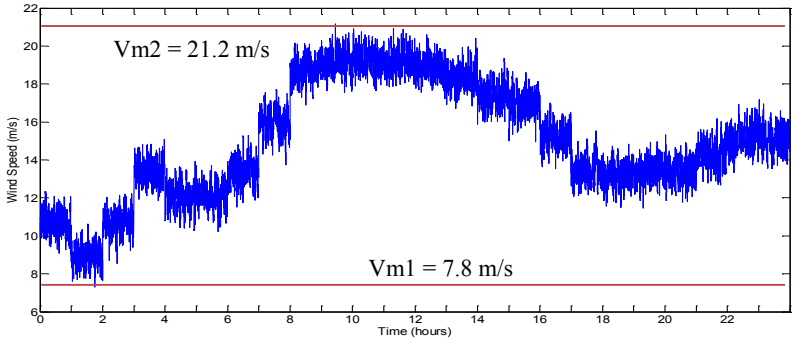

a. Wind Speed during a day ahead.

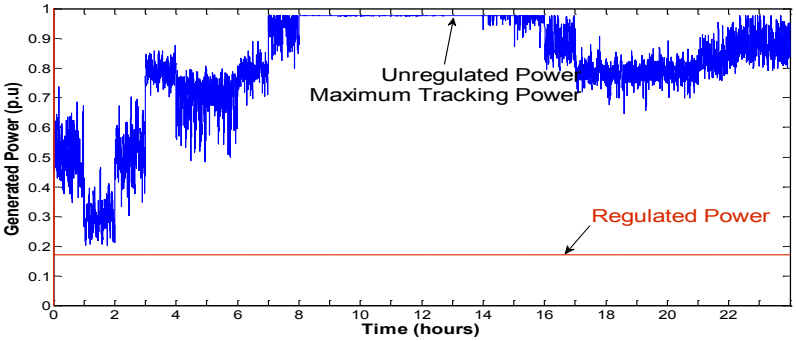

b. One level power regulation.

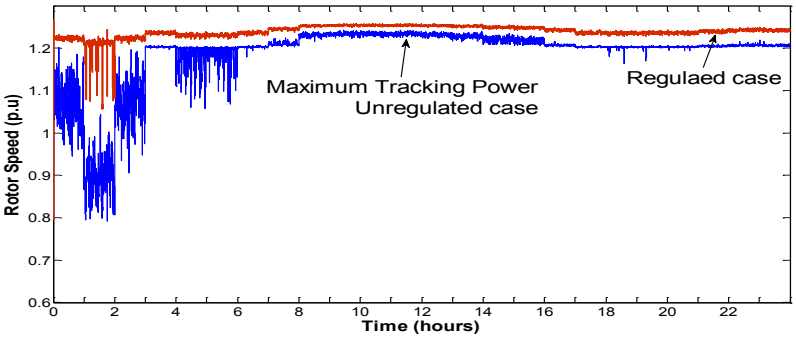

c. Rotor speed.

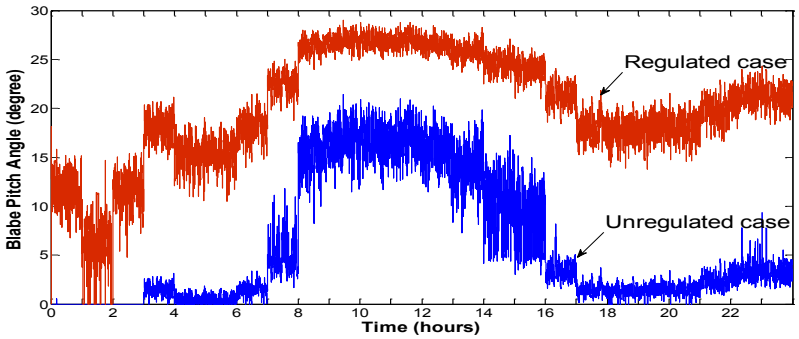

d. Blade pitch angle variations.

Figure 2-8. First case simulation results

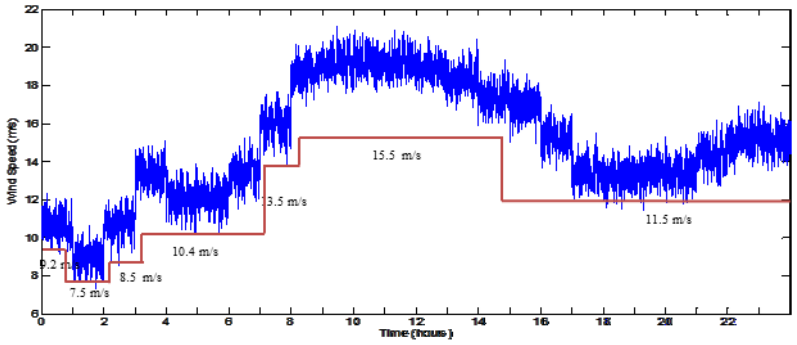

a. Wind Speed during a day ahead.

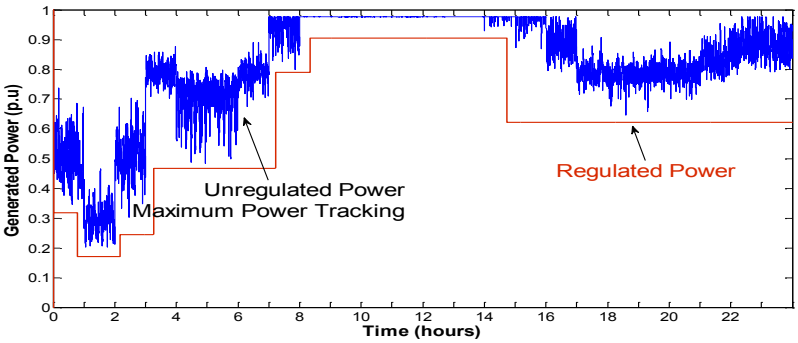

b. Multi levels power regulation.

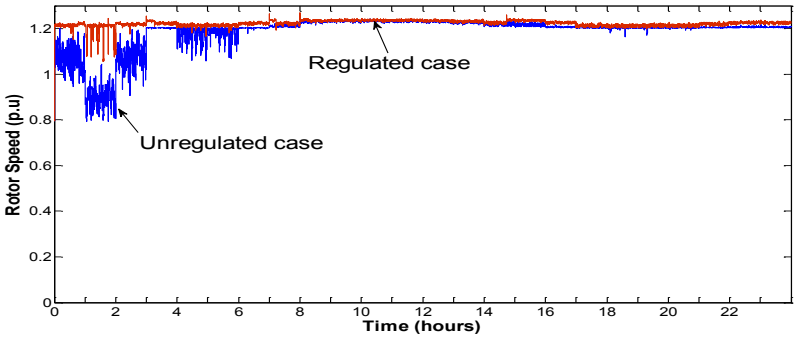

c. Rotor speed.

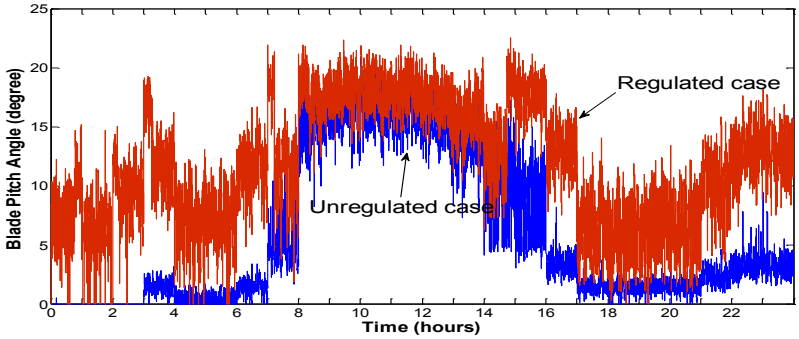

d. Blade pitch angles variations.

Figure 2-9. Second case simulation results

Chapter 3: Fluctuation Reduction and Load Supply of Large-Scale Wind Power Systems

In this chapter a new method is presented for enhancing the operation of large-scale WECS using multiple storage facilities. The previous chapter was about smoothing the fluctuations based on changing the operation of a wind power system to not operate at MTPP. In this chapter the wind power system will operate at its designed operation strategy; that is at MTPP. The goals of this method are to reduce the output power fluctuations of wind power systems and to make the generated power capability follow the system load demands. Two types of grid connections are considered: standalone and grid-connected wind power systems. The results are compared with the real-time data [81].

3.1 Introduction

A considerable amount of research has been published in area of reducing output power fluctuations of wind power systems by using power storages. One example is the use of an ultra-capacitor storage system for regulating active power of renewable power systems [65]. Another is the use of superconducting magnetic energy storage (SEMS) technology for power regulation and compensation of the fluctuation [66]. Finally the battery storage facilities [67]-[69] for smoothing the fluctuations of output power from the wind power systems are examined. All the above studies considered only the fluctuation reduction of output power and did not deal with planning management for supplying the load.

In this chapter, a new method is presented for reducing the output power fluctuations of wind power systems. The method is based upon two factors: the estimation of the

output power and the estimation of the stabilizer facilities. The generated power from wind power systems can be estimated through using weather forecasting data (wind speed) during the designated forecast period. The period of the forecast is used for planning the system power management. Furthermore, the fluctuation's characteristics and behaviors will be known from the estimation of generated power. The stabilizing facilities considered in the method are battery energy system (BESS) and pumped-hydropower storage system (PHSS). The charging/discharging of the BESS will be used for smoothing the fluctuations. The information about the fluctuations will be significant for detecting the rates of charging/discharging and the capacity of the BESS. The BESS is connected to the bus through a DC-AC bidirectional converter which consists of power electronic components, and it is controlled through a pulse width modulation (PWM). The PWM will enhance the charging/discharging modes for suppressing the fluctuations. However, due to a limitation in the capacity of the BESS, the BESS will not be able to support the output power of wind power systems to cover the system loads in standalone grid, and cannot give the desired levels of output power in the grid-connected wind power systems. Therefore, it is necessary to add another storage facility, such as PHSS, to the system in order to compensate the output power in both types of the grid. The PHSS, which is based on pumping/generating modes, is not fast enough for smoothing the output fluctuations, but has the ability to provide/store large power which is needed by the output power of the wind power systems to cover the load demands or to give the desired level of power generation in standalone and grid-connected wind power systems, respectively.

3.2 Wind Power System and Storage Facilities Model

3.2.1 System Configuration

Figure 3-1 shows a configuration of a power system which includes the following components:

1. Wind farm
2. Battery energy storage system (BESS)
3. Pumped-hydropower storage system (PHSS)

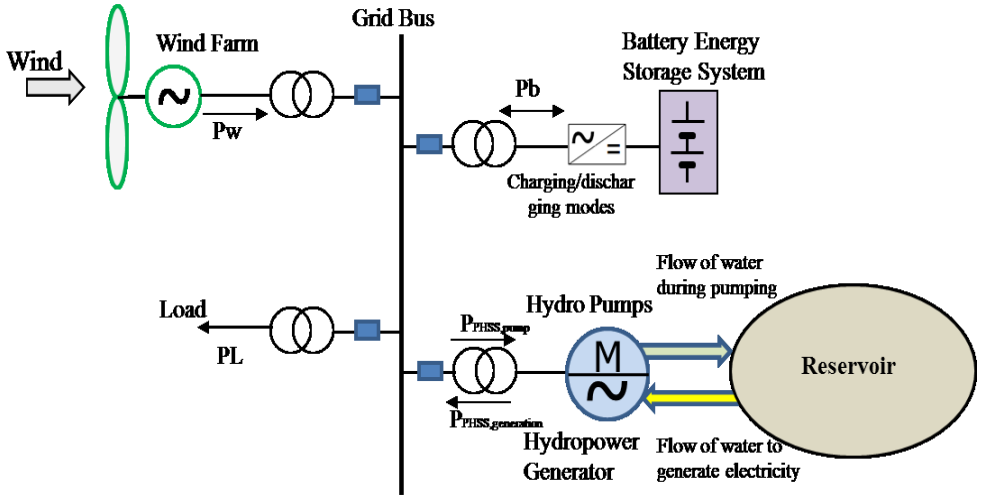

Figure 3-1. Wind power system with two storage facilities for power fluctuation reduction systematic diagram system model

3.2.2 Wind Farm

A wind farm consists of multiple wind turbines, each provided with a blade pitch angle controller and a DFIG with a capacity of 2 MW. The blade pitch angle controller is used to regulate the turbine speed when the wind speed is above the rating wind speed and DFIG is used since it can generate power in a wide-range of rotor speeds with the

ability to control voltage and frequency. The controls on the wind turbines will operate as planned by the operators, most commonly on maximum power point tracking.

To estimate the generated power from a single unit of a wind power system, 24 hours of weather forecasting data is required. Referring to the forecasting wind speed data in Figure 1-9, Figure 3-2 shows the corresponding prediction of the generated power for any wind power system unit in the wind farm, in which rated wind speed for WECS is 12 m/s.

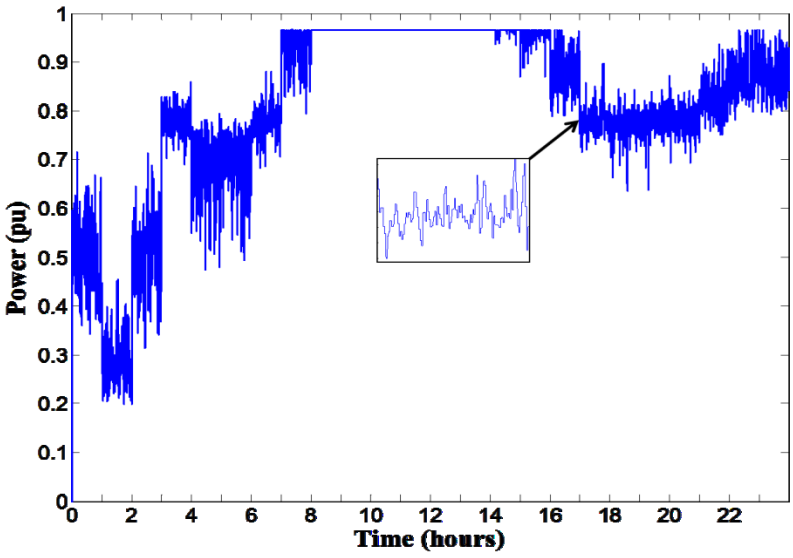

Figure 3-2. Wind power forecasting data based on wind speed in Figure 1-9 (Base power is 2 MW)

3.2.3 Battery Energy Storage System

The battery energy storage system (BESS) is used to regulate the output power of the wind power systems. The BESS is connected to the bus through a bidirectional AC-DC power converter. The converter has the capability of passing power in both directions according to the controlling system that regulates this process. A pulse width

modulation (PWM) is used to control the bidirectional converter for charging/discharging of BESS.

The charging/discharging controller of BESS will be based on the following:

1. The output power of BESS, *Pb*, will be in charging mode when battery storage is not full ($Pb=P_{ch}$).
2. The *Pb* will be in discharging mode when the generated power from the wind farm is less than the demand ($Pb=P_{disch}$).
3. The charging/discharging power, (P_{ch}/P_{disch}), is based on the capacity of the BESS.
4. To protect the BESS, the battery will not be charged when the battery is full, and will not be discharged when the discharging level is less than 20% of the rated capacity of the battery

In this study, a sodium-sulfur (NaS) battery is used. Large energy capacity and fast, precise response are the major features of NaS battery performance. A standard 1 MW NaS battery storage system can discharge 6 MWh of stored energy. The characteristics of NaS battery are presented in Appendix C [82].

3.2.4 Pumped-Hydropower Storage System

The pumped-hydropower storage system (PHSS) is one of the methods for hydropower generation that stores energy in the form of potential energy of water in an upper reservoir, pumped from a second reservoir at a lower elevation.

The PHSS use surplus power generation, in cases of low demand, to pump water to a reservoir and use it at a later time through a turbine when it is required to cover peak loads or when the demand on the electricity increases [83].

Based on the type of equipment, there are three PHSS configurations:

1. A separate pump coupled to a motor and a turbine coupled to a generator. This configuration requires four units and a large space.
2. A pump and turbine are both coupled to a single reversible motor/generator. This configuration requires three units.
3. The most widely used PHSS is a revisable pump/turbine, which is coupled to a reversible motor/generator. This configuration takes up less space than the other two and has a lower installation cost than the others [84].

The PHSS system turnaround/cycle efficiency is defined as the ratio between the energy supplied while generating and the energy consumed while pumping. This efficiency depends on both pumping efficiency (η_p) and generation efficiency (η_g). The turnaround efficiency of any PHSS system (η_{ph}) is given as the product of pumping efficiency and generation efficiency:

$$\eta_{ph} = \eta_p \, \eta_g \tag{3.1}$$

The turnaround efficiency usually ranges between 70-85%. In general, PHSS can be brought in service within 90 seconds and can be functioning at full power within 120 seconds. It can also switch from pumping to generation or from generation to pumping mode in 180 to 240 seconds [85].

While in generation mode, the PHSS output power, $P_{PHSS,generation}$, can be calculated from the following expression (from [86][87], *© 2012 & 2008 Elsevier, used by permission*):

$$P_{PHSS,generation} = \rho g H V_g \eta_g \qquad Watt \tag{3.2}$$

where ρ is the density of water in kg/m^3 , V_g is the volumetric flow rate during generation mode in m^3/s, g is the acceleration due to gravity in m/s^2, and H is the head or difference in elevation of the reservoir in m.

The power consumed, $P_{PHSS,pumped}$, while the PHSS system is in pumping mode can be calculated from:

$$P_{PHSS,pumped} = \frac{\rho g H V_p}{\eta_p} \qquad Watt \tag{3.3}$$

where V_p is the volumetric flow during pumping mode in m^3/s [86][87].

3.3 Fluctuation Reduction and Load Supply Method

3.3.1 Wind Power Generation

The fluctuation reduction method requires having the estimation of total generated power from all wind power systems. Since the best weather forecasting data is short-term, the planning ahead for smoothing fluctuations using both BESS and PHSS will be based on the combination of all generated power from the wind power systems during the short-term weather forecasting data.

Based on the clustering technique which was proposed by Ali et al. [88], the total power generation of the wind farm at any given time, t, can be estimated as follows:

$$P_{tw}(t) = \sum_{i=1}^{c1} Ps_k(t) + \sum_{i=1}^{c2} Ps_k(t) + \cdots + \sum_{i=1}^{cn} Ps_k(t) \tag{3.4}$$

where P_{tw} is the total power of wind farm, PS_k is the wind power system i, and $c1$, $c2,..,cn$ is the number of the units in each cluster. Knowing that the total number of unites in the wind farm is $c1+c2+\cdots+cn$.

3.3.2 Power Smoothing by BESS

BESS is connected to the bus through a bidirectional AC-DC converter, which is controlled by a PWM, and due to a high rate of charge/discharge capability of BESS, the BESS can respond very quickly to the variation of output power of wind power systems, P_{tw}. However, due to the limitation of the capacity of BESSs and their sizes, they are not able to make the entire output power, P_{tw}, a straight smoothing line. Therefore, P_{tw} can be divided into equally intervals, k, with each interval having a specific value of the smoothed power based on the previous value as shown in Figure 3-3. Therefore, the smoothed power from (3.4) can be reconstructed as follows:

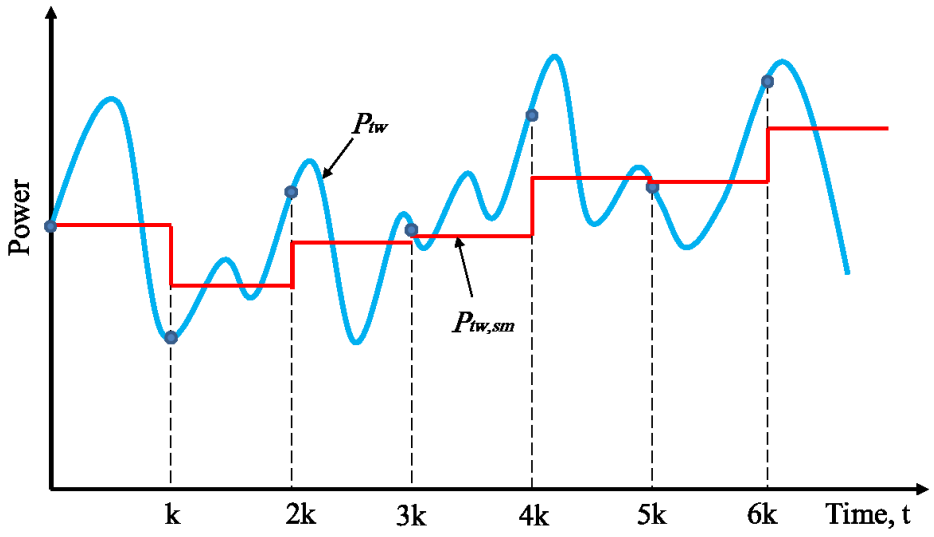

Figure 3-3. Smoothing procedure

$$
\begin{aligned}
P_{tw,sm}(0) &= P_{tw}(0) \\
P_{tw,sm}(t) &= P_{tw,sm}(0) \qquad 0 \le t < k \\
P_{tw,sm}(k) &= \frac{1}{2}[P_{tw,sm}(0) + P_{tw}(k)] \\
P_{tw,sm}(t) &= P_{tw,sm}(k) \qquad k \le t < 2k \\
P_{tw,sm}(2k) &= \frac{1}{2}[P_{tw,sm}(k) + P_{tw}(2k)] \\
P_{tw,sm}(t) &= P_{tw,sm}(2k) \qquad 2k \le t < 3k \\
P_{tw,sm}(nk) &= \frac{1}{2}[P_{tw,sm}((n-1)k) + P_{tw}(nk)] \\
P_{tw,sm}(t) &= P_{tw,sm}(nk) \qquad nk \le t < (n+1)k,\ n > 0
\end{aligned}
\tag{3.5}
$$

where n is the number of intervals, and $P_{tw,sm}$ is the smoothed output power.

The fluctuations in total generated power from the wind farm, P_{tw}, can be partially smoothed using charging/discharging BESS. The smoothed line, $P_{tw,sm}$, will separate charging and discharging levels for BESS. This can be estimated through:

$$
P_{ch/disch}(t) = P_{tw}(t) - P_{tw,sm}(t) \tag{3.6}
$$

where $P_{ch/disch}$ is the BESS power for damping the fluctuated power at time t.

State-of-Charge (SOC) of the BESS can be detected from (3.6), in which the positive part represents the charging state of the BESS, and negative part represents discharging state of the BESS. Figure 3-4 shows the SOC.

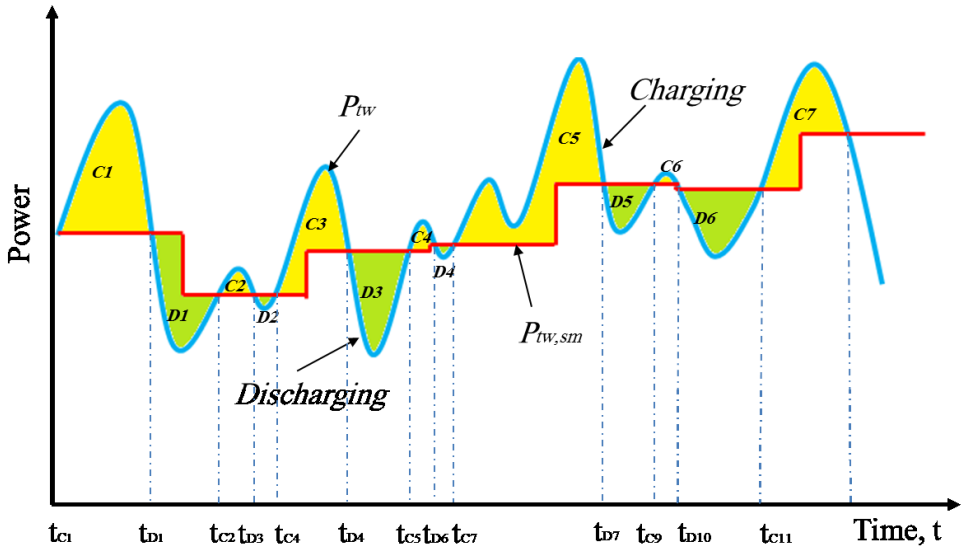

Figure 3-4. State – of – Charge of BESS

The total charging energy can be given by:

$$P_{ch} = \sum_{i=1}^{p} C_i \tag{3.7}$$

where $$C_i = \sum_{t=t_{Ci}}^{t_{Di}} (P_{tw}(t) - P_{tw,sm}(t))$$

and, the discharging energy can be given by:

$$P_{disch} = \sum_{i=1}^{q} D_i \tag{3.8}$$

where $$D_i = \sum_{t=t_{Di}}^{t_{Ci+1}} (P_{tw,sm}(t) - P_{tw}(t))$$

In (3.7) and (3.8), p and q represent the total areas of charging and discharging, respectively, and t_{ci} and t_{Di} are starting time for charging and discharging, respectively.

The capacity of the BESS in the interval for estimating the total generated power from wind power systems, P_{tw}, can be detected by P_{ch} and P_{disch}. Therefore, three cases can be classified based on the capacity of the BESS:

1. $P_{ch} > P_{disch}$: this means that the battery(s) will be charged more than discharged. If the battery(s) charged in full, the surplus power should be absorbed by the PHSS. In the case the surplus power is not sufficient for running PHSS, the local resistance (or capacitance) should be available to absorb this extra power.
2. $P_{ch} < P_{disch}$: this means that the battery(s) will be discharged more than charged. If it reached its limited level for discharging (less than 20%), a protection system should disconnect the BESS from the bus. The PHSS should release its power to cover the power deficiency (or using the charged capacitors if they are available).
3. $P_{ch} = P_{disch}$: this is the optimum case, where the charging and discharging are equal.

Furthermore, the power electronic for the bidirectional AC-DC converter should be capable to change the modes within the time equal to t_i + 0.1or less for stable and optimal BESS operation.

The BESS regulates the output power of wind power systems when the charging and discharging are within its capacity and when very fast response to the variations in P_{tw} are required. The maximum power which detects the capacity of the BESS can be given by:

$$P_{BESS,\max} = \max\left|P_{tw}(t) - P_{tw,sm}(t)\right| \tag{3.9}$$

3.3.3 Load Supplying Support by PHSS

The PHSS will be in generation mode when there is a large deficiency of generated power, P_{tw}, and when BESS is in charging mode, and it will be in pumped mode when there is a large surplus of power available on the system. In normal grid operation, these two cases are highly depending on the system load demands. That is, when the generation is more than the consumption there will be a surplus power on the system, and when the power consumption is larger than the power generation there will be a power deficiency. In these cases, PHSS is necessary in the system because the power generation of wind power systems is not controllable and they usually designed to operate at maximum tracking power point (MTPP), and the BESS does not have sufficient capacity to supply or to store large power. The two mode operations of PHSS are shown in Figure 3-5.

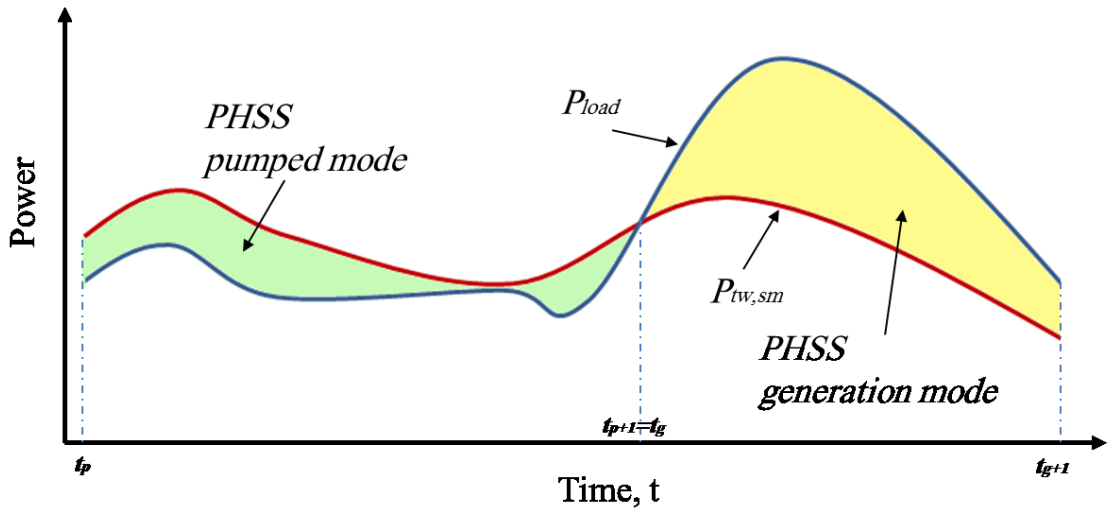

Figure 3-5. PHSS generation and pumped modes

The total energy required in pumped mode and in generation mode can be determined by the following:

$$P_{PHSS,pumped} = \sum_{t=t_p}^{t_{p+1}} (P_{tw,sm}(t) - P_{load}(t)) \tag{3.10}$$

and,

$$P_{PHSS,generation} = \sum_{t=t_g}^{t_{g+1}} (P_{load}(t) - P_{tw,sm}(t)) \tag{3.11}$$

where t_{gi} and t_{pi} are the starting time for generation mode and pumped mode, respectively.

The rating of PHSS can be evaluated from the accurate load and power generation from wind power systems forecasting data. In general, the rating PHSS is:

$$P_{PHSS,\max} = \max\left|P_{load}(t) - P_{tw,sm}(t)\right| \tag{3.12}$$

3.4 Fluctuation Reduction and Load Supply Algorithm

The algorithm of the fluctuation reduction method is in the flowchart in Figure 3-6.

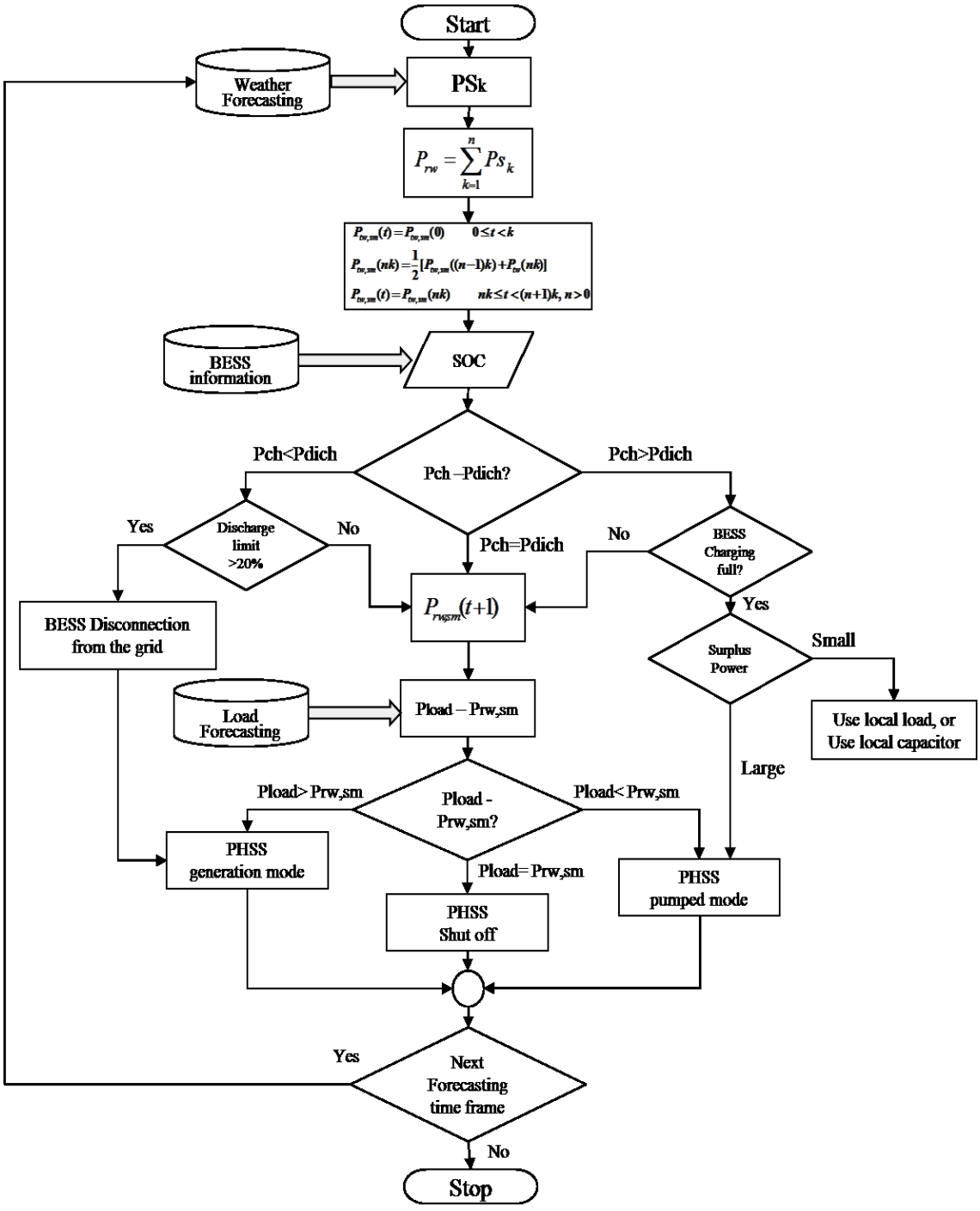

Figure 3-6. Flowchart diagram for system operation and management

3.5 Simulation and Results

The wind farm shown in Figure 3-7, presented by Ali et al. [88] (*© 2013 IEEE, used by permission*), consists of 49 identical DFIG-based WECSs with 2 MW each is used as an illustrative example.

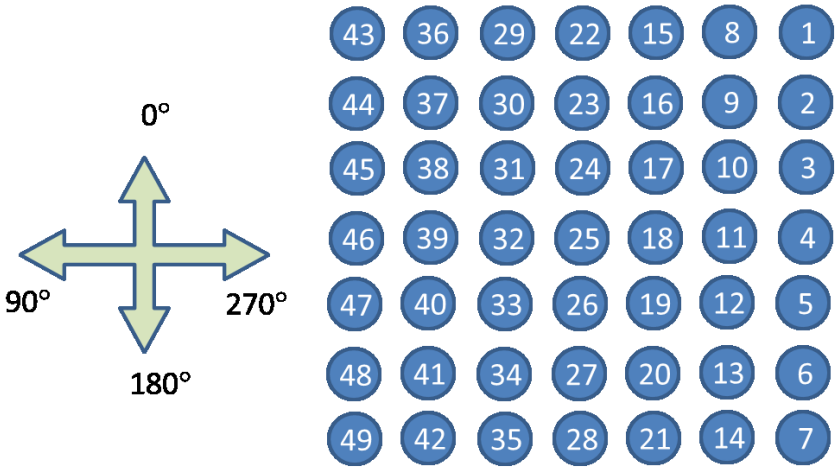

Figure 3-7. Wind Farm Layout of 49 wind turbines [88]
(© 2013 IEEE, reused by persimmon)

The MATLAB® Simulink® is used for designing a model of the above system, and according to the system flowchart in Figure 3-6, the procedure of the running system is as the following:

First: Ali et al. gave three clusters for the aggregation wind farm: cluster 1 includes turbines 1-35, cluster 2 includes 36-42, and cluster 3 includes turbines 43-49. From these clusters and using (3.4), the total power generation, P_{tw}, from the wind power systems is calculated and the result is shown in Figure 3-8.

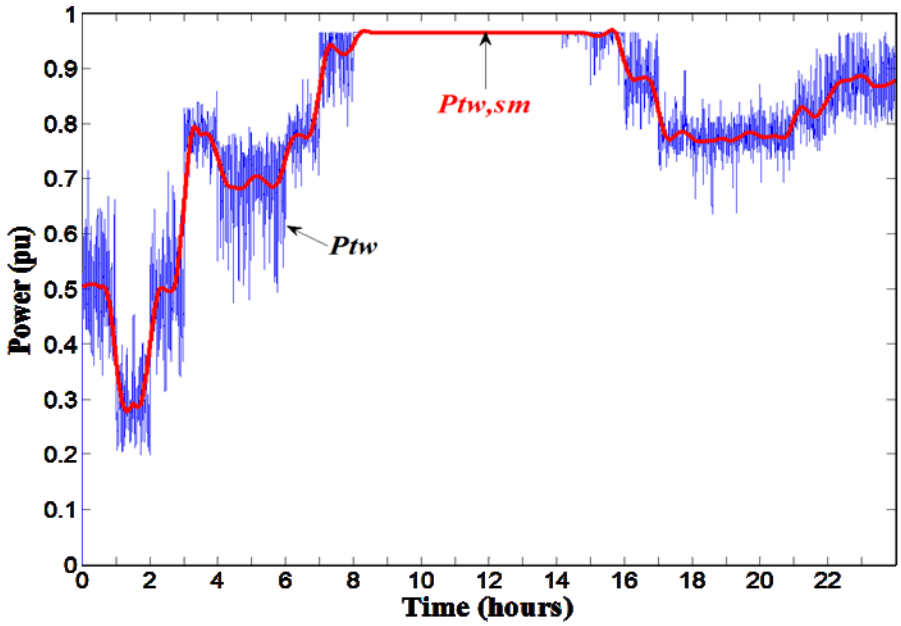

Figure 3-8. Combination of wind farm and smoothed power line (Base is 98 MW)

Second: Using (3.5) and for *k=10* sec, the output power of the wind farm can be smoothed, and the result of smoothed output power is shown in Figure 3-8 ($P_{tw,sm}$ line).

Third: in this paper, two types of grids are considered: standalone and grid-connected wind power systems:

A. Standalone System

In a standalone power system, wind power systems are responsible for providing the power to the system load demand. Different techniques are available for modeling the short term load forecasting. For instance, time series have been popular in load forecasting [89], the load forecasting output of an artificial neural network as a model that is compensated by rough set theory for better accuracy [90], and the back propagation of neural network [91]-[93]. Overall, the artificial neural network has been proven reliable in prediction errors, but very large historical recorded data is required.

Fuzzy logic technique, on the other hand, does not need as much historical recorded data for predicting process [94]-[96].

However, the best estimation of short term load forecasting process is collecting historical data. This data should be classified as a day of the week, since weekends usually have a lower load than weekdays, and also by the coordinate temperature and weather condition, the season and the time of day. It should be taken into account that load will increase each year as the number and type of customers change. In this study a short term load forecasting is adapted to the grid since the grid contains wind power systems. Usually, the perdition of generated power from these power systems is more accurate in short-term rather than long-term, at least with the current weather forecasting technologies. A typical load forecasting data is shown in Figure 3-9 [97]. Figure 3-10 shows the difference between load and total generated power from wind power systems.

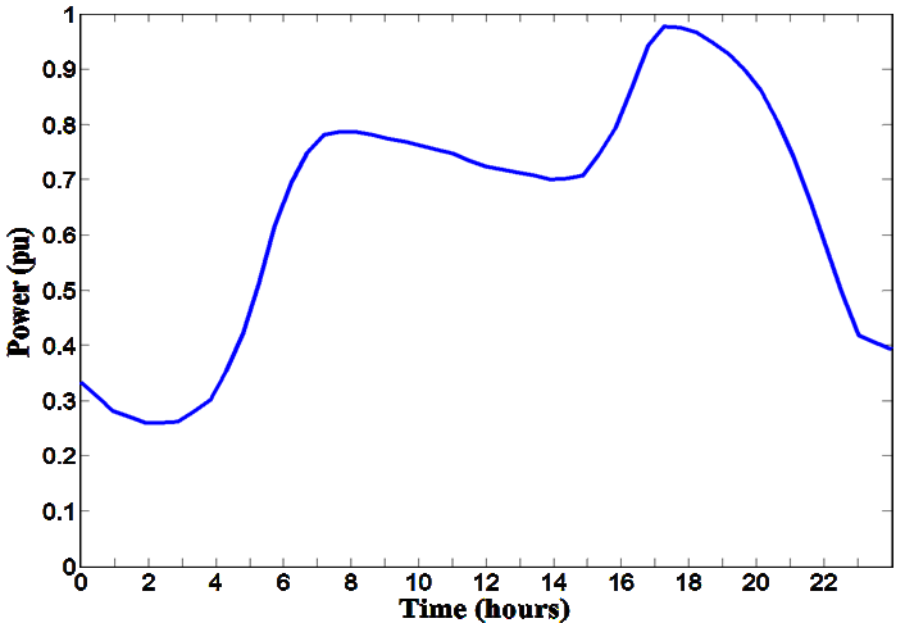

Figure 3-9. Typical load forecasting data in 24 hrs (Base is 98 MW)

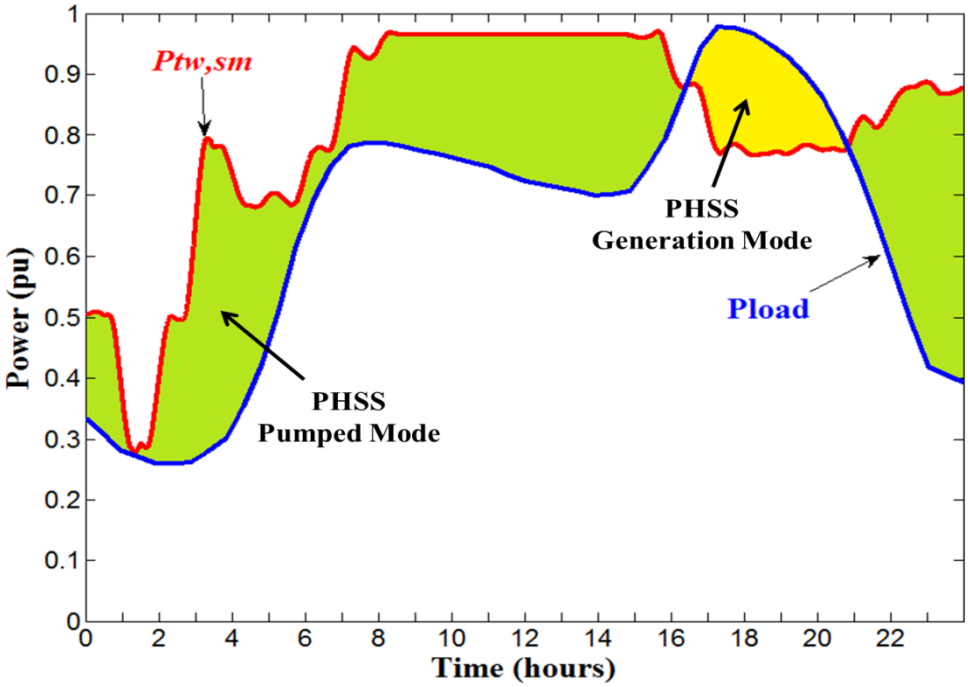

Figure 3-10. Difference between load and generated power from wind farm after regulation by BESS

Using the PHSS, the generated power from the wind power systems can be regulated to provide the power consumption (load). Thus to retain the balance between power generation and consumption, the PHSS is needed to operate as pumping when the generation is larger than the consumption and operate as generator when generation is less than consumption. Figure 3-10 shows the generation and pumping requirement modes based on the differences between load and power generation, and Figure 3-11 shows the total operation of PHSS as generation and pumping.

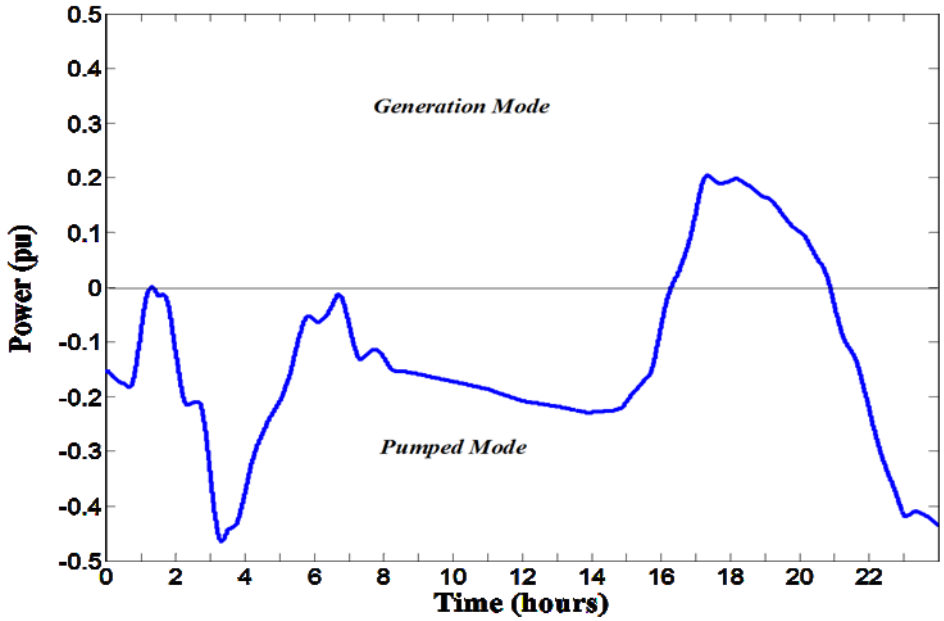

Figure 3-11. PHSS generation and pumped modes to support wind power systems

B. Grid-Connected Wind Power System

In grid-connected wind power systems, the wind power system shares the load with other power systems. In this case, the power generated from wind power systems is forced to have a certain level of power generation. Also, the system manager may require different levels of generation from the wind power systems. In both cases, the PHSS can be employed to provide certain levels of the output power generation from the wind. Hence, $P_{tw,sm}$ can have a constant level(s) according to generation/pumped modes of the PHSS. Figure 3-12 shows the contribution of the PHSS for giving a constant level and variable levels of the output power of the wind power systems.

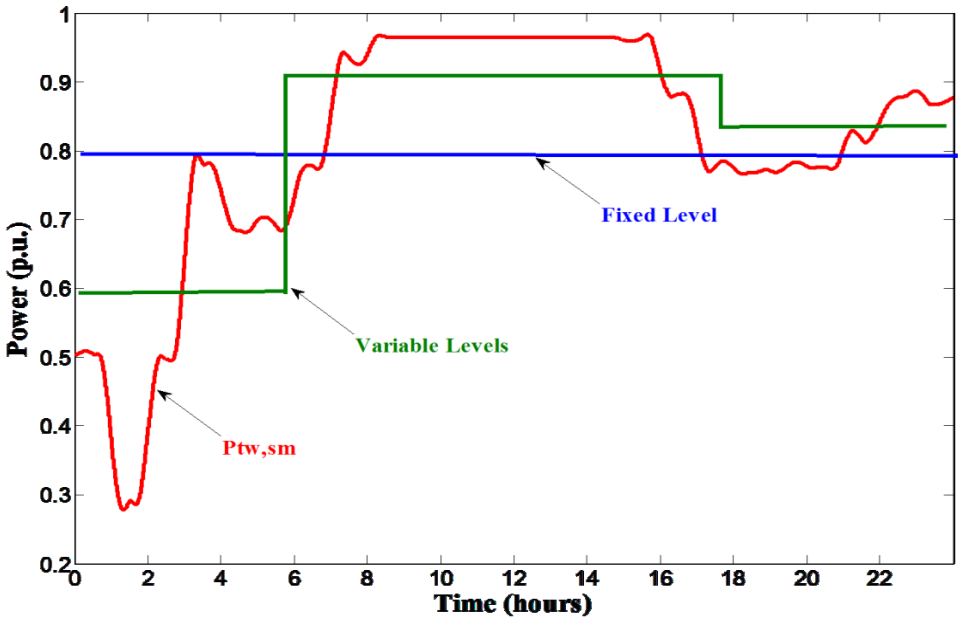

Figure 3-12. Different levels of the output power

3.6 Comparison and Discussion of the Simulated Results with the Actual Wind Speed and Load Data

The implementation of the method has been applied to the actual data. Figure 3-13 shows the implementation of the method on the actual data. The difference between total generated power from the wind farm and the load is shown in Figure 3-14.

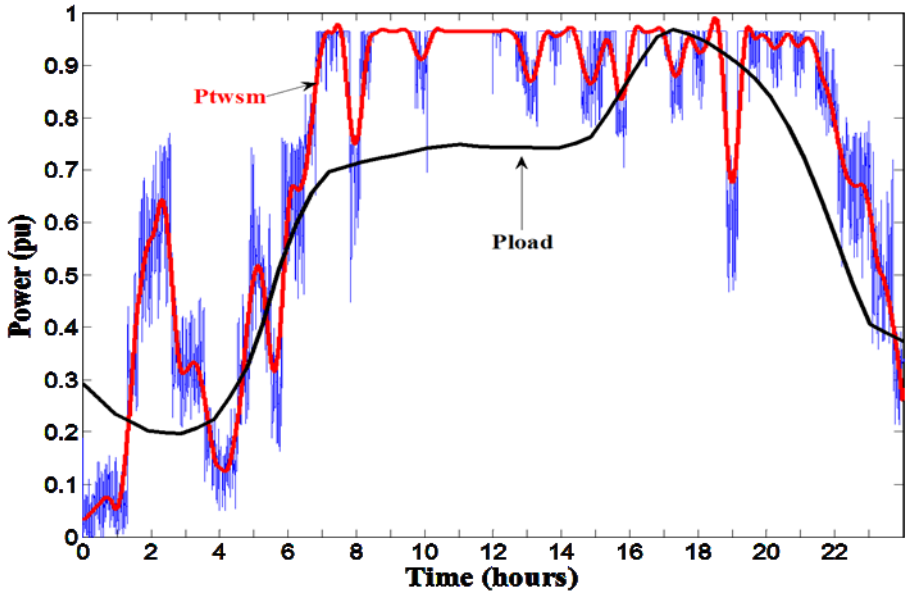

Figure 3-13. Implementation of the method on the real-time operation

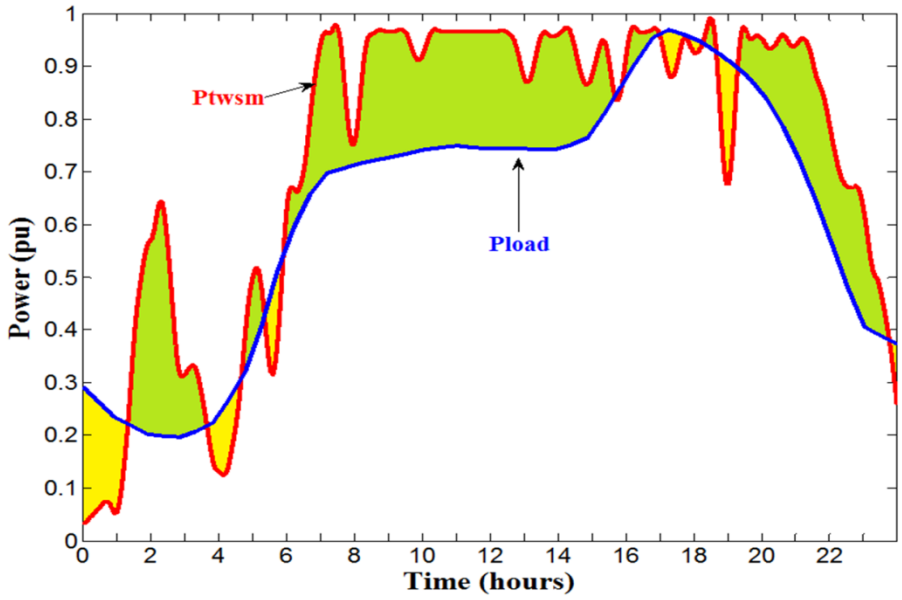

Figure 3-14. Difference between load and generated power from wind farm after regulation by BESS

For the purpose of the comparison between forecast and actual operation of the system containing wind power systems and supported by energy storage facilities for fluctuations' reduction and making wind power systems to follow the load demands, the same time frame has been chosen for wind speed and load. Figure 3-15 shows the difference between forecast and actual smoothing output power using the BESS, and Figure 3-16 shows the difference between forecast and actual PHSS response during generation/pumped modes.

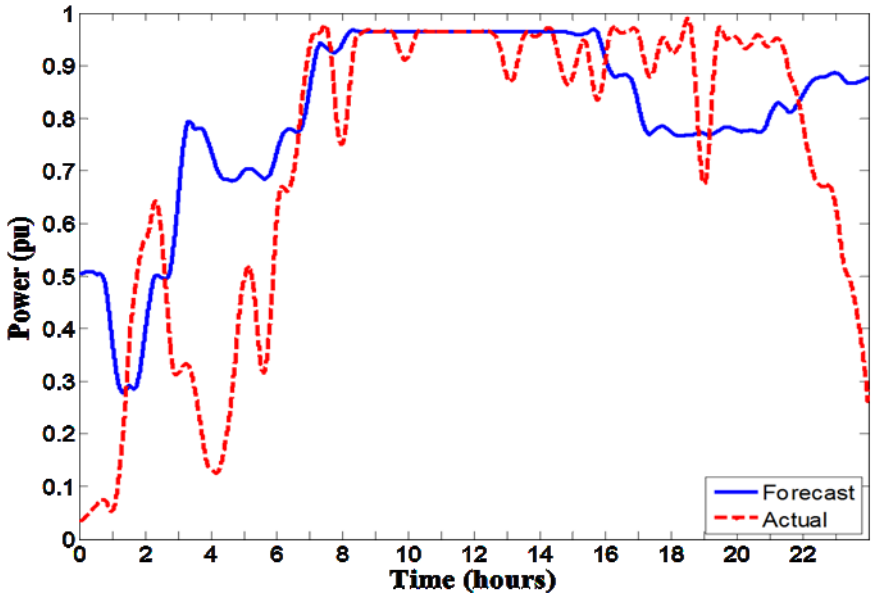

Figure 3-15. Difference between forecast and actual $P_{tw.sm}$

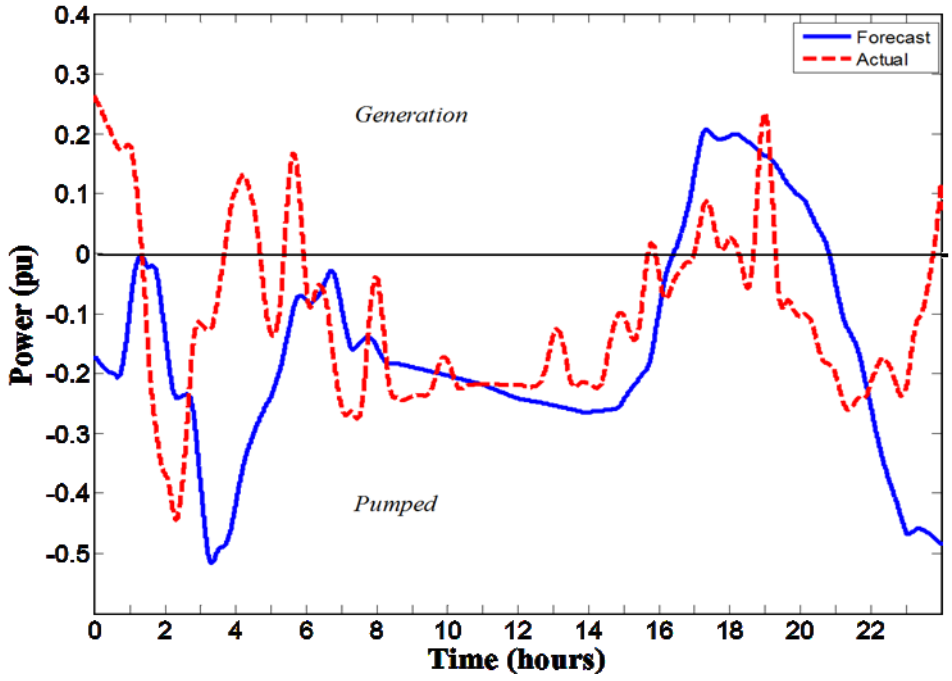

Figure 3-16. The generation/pumped modes of PHSS

Figure 3-17 shows the difference between actual and forecast output power when different generation levels are required by the system operators. Referring to Figures 3-8 and 3-13, the charging/discharging BESS required for providing the fluctuation reduction in the output power of the wind farm can be computed using (3.7) and (3.8). Similarly, referring to Figures 3-10, 3-11, 3-15, and 3-16, the generation/pumped of PHSS required for providing the balance between power generation and consumption can be computed using (3.10) and (3.11). The results for the computations of all the above cases including: forecast, actual, standalone, and grid-connected are tabulated in Table 3-1.

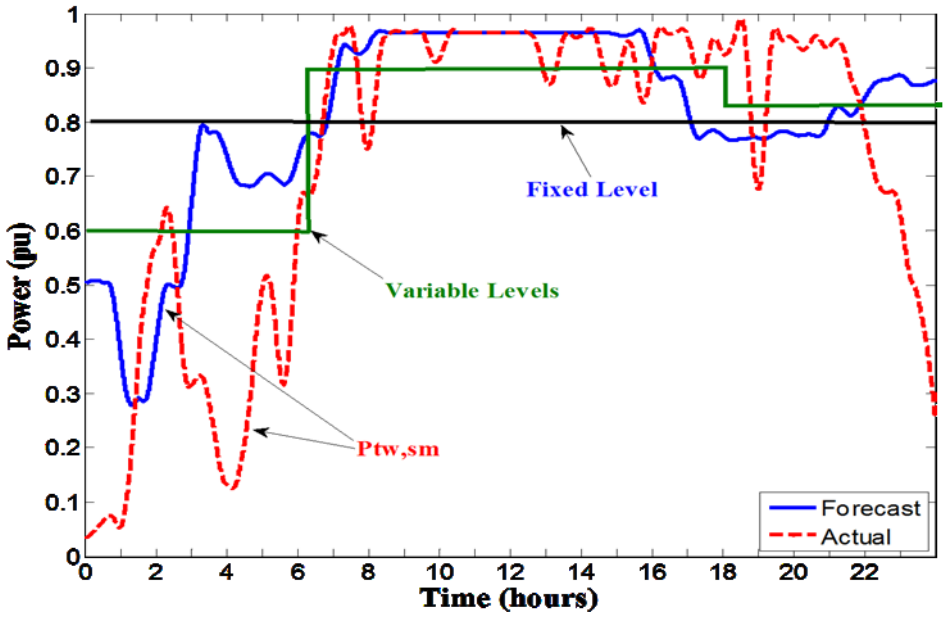

Figure 3-17. Regulating the output power based on system operating requirements

Table 3-1. BESS and PHSS Energy Calculations

Energy Facility		Forecast Data (MWh)	Actual Data (MWh)
BESS	Charging Energy	25.964	40.12
	Discharging Energy	26.055	39.88
PHSS Standalone Grid	Generation Mode	55.55	48.70
	Pumped Mode	393.16	286.03
PHSS Grid-Connected Fixed Level	Generation Mode	131.52	317.73
	Pumped Mode	152.25	178.70
PHSS Grid-Connected Variable Levels	Generation Mode	84.2	232.17
	Pumped Mode	88.71	79.95

From the results, it can be seen that the error in forecasting data causes different values of energy requirements for achieving the fluctuation reduction and load supplying. Also, from these results, the system planner and manager can detect the capacity and the size of both BESS and PHSS that are needed for implementing this method and getting the optimal system performance.

According to the charging/discharging energy of BESS, the best suited type for providing this energy can be a sodium-sulfur (NaS) battery. Large energy capacity and fast, precise response are the major features of NaS battery performance. A standard 1 MW NaS battery storage system can discharge 6 MWh of stored energy [82]. Since the maximum capacity for charging is 40.12 MWh, therefore, 7 units of NaS can be employed to perform the smoothing output of a wind farm of 98 MW.

Similarly, the results showed that the maximum pumping rate is 396.73 MWh and the maximum generation rate is 317 MWh of PHSS , respectively, therefore, by using (3.2) and (3.3), the PHSS can have the following parameters: $H = 400\ m$, $V_g = 100\ m^3/s$, $V_p = 80\ m^3/s$, $g = 9.81\ m/s^2$, $\eta_g = 0.85$, $\eta_p = 0.78$, and $\rho = 1000\ kg/m^3$.

Chapter 4: Microprocessor Based Controller of WECS

This chapter describes a microprocessor based system used to control the operation of the wind energy conversion system.

4.1 Microprocessor Based Controller

A microprocessor system automatically controls the operation of the wind power system. During startup, synchronization, and shutdown sequences, the microprocessor adjusts the blade pitch angle to control the rotor speed. Also, the blade pitch angle is adjusted to limit the output power to the rating power when the wind speed exceeds rating of wind speed (12 m/s). The yaw motion of the nacelle is also controlled by the microprocessor.

Overall, the microprocessor is programmed to perform the following primary functions for operating the wind power system: starting and stopping control, yaw control, blade pitch angle control, monitoring the operation, sending and receiving signals, and remote control.

The schematic diagram of a nacelle interior which is used as a wind power system in this chapter is shown in Figure 4-1 [98], in which all mechanical parts are shown in the nacelle interior for the wind turbine.

The modification to the control system in [99] and architecture of the microprocessor based system to the different types of control signals is shown in Figure 4-2. The microprocessor based control system consists of various input and output control and sensor signals which are used for controlling, operating, and the wind power system. The functions of these signals are described in the next section.

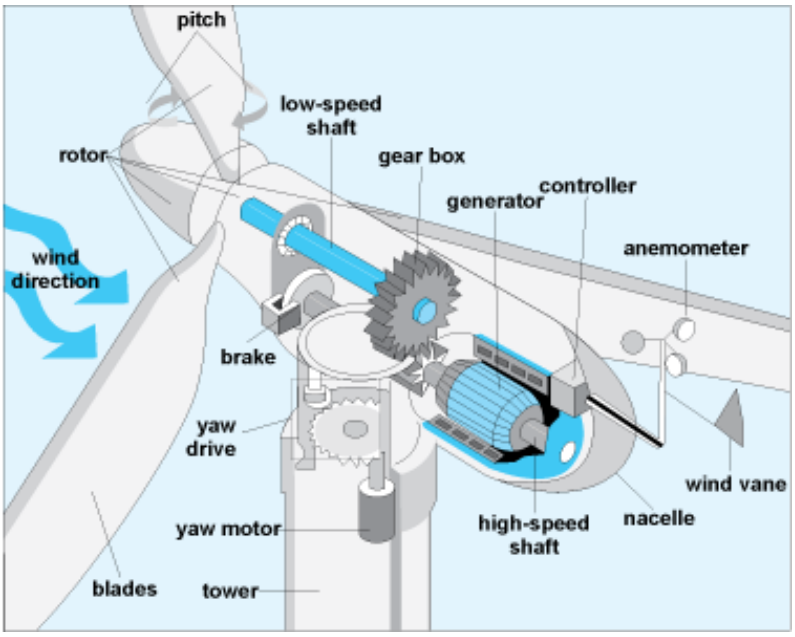

Source: U.S. Energy Information Administration, 2012

Figure 4-1. Wind turbine nacelle diagram [96]

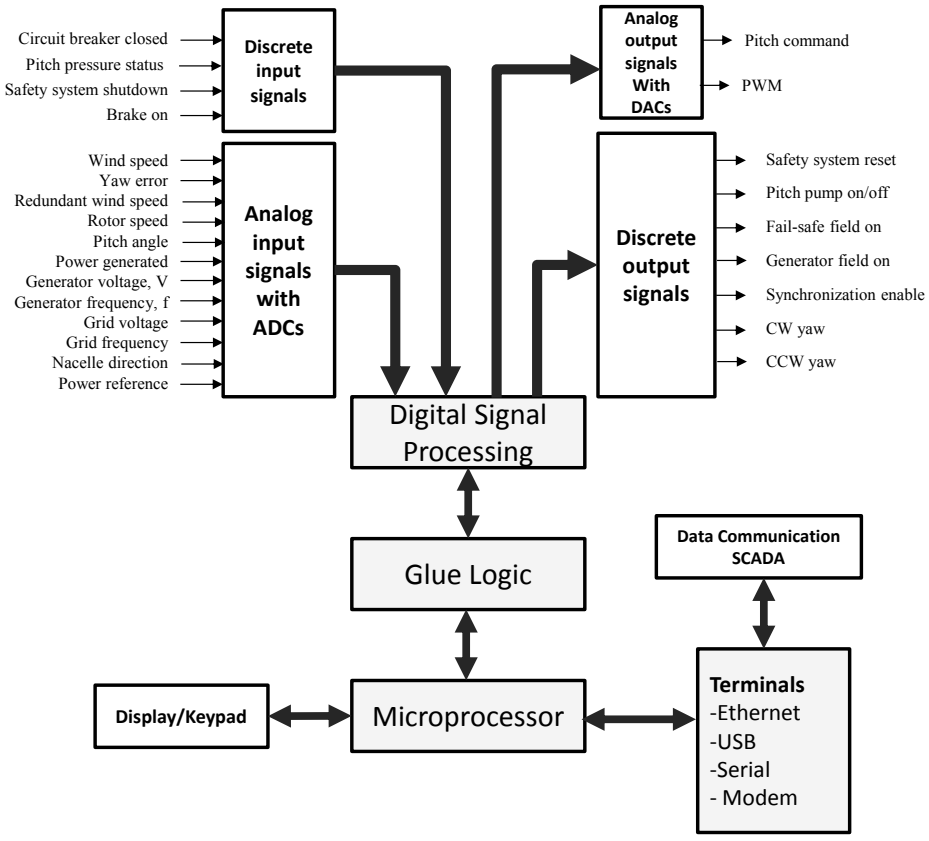

Figure 4-2. Microprocessor control architecture

4.2 Wind Turbine Control Signals

In general, the control signals from the wind turbine can be classified to continuous input signals, input discrete signals, continuous output signals, discrete output signals, and data communication.

1. Continuous input signals include the following signals: wind speed, redundant wind speed, yaw error, rotor speed, blade pitch angle, power generated, voltage, frequency, nacelle direction, and power reference.
2. Discrete input signals include the following signals: circuit breaker closed, pitch pressure status, safety system shutdown, disk brake on.
3. Continuous output signal include the pitch command signal.
4. Discrete output signals include the following signals: safety system reset, pitch pump on/off, failsafe disable, generator field on, synchronization enable, clockwise and counterclockwise yaw.
5. Data Communication includes SCADA receiving and transferring data.

4.3 Microprocessor Layout

The microprocessor system can be provided with the start and stop buttons for enabling and disabling the controlling system to operate and manage the wind power system. Also, the microprocessor system can be remotely started and stopped for the same purpose.

The display (LCD) built into the microprocessor front panel shows the status of all control signals. The status display is used to indicate the operating state of the wind power system. It is also used to indicate the particular fault detected during operation.

The status at the same time can be seen from the remote controller screen when it is needed.

The microprocessor accompanied with the memory to retrieve the recorder information may be used to study the past performance of the wind power system.

The microprocessor may controls four hour-meters and four mechanical pulse counters that are used in gathering operational data. The hour-meters measure total yaw time, synchronization time, wind available time when the wind speed is greater than 4 m/s, and outage time when the turbine is disabled. Three pulse counters give measures of total wind energy available, energy available during startup and shutdown, and outage energy. These energies are calculated by assuming a linear relationship between power and wind speed with zero output at 4 m/s and 1.5 MW at 12 m/s. The fourth counter indicates total energy generated as determined from the average of power-generated measurement.

4.4 Microprocessor Performance and Specifications

The wind power system uses various sensors to collect data such as wind speed, wind direction, current, voltage, frequency, etc. The microprocessor which is used in the embedded controller system must meet the following requirements to be considered for use in the controller of wind power systems:

1. Low power consumption
2. Sufficient amount of memory
3. Moderate to fast processor speed
4. Sufficient number of I/O data lines
5. Package type that work with the system

6. Programming language that is powerful but not difficult
7. Ability to add development board
8. Ability to interface with an LCD
9. Analog to Digital Converter
10. Low cost
11. Ability to work in different environmental conditions

The Intel® Atom™ processor is designed specifically for low power embedded systems [100]. The thermal design power (TDP) specification is 0.6 – 3 watt range, though it can scale to 1.8 GHz, making it a smart choice for use in the controlling system of a wind power system. Table 4-1 gives the specifications of the embedded system which is implemented in this type of microprocessor [100]-[103].

Table 4-1. Intel® Atom™ embedded system specifications

Term	Specification
Processor (CPU)	Intel® Atom™ Processor D510
Cores	2
Threads	4
Clock Speed	1.66 GHz
L2 Cache	1 MB
DMI	2.5 GT/s
Instruction Set	64-bit
Instruction Set Extension	SSE2, SSE3
Lithography	45 nm
Max TDP	13 W
VID Voltage Range	0.8 – 1.175 V
RAM	4 GB DDR2 – 667/800
Memory Bandwidth	6.4 GB/s
Physical Address Extension	32-bit

The embedded controller components are as follows:

1. One 16-channel multiplexer analog-to-digital converter (ADC) with ±10 DC V inputs and 12-bit resolution
2. Twelve 120 AC V discrete inputs
3. Eight 120 V ac, 2 A discrete outputs (relay)
4. One 2-channel digital-to-analog converter (DAC) converter with ±10 V output
5. 8 MB EPROM (Erasable Programmable Read-Only Memory)
6. I/O Controller: USB, RS232
7. Network connection: 1000 Mb/s Ethernet Controller
8. PCI connector
9. Serial ATA Interface: STA interface with 300 MB/s transfer rate
10. Integrated Graphics and Video memory

The operating system can be Windows CE or Windows Embedded Standard, and the TwinCAT2 automation software or Borland C++ transforms this embedded controller system into a power PLC and Motion Control system.

4.5 Microprocessor Based Controlling Operations

The microprocessor embedded based controller is responsible for performing certain monitoring and controlling operations on wind power system.

4.5.1 DFIG Voltage and Frequency Control

The integration of the wind power system with the grid requires that the wind power system operates at constant system, voltage; otherwise the wind power system acts as a motor and consumes power from the grid instead of producing power to the grid. The voltage control in DFIG can be done by controlling the rotor current. This current in

DFIG is controlled through AC-DC-AC through a DC-Link which controlled through the PWM converter. The microprocessor software will be responsible for generating desired characteristics of optimized PWM to minimize the total harmonic distortion in the inverter.

The PWM function *f(t)* is periodic function and therefore it can be decomposed into Fourier series as:

$$f(w_m t) = \sum_{n=1}^{\infty} [A_n \cos(n w_m t) + B_n \sin(n w_m t)] \tag{4.1}$$

where $A_n = \frac{1}{\pi} \int_0^{2\pi} f(w_m t) \sin(n w_m t) d(w_m t)$

and $B_n = \frac{1}{\pi} \int_0^{2\pi} f(w_m t) \cos(n w_m t) d(w_m t)$

using the quarter and half-wave symmetry of $f(w_m t)$, $A_n = 0$ for even n, $B_n = 0$ for all n. Since $f(w_m t)$ has a constant value between two consecutive switches of the PWM waveform, the computation of V_n for odd n is considerably simplified, and can be expressed as the following:

$$V_n = \frac{4}{n\pi} [1 + 2 \sum_{k=1}^{N} (-1)^k \cos(n \alpha_k)] \tag{4.2}$$

For 2-level PWM, and

$$V_n = \frac{4}{n\pi} \sum_{k=1}^{N} (-1)^{k+1} \cos(n \alpha_k) \tag{4.3}$$

For 3-level PWM, n corresponds to the harmonic order and N equals the number for switching angles per quarter cycle of the PWM waveform. The asynchronous PWM modulating signal is presenting in Figure 4-3.

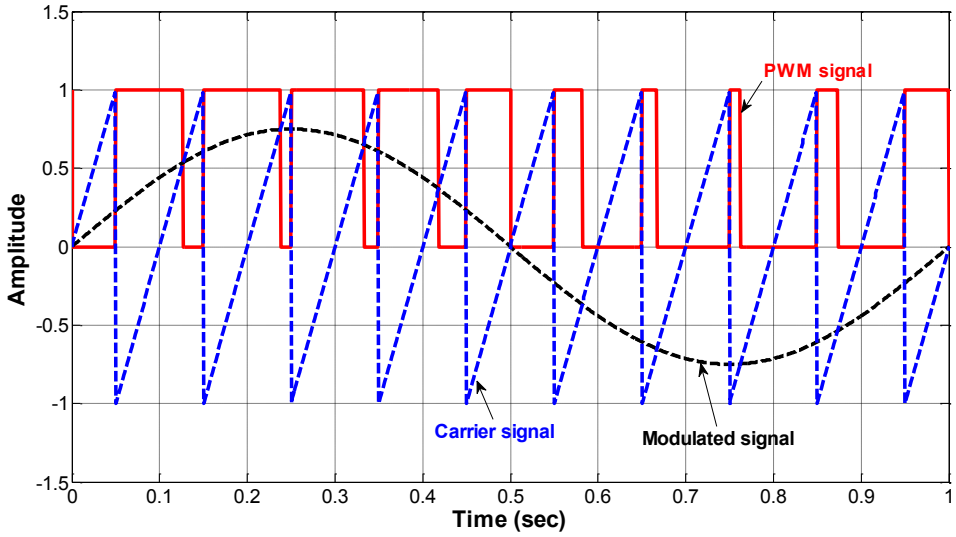

Figure 4-3. Asynchronous PWM modulating signal

The microprocessor is responsible for generating the PWM control signals with the help of i8255 Programmable Peripheral Interface (PPI) chip, 8255 programmable interval time (PIT), 8259 programmable interrupt controller (PIC), and analog-to-digital converter (DAC). A DC control signal is converted to a digital number by DAC. This digital number represents the carrier time period T, which corresponding to the desired output frequency. The programmable input/output ports are used to output six PWM control signals, and to input the digital number, corresponding to the desired output frequency. The 8253 programmable inverter (PIT) has three counters. The output signal from the counter changes from low to high after the loaded number has been finished. The 8259 programmable interrupt (PIC) is used to identify the source of the interrupt signals. Also, it determines the priority of the interrupt signals.

4.5.2 Microprocessor Based Power Smoothing using De-loaded technique

The microprocessor embedded control system is capable for regulating the generating output power both at maximum tracking power and power smoothing for wind power

system. According to the procedure of de-loaded technique, which was presented in Chapter 2, and when power smoothing is required from the wind power system to eliminate the fluctuation effects on other power plants, the central control manager sends a signal through SCADA to order the microprocessor to perform a regulation procedure. Also within the SCADA signal the metrological data for short-term wind speed forecasting and the power characteristic of the wind power system which is stored in the controller memory data bank. The microprocessor can detect the reference power signal which will be used for generating power in the range of the wind speed variations.

4.5.3 Microprocessor Based Power Smoothing using BESS and PHSS

In this type of smoothing output power, multiple microprocessor controllers are required for controlling each energy storage system separately. Controlling charging and discharging the BESS, Chapter 3, and detecting the full charge and minimum level of discharging are all done through a continuously running programmed microprocessor embedded system. This system will send signals to the central control manager indicating the instantaneous status of BESS. On the other hand, the pumping/generation modes of the PHSS are supervised by another microprocessor controller system. This system is responsible for directing the type of PHSS operation as needed based on the wind farm and system load requirements. Figure 4-4 shows the microprocessor controller systems for BESS and PHSS, respectively.

4.6 Discussion

In this chapter, the microprocessor embedded control system for monitoring and operating the wind power system is presented. The Intel® Atom™ processor is

suggested for this purpose due to its low power consumption and high speed computations. This does not mean that other microprocessors cannot be implemented for the same purpose. The ARM and ATmega family can also be used.

The microprocessor increases efficiency by ensuring all components of the wind power system are monitored and controlled. The response to the multifunction of these components can be easily detected, and a certain action can be done to the wind power system to eliminate the effects of this unit to the other units in the wind farm, and consequently to the grid. Furthermore, the remote communication and data collection with the presence of the microprocessor are easier and more efficient. Therefore, all units in the farm can be monitored and controlled.

Overall, the self-correction and dynamic performance of the wind power system can be enhanced with the presence of the high speed microprocessor.

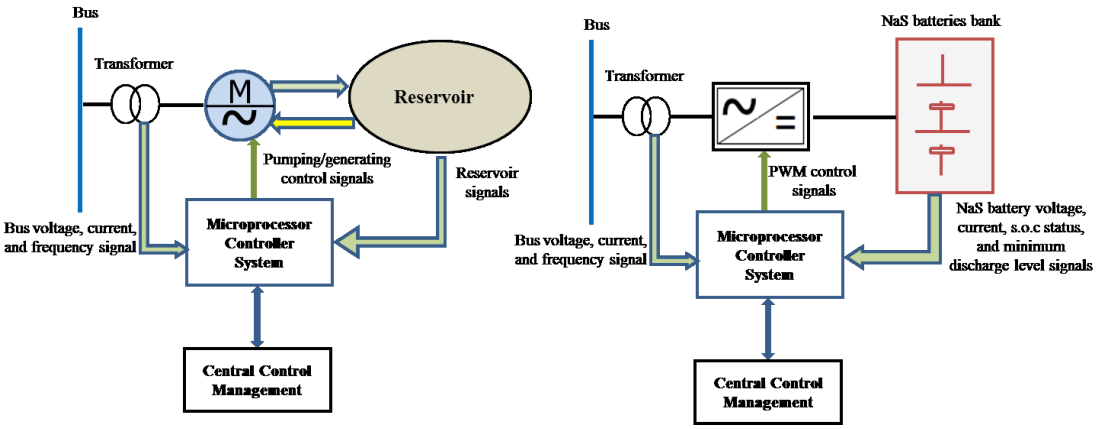

(a) BESS controller system (b) PHESS controller system

Figure 4-4. BESS and PHSS microprocessor controller architectures

Chapter 5: Optimization of the Grid Power Management

In this chapter the short term grid power planning with the presence of wind power system is presented. This future planning is optimized by adapting the weather forecasting data, load forecasting data, wind farm installed capacity, and the installed capacities for each conventional power plant providing demanded power to the grid. The wind power systems are assumed to have significant load sharing with other conventional power plants [104].

5.1 Bases of the Grid Containing Wind Power Systems

In order to utilize massive amounts of wind energy with the current and future power system, it is recommended that first the power grid be modernized by installing advance digital controls, power electronic switches, computerized controlling, monitoring, higher capacity transmission lines, etc. Such a power grid, as defined by the U.S. Department of Energy, is categorized as a smart grid and should have the following characteristics [105]:

1. Supplying a quality power for 21st century electric demands
2. Optimizing the operating efficiency
3. Dynamic self-correction capabilities to power disturbance and errors
4. Activating the customers' participation in demand response operating resiliency to physical and cyber attacks
5. Efficient usage of generations and storages
6. Providing new products, services, and markets
7. Smoothing transition ability for supplying loads form conventional power plants to renewable power systems

In this chapter, a method is presented for planning the grid power management for the next 24 hours. The method is based on adapting two uncertain quantities, weather and load. The following sections will describe the procedure for the implementation of this method.

5.2 Behavior of Power Plants on the Grid

Regarding the load demanded curve, power plant operation is conventionally broken down into different timescales ranging from seconds to days. Power plants that respond within minutes to load variations are partly loaded plants which respond through governor action. Power plants responding to this timescale are known as baseload providers. The peak load and intermediate provider in the timescale involves the plants that balance the load increasing and decreasing. This portion of timescale covers several minutes to several hours according to the demand on the basis of power pants operation strategies [106]. Figure 5-1 shows a typical timescale load demand curve.

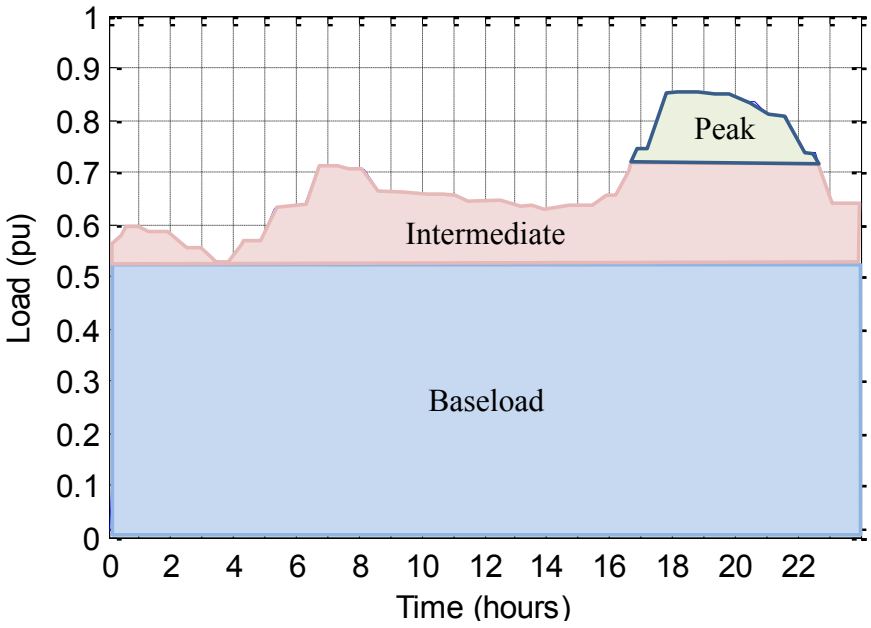

Figure 5-1.Timescale load demand in 24 hours

In general, baseload power plants involve large scale hydropower plants, coal power plants, gas power plants, and nuclear power plants. Except for scheduled maintenance or repairs, theses power plants will be on duty all the time. Since these power plants are slow to start up and shut down, they work more efficiency to provide baseload. Furthermore, the baseload power plants provide the majority of the power required by the grid.

On the other hand, the peak and intermediate loads are supplied by smaller power plants like diesel, oil or natural gas fired power plants. The behaviors of these power plants meet the requirement of the peak and intermediate load which occurred in periods and varies from time to time. These power plants can be brought online and shut down quickly.

In contrast to the other power plants, WECSs are not considered to serve baseload, peak, or intermediate loads as they produce power intermediately. However, these power systems can work as negative load to the power grid and reduce the total loads.

5.3 Load Forecasting and Customers Usage

Accurate data for electric power load forecasting is essential for operating and planning utility companies. The power industry requires forecasts for production as well as for financial perspective. It is necessary to predict hourly loads as well as daily peak loads. Accurate tracking of the load by the system generation at all times is a basic requirement in the operation of power systems and must be accomplished for various time intervals. Since electricity cannot be stored efficiency in large quantities, the amount of power generated at any given time must cover all the demand from consumers as well as grid losses [107].

Forecasts of the load are used to decide, under normal system operation, whether extra generation must be provided by increasing the output of online generators, by committing one or more extra units, or by the interchange of power with neighboring systems. Similarly, forecasts are used to decide whether the output of already running generation units should be decreased or shutoff.

Load forecasting can be divided into three categories: short, medium, and long term. Short-term forecasting usually starts from one hour to a week. Medium term forecasting is from a week to a year. The load forecasting longer than a year is counted as a long-term. For short-term load forecasting several factors should be considered such as time factors, weather data, and possible customers' classes. The medium and long terms of load forecasting take into account the historical load and weather data, the number of customers in different categories, the appliances in the area and their characteristic including age, the economic and demographic data and their forecasts, the appliance sales data, and other factors.

The time factor includes the time of the year, the day of the week, and the hour of the day. There are significant differences in load between weekdays and weekends. On the other hand, most electric utilities serve customers of different types such as residential, commercial, and industrial [108].

For the purpose of the proposal method for grid power management in this chapter, the short-term load forecasting is adapted to the grid power management process since the grid contains wind power systems. Usually, the prediction of generated power from the wind turbine is more accurate in a short-term rather than in a long-term at least with the current weather forecasting technologies.

There are different technologies available for modeling the short-term load forecasting. For instance, time series have long been used in load forecasting [107], the load forecasting output of artificial neural network as a model which is compensated by rough set theory for better accuracy [110], and the back propagation of neural network [111]-[113]. In general, the artificial neural network has been proven more reliable in prediction errors, but very large historical recorded data is required. Fuzzy logic technique, on the other hand, does not need huge historical recorded data for predicting process reported in [114]-[116].

The main objective of the short-term load forecasting is to advise dispatcher in making a decision to:

1. Supply load with stability aspect and consistence
2. Estimate full allocation
3. Determine operation constraints
4. Update the system
5. Determine equipment limitation, and
6. Power management between different power plants

In general, the best estimation of the short-term load forecasting process is collecting historical data. This data should be classified as day of the week, as weekends usually have lower load than other weekdays. Also, the coordinate temperature and weather condition, the season, and the day time of day should be classified. It should also be taken into account that load will increase each year as the number and types of customers are continuously changing [97]. A typical load forecasting and actual load are shown in Figure 5-2.

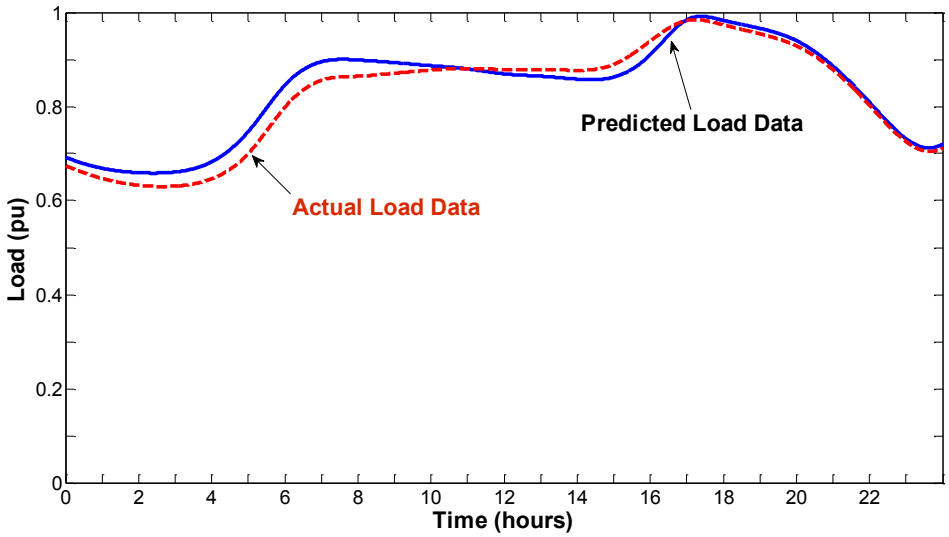

Figure 5-2. Hourly actual and predicted load data

5.4 Predicted and Actual Wind Power Generation

From (1.7) it was shown that the mechanical power of the wind turbine changes with the cube of the wind speed. In order to estimate the power that can be produced from the WECS, it is necessary to have sufficient information about wind data. The wind speed both predicted and actual recorded are given in Appendices A and B, respectively.

For the purpose of simplification, the wind data is not reconstructed according to the ARMA model which was given in section 1.5.3. Figure 5-3 shows the 24 hours wind speed both actual and predicted. Therefore, from using the MATAB simulation the actual and predicted generated powers from the WECS can be estimated. Based on the wind data in Figure 5-3, Figure 5-3 shows the difference between the actual and predicted powers of the WECS. The simulation is carried out on the DFIG wind turbine which has the following parameters' values; blade length (26 m), C_p (0.4), site location air density (1.23 Kg/m^3), generator efficiency (0.9), and neglecting the gear box losses.

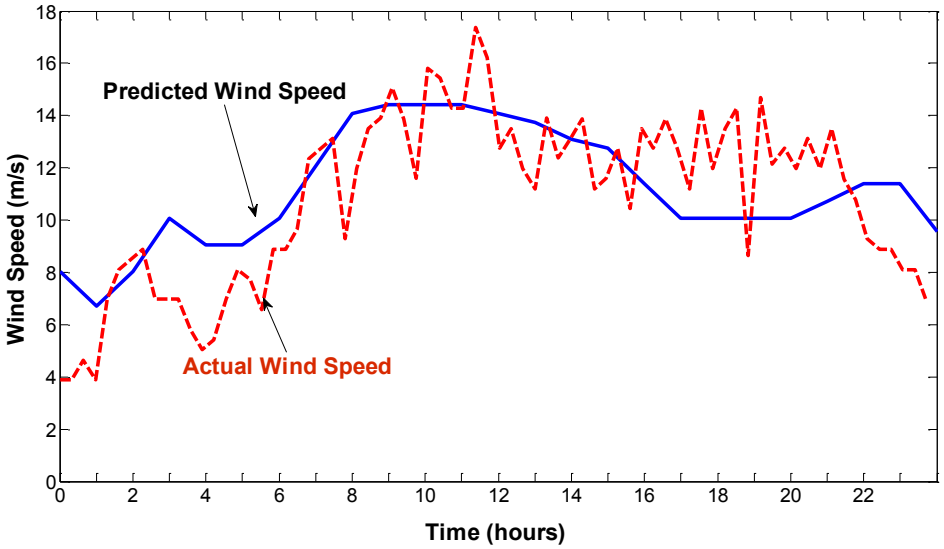

Figure 5-3. Predicted and actual wind speed observation

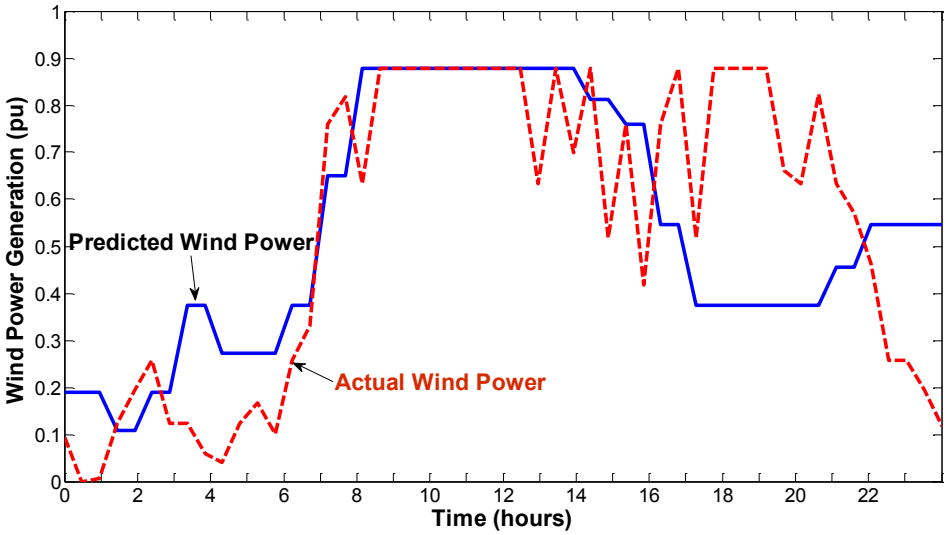

Figure 5-4. Predicted and actual wind power generation

5.5 Redistribution of the Load and Power Optimization of the Grid Power

5.5.1. Grid Power Balancing

In general, the power system requires equilibrium between power generations and loads. However, the reliable grid requires having a total installed capacity larger than the load demands. This extra capacity refers to a safe margin which ensures the guarantee for continuous supplying power to the grid when one or more units suddenly shut off due to faults or pulling a power plant from the network due to natural disasters. The grid installed capacity can be given by:

$$G = \sum_{i=1}^{n} PS_i \tag{5.1}$$

where G is the grid capacity, PS_i refers to the i^{th} power plant, and n represents the number of the power plants available on the system. The relation between generation and consumption can be giving by the following expression;

$$G \geq \sum_{j=1}^{m} L_j + Losses \tag{5.2}$$

where L_j is the load at pont j, m is the total load points on the grid, and Losses represent the summation of different system losses such as transmission lines loss, transformers losses, etc.

The vision of the future load demands L_j and the availability of the grid capacity G. Even for the short term it is very necessary to plan the load sharing between power plants. The grid capacity G depends not only on the installed number of power pants and their ratings, but also on multiple other factors. These factors are characteristics of the power plant, economic issues, availability of the power plants, weather and seasons, environmental issues, scheduled and unscheduled maintenances, etc. The variations of

these factors make the grid capacity to be inconstant. Grid management and central controlling require the study of all these factors to know the grid capacity. On the other hand, knowing in advance the behavior of the load is highly recommended for grid power management.

Furthermore, there is a steady increase of large-scale wind power systems in the grid. Therefore, the grid power management also requires predicting the generated power from these systems and adding them to the grid capacity. But the intermittence behavior of the power generation from WECSs makes merging their capacity to the capacities of the conventional power plants not an easy procedure. The power smoothing of wind energy conversion systems can be useful for the merging process, but let's consider an alternative method and assume the power smoothing has not been done on these systems. Therefore, one can detect that there are two variable quantities on the power systems, load and wind power, assuming all conventional power plants can provide stable and constant powers. The accurate detection of these variations highly depends on accurate forecasting methods. Since loads and wind power systems carry similar characteristics, let's consider merging the available capacity from the wind power systems to the other power plants capacities. Therefore loads and wind power systems can merge together and provide a new load demand curve (NLDC) to the grid. Therefore, (5.1) and (5.2) can be re-written such as

$$\sum_{i=1}^{n} PS_i \geq \sum_{j=1}^{m} L_j + Losses - P_W \tag{5.3}$$

where P_W represent the total power of the wind farm.

Assuming that all wind turbines in the wind farm receives the same wind speed, thus, wake effect is in its minimum influence. Therefore, the total power of the wind farm

can be represented by the total power than can be generated by a single wind turbine [54]-[57].

$$NDLC = \sum_{j=1}^{m} L_j - P_W \tag{5.4}$$

5.5.2. Technique of the Power Optimization

The procedure of the power optimization of the grid containing wind power systems can be described through the following algorithm steps [117]:

Step 1: Start

Step 2: Fetching grid information; such as the status of all power plants, the status of all wind farms, transmission line status, etc.

Step 3: Estimating the load data for a specific time frame; using an appropriated short-term load forecasting method for constructing load demand curve.

Step 4: If wind power systems provide significant contributions go to *Step5*, otherwise go to *Step 8*.

Step 5: Collecting the wind forecasting data for 24 hours ahead.

Step 6: Estimate the power generation of the wind power systems.

Step 7: Construct a new load demand curve (NLDC) using (5.4).

Step 8: From NLDC (or just load demand curve when no significant contributions from the wind farms).

Step 9: Set the baseload power plant(s) supplier, according to the variation of the load curve, arrange setting for all other power plants based on their types and capacities, and distribute the load sharing.

Step 10: Observe and monitor the performance of the system during real-time operation and respond to forecasting errors for re-distributing load sharing on all power plants.

Step 11: Go to *Step 2* for next time frame, next 24 hours.

Step 12: End

The corresponding procedure to the above steps and to continuous the load distribution and re-distribution is shown in Figure 5-5 [104]:

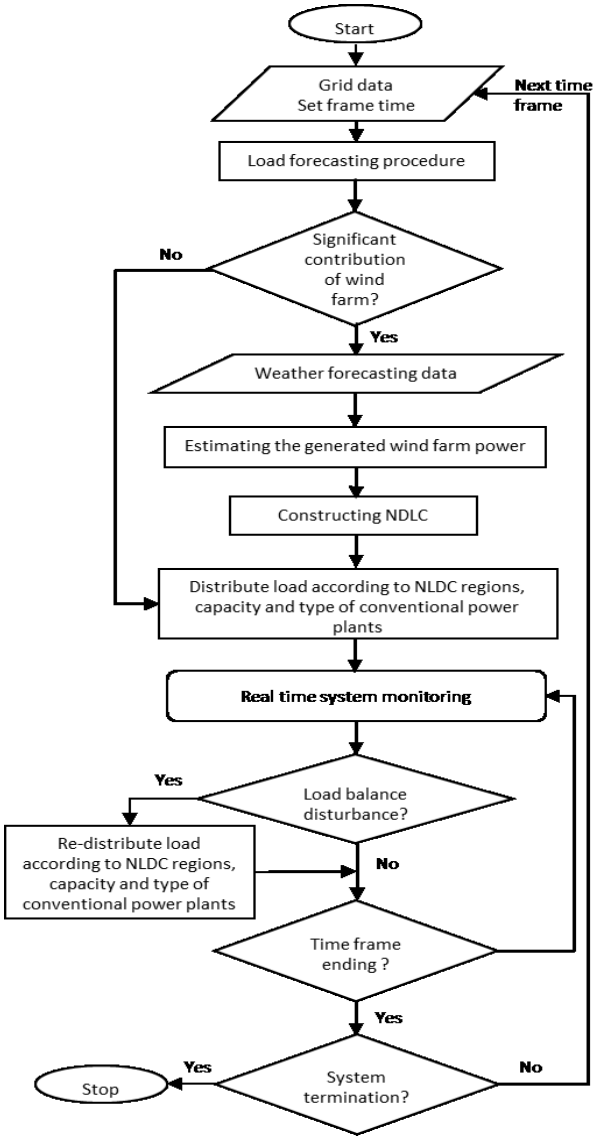

Figure 5-5. Flowchart of the system operation

5.5.3. Illustrative Example

For the sake of the explanation of the power management process, an illustrative example of a power system is presented (Figure 5-6) which has the loads given in Figure 5-2. The system is formed of the following power plants; steam power plant (Ps), hydropower plant (*Ph*), gas power plant (*Pg*), diesel power plant (*Pd*), and wind farm (*Pw*). Their ratings are shown on the diagram in Figure 5-6. The installed capacity of this system is;

$$G = Ps + Ph + Pg + Pd + Pw \tag{5.5}$$

With the giving installed capacity of each power plant, *G* is 1234 MVA.

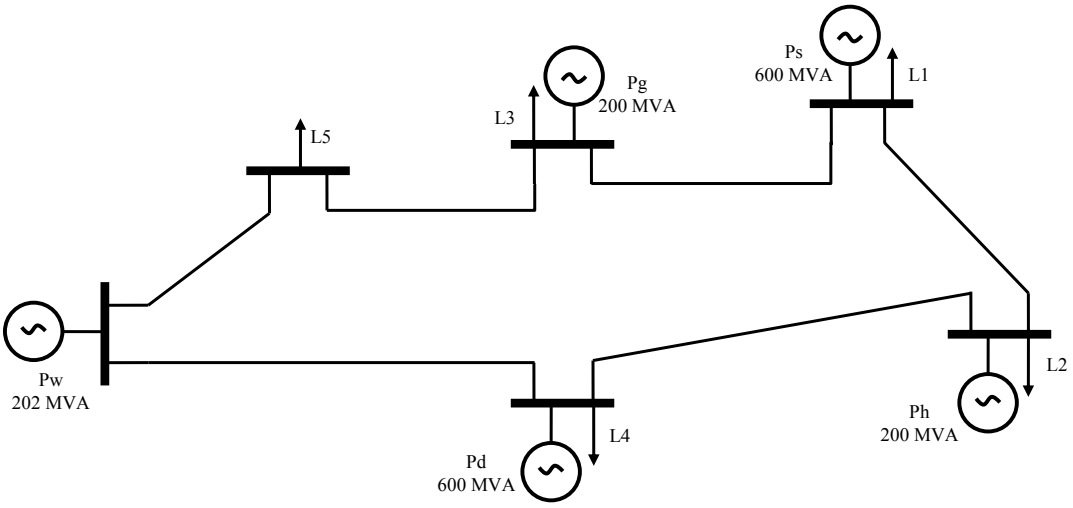

Figure 5-6. Illustrative example of grid diagram

From (5.4) the NLDC can be constructed for the base power of 1234 MVA and it is shown in Figure 5-7.

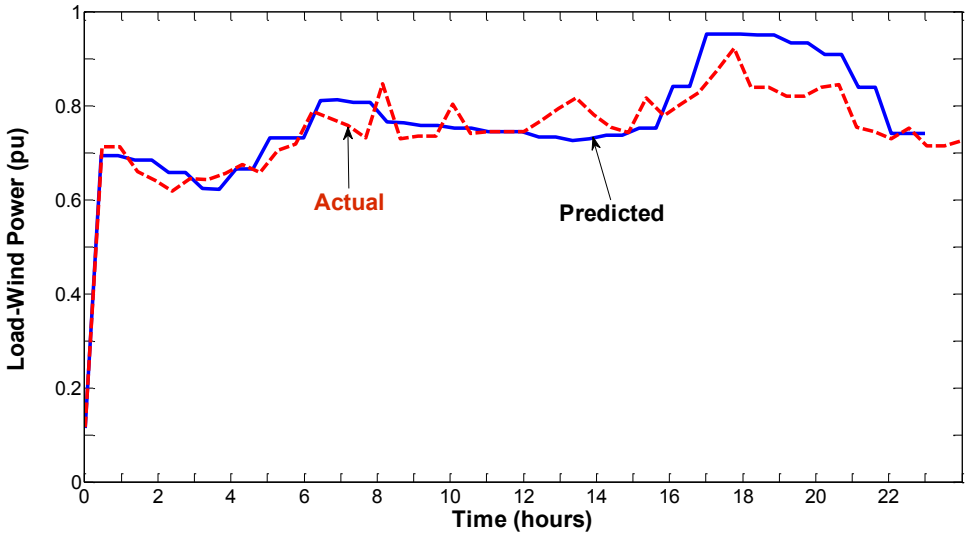

Figure 5-7. Actual and predicted NLDCs

Assuming that all power plants are available and operating under normal operating condition, and they share the load based on their ratings. Therefore, for this system, the load can be divided as the following;

$$\begin{aligned} Ps &= 600/200Ph \\ &= 600/200Pg \\ &= 600/32Pd \\ &= 600/202Pw \end{aligned} \tag{5.6}$$

and, from (5.5) and (5.6),

$$G = 2.05667Ps \tag{5.7}$$

Therefore, from (5.7) the maximum contribution of each power plant is given in Table 5-1.

Now, let Ps and Pg be the baseload provider. Therefore,

$$L_{\min} \geq Ps + Pg \tag{5.8}$$

Table 5-1. Contribution of Power Plants

Power Plant	Percentage of Contribution
Steam Power Plant, Ps	48.5
Hydropower Power Plant, Ph	16.2
Gas Power Plant, Pg	16.2
Diesel Power Plant, Pd	2.6
Wind Farm, Pw	16.4

where L_{min} is a minimum load value on NLDC. The distribution of the load will be given by

$$\begin{aligned} &L_{\min} = Ps + Pg \quad \text{if} \quad L_{\min} \le Ps + Pg \\ &\text{and}, \\ &L_{\min} = Ps + Pg + Ph + Pd \quad \text{if} \quad L_{\min} > Ps + Pg \end{aligned} \tag{5.9}$$

The baseload provider is 64.8%, which is greater than the L_{min}, where L_{min} is predicted to be 0.6 as detected from NLDC (Figure 5-6). Thus, from (5.9), the load sharing between *Ps* and *Pg* will be as the follows:

$$\begin{aligned} &L_{\min} = 4/3 Ps \\ &or, \\ &Ps = 0.75 L_{\min} \\ &Pg = 0.25 L_{\min} \end{aligned} \tag{5.10}$$

For $L_{min} = 0.6$;

Ps = 0.45 p.u. or 555.3 MVA, and

Pg=0.15 p.u or 185.1 MVA

However, these values for *Ps* and *Pg* will be constant as long as the following expression is true:

$$L(t) \ge Ps + Pg + Pd + Ph \tag{5.11}$$

5.5.4. Simulations and Results

Based on the algorithm in section 5.5.2 and following the procedures in previous section, a simulation using MATLAB software is carried on the power system which was shown in Figure 5-6. The system includes steam power plant, hydropower plant, diesel power plant, gas power plant, and a wind farm which consists of 122 DFIG-based WECSs each of 1.6 MVA. The simulations are run with two types of the wind speed and load data; predicted and actual. The results for each power plant are shown in Figures 5-8 to 5-13, respectively.

5.6 Discussion

In this chapter, the load forecasting and wind speed forecasting data were adapted into the power system which involves a significant contribution of the WECS. The case study implemented in the simulation consists of more than 15% of wind power in total of the grid power. The load distribution and re-distribution between different power plants gave the optimization of the generated power. Thus, the influence of the intermittent behavior of the wind power system is minimized through a good estimate of the upcoming 24 hours of wind and load forecasting data. The simulation results show the behavior of the steam and gas turbine while they supply baseload and other plants supply intermediate and peak loads. The achievement of the optimization has been successful since the grid previously planned for distribution loads, and the correction due to errors in forecasting take place without disturbance to the baseload or influencing the balance between generation and consumption. There is a slight difference between Figures 5-7 and 5-13 because of the losses in the system as indicated by (5.3).

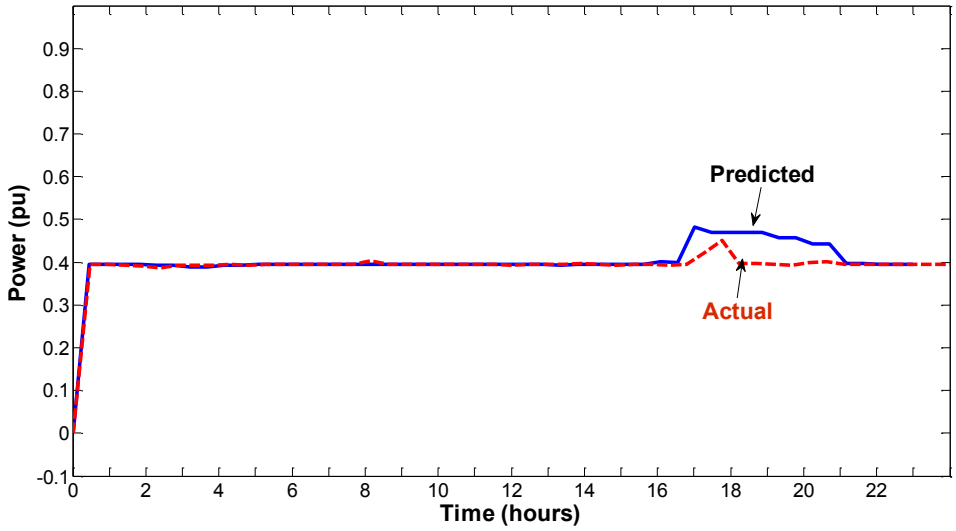

Figure 5-8. Steam Power Plant, *Ps*

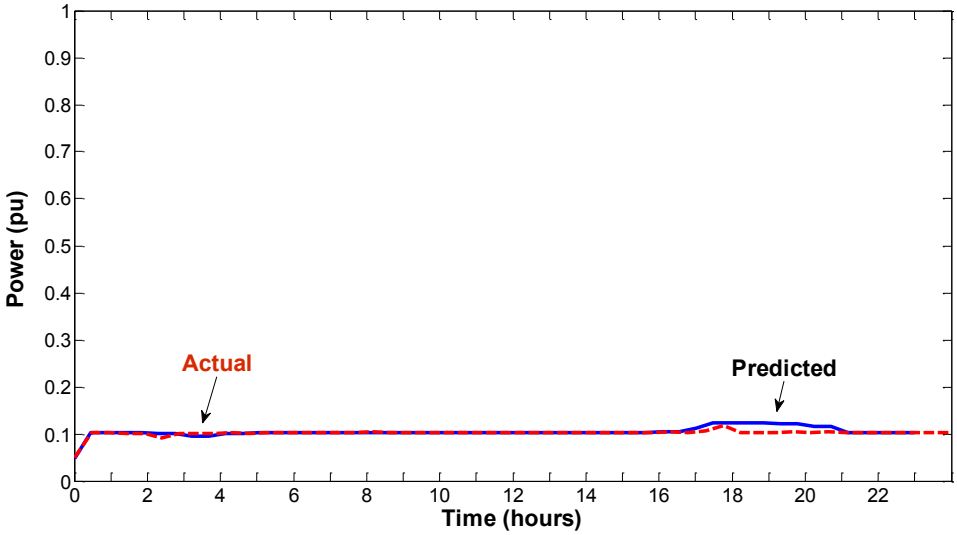

Figure 5-9. Gas Power Plant, *Pg*

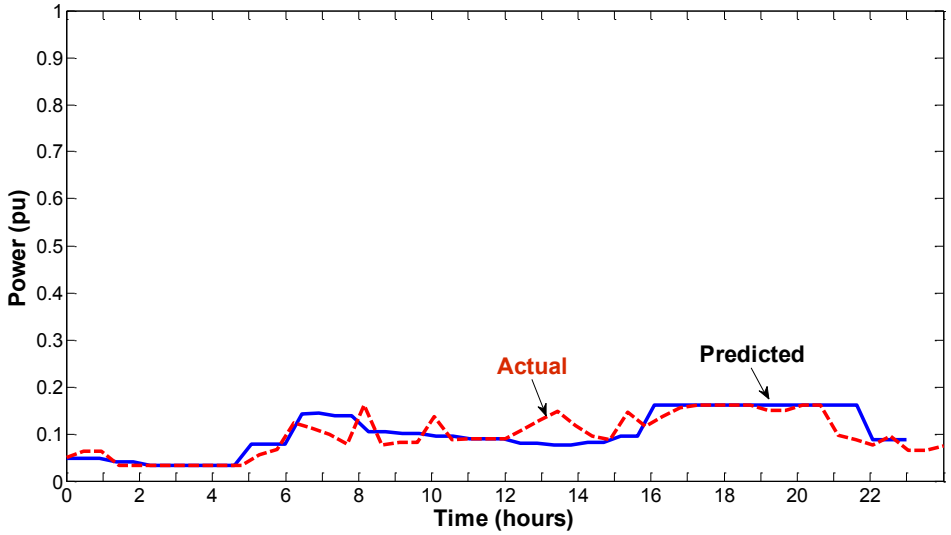

Figure 5-10. Hydropower Plant, *Ph*

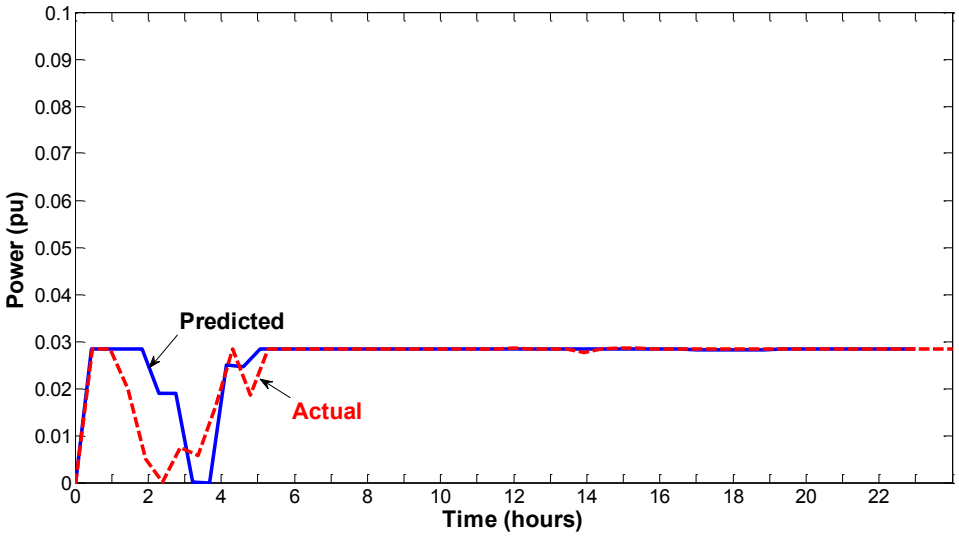

Figure 5-11. Diesel Power Plant, *Pd*

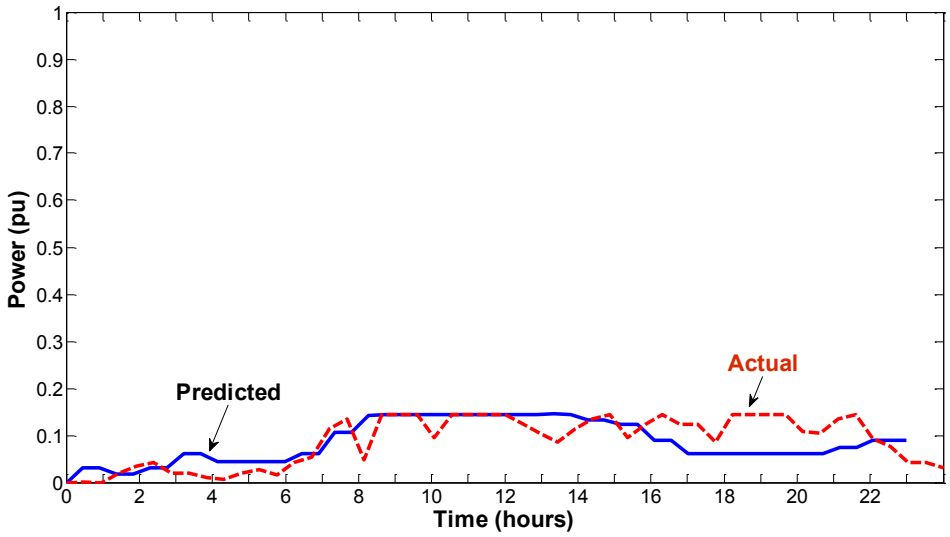

Figure 5-12. Wind farm, *Pw*

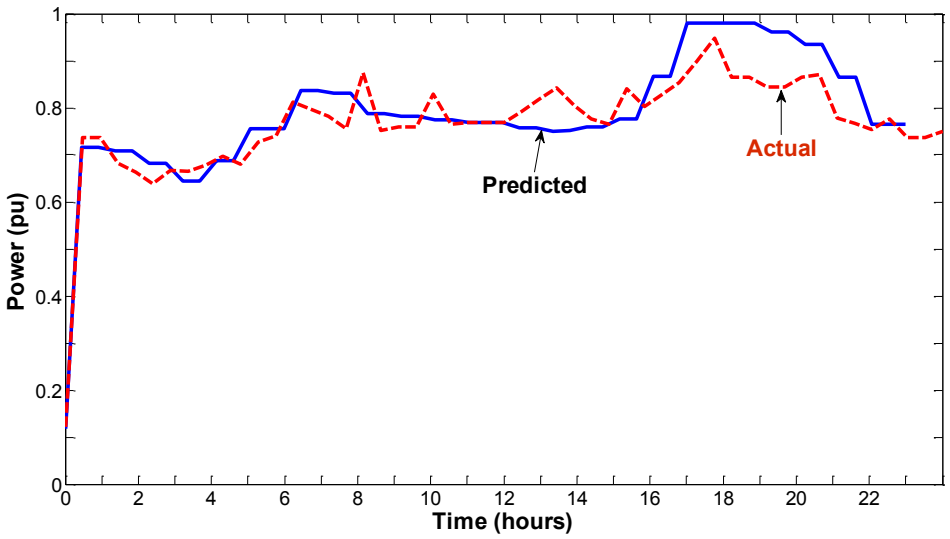

Figure 5-13. Total grid generated power

Chapter 6: Conclusions and Future Works

6.1 Conclusions

In this dissertation, the integration of large-scale wind power systems to the power grid has been studied. Due to the nature of wind energy, wind power systems can only generate irregular power to the system. Output power fluctuations and load supply problems of the wind power systems are the main problems caused by this power irregularity. These problems increase the grid instability, disturb the balance between power generation and consumption, influence the operations of other power plants influenced, etc.

In this research, different methods are presented and implemented for overcoming and eliminating the effects of these problems and for improving the performance of wind power systems to act more as conventional power plants. The major conclusions of these methods are highlighted as follows:

1. The de-loaded method is presented for power regulating and smoothing, which is based on the power characteristics of the wind turbine and short-term wind speed forecasting data. The method also gives the optimum power smoothing of the DFIG-based WECS.
2. The utilization of multiple-types of energy storages for reducing the power fluctuation and load supply of large-scale wind power systems in standalone and grid-connected systems has been presented. The method is different from the de-loaded technique in which wind power systems are operated under maximum tracking power points to capture as much power as possible from the wind energy. The BESS is used for suppressing these fluctuations,

while the PHSS is used for supporting the wind power systems in load supply. The simulation results showed that both types of energy storages, BESS and PHSS, can successfully reduce the fluctuations and load supply of the wind power systems in standalone and in grid-connected systems. The results also showed that the forecasting data, when compared with actual data for validating the application of the method, can be used for detecting the actual ratings of BESS and PHSS for any given wind farms.

3. The power management method has been presented to manage the grid power with an illustrative system and simulation results. The two fluctuated quantities, wind power and load, can be merged together and form a new load demand on the grid. Therefore, the sharing and distribution of the loads can be done through this new load demand and the capacity of each power plant on the grid.

4. The microprocessor embedded controller system is presented to optimize the operation of the wind power system. Monitoring, self-correction, and dynamical real time operation are done through high speed general purpose microprocessor. Furthermore, the microprocessor controller system provides the self-testing routine to ensure all components are functioning correctly, and provides safe shut off in the case that malfunctions are indicated. Overall, the implementation microprocessor is enhancing the power management and performance of the wind power systems.

Overall, the presented methods in this dissertation improve the performance of the DFIG-based WECS and enhance the integration of large-scale wind power systems to the power grid and share loads like other conventional power plants.

6.2 Future Works

The integration of large-scale wind power systems to the power grid can be investigated more to include different types of system faults, transient behavior during system voltage sags/swells, etc. More advanced studies are still needed to achieve a standard wind farm model as wind farms are expanded to include more WECS units than currently available.

This work can be extended to include the power management planning for longer periods when the accurate weather forecasting becomes available for medium and long terms. Also, other renewable energy sources can be included as they gain more focus, such as solar energy. The photovoltaic power systems also have the power fluctuations' problem and the same procedures of the wind power systems with some modifications can be applied to them to produce constant power.

References

[1] S. K. Khadem, M. Basu and M. F. Conlon, "Power Quality in Grid connected Renewable Energy Systems: Role of Custom Power Devices," *International Conference on Renewable Energies and Power Quality (ICREPQ'10),* Granada, Spain, 23rd-25th ,2010

[2] Wei Qiao; Harley, R.G., "Grid Connection Requirements and Solutions for DFIG Wind Turbines," *Energy 2030 Conference, 2008. ENERGY 2008. IEEE,* pp.1,8, 17-18 Nov. 2008

[3] REN21.2012. Renewables Global Status Report, 2012, available online at www.ren21.net

[4] International Energy Outlook 2011, Independent Statistics and Analysis, U.S. Energy Information Administration, September, 2011, Report Number DOE/EIA-0484(2011)

[5] B. Kirby, J. Kueck, H. Leake, and M. Muhlhiem, "Nuclear generating stations and transmission grid reliability," *39th North American Power Symposium, NAPS'07*, 12 December 2007

[6] Annual Energy Outlook with projections to 2035, U.S. Energy Information Administration, U.S. Department of Energy, April, 2011, Report No. DOE/EIA-0383,2011

[7] 20% wind energy by 2030 Increasing Wind Energy's Contribution, US Department of Energy, U.S. Electricity Supply, Report No. DOE/GO-102008-1567, July 2008.

[8] Global Wind Energy Council, 2006 report available online at: http://www.gwec.net

[9] Olken, M, "The rise of the sun," *IEEE Power and Energy Magazine*, vol.7, issue 3, pp.4, 2009

[10] Technology Roadmap Solar photovoltaic energy, International Energy Agency, 2010, OECD/IEA, May, 2010 Available online at: http://www.iea.org/publications/freepublications/publication/pv_roadmap.pdf

[11] A. Hansen and L. Hansen, "Market penetration of wind turbine concepts over the years," *in Proc. European Wind Energy Conference and Exhibition 2007(EWEC 2007)*, Milan, Italy, May 2007

[12] Luna, A., Lima, F.K.A., Santos, D., Rodriguez, P., Watanabe, E.H., Arnaltes, S., "Simplified Modeling of a DFIG for Transient Studies in Wind Power

Applications," *Industrial Electronics, IEEE Transactions on* , vol.58, no.1, pp.9,20, Jan. 2011

[13] Endusa Billy Muhando, Tomonobu Senjyu, Aki Uehara, Toshihisa Funabashi, and Chul-Hwan Kim, "LQG Design for Megawatt-Class WECS With DFIG Based on Functional Models' Fidelity Prerequisites," *IEEE Trans. on Energy Conversion*, vol. 24, no. 4, pp. 893-904, Dec. 2009

[14] L.S.T. Ackermann, "Wind Energy Technology and current status. A Review", *Renewable and Sustainable Energy Review*, 4:315-375, 2000

[15] S.M. Barakati, M. Kazerani, and J.D. Aplevich, "Maximum power traking control for a wind turbine system including a matrix converter," *IEEE Trans. On Energy Conversion*, vol. 24, no. 3, September 2009

[16] Hugh Sharman, Bryan Leyland, and Martin Livermore," Renewable Energy Vision or Mirage?" *Adam Smith Research Trust*, London, 2011

[17] Lange M, Focken U, "Physical Approach to Short-Term Wind Power Prediction," *Springer-Verlag*: Berlin, Heidelberg, 2006

[18] A. Kusiak, H., Y. Zheng, and Z. Song, "Wind Farm Power Prediction: A Data-MiningApproach," *Wind Energy*, vol. 12, no. 3, pp. 275–293, 2009

[19] AccuWeather, Inc, 2011, http://www.accuweather.com/

[20] Weather Underground, 2011, http://www.wunderground.com

[21] M. Magnusson and A., S. Smedman, " Air flow behind wind turbines," *Journal of wind engineering and industrial aerodynamics*, vol. 89, pp. 169-189, 1999

[22] Moskalenko, N., Rudion, K., Orths, A., "Study of wake effects for offshore wind farm planning," *Modern Electric Power Systems (MEPS), 2010 Proceedings of the International Symposium* , vol., no., pp.1,7, 20-22 Sept. 2010

[23] D. Joshi, K. S. Sndhu, M. K. Soni, "Constant voltage constant frequency operation for a self-excited induction generator," *IEEE Transactions on Energy Conversion,* issue: 1, vol.21, pp. 228-234, March 2006

[24] Gipe, Paul, "Wind Power, Revised Edition: Renewable Energy for Home, Farm, and Business," *Chelsea Green Publishing Company*; Rev Exp edition, 2004

[25] Sangshin Kwak, and Hamid Toliyat," An Approach to Fault-Tolerant Three-Phase Matrix Conveter Drives," *IEEE Transactions on Energy Conversion*, vol. 22, no. 4, December 2007

[26] Ching-Tsai Pan, and Yu-Ling Juan," A Novel Sensorless MPPT Controller for a High-Efficiency Microscale Wind Power Generation System," *IEEE Transactions on Energy Conversion*, vol. 25, no. 1, March 2010

[27] Yasser Mohamed, Ehab El-Saadany, and Magdy Salama," Adaptive Grid-Voltage Sensorless Control Scheme for Inverter-Based Distributed Generation," *IEEE Transactions on Energy Conversion*, vol. 24, no. 3, June 2009

[28] Yateendra Mishra, S. Mishra, Fangxing Li, Zhao Yang Dong, and Ramesh Bansal," Small-Signal Stability Analysis of a DFIG-Based Wind Power System Under Different Modes of Operation," *IEEE Transactions on Energy Conversion*, vol. 24, no. 4, December 2009

[29] Mohammad Marwali, Jin-Woo Jung, and Ali Keyhani," Stability Analysis of Load Sharing Control for Distributed Generation Systems," *IEEE Transactions on Energy Conversion*, vol. 22, no. 3, June 2007

[30] Bhim Singh, S. S. Murthy, and Sushma Gupta," Analysis and Design of Electronic Load Controller for Self-Excited Induction Generators*," IEEE Transactions on Energy Conversion*, vol. 21, no. 1, June 2006

[31] Shu Fan, James Liao, Ryuichi Yokoyama, Luonan Chen, and Wei-Jen Lee," Forecasting the Wind Generation Using a Two-Stage Network Based on Metrological Information*," IEEE Transactions on Energy Conversion*, vol. 24, no. 2, June 2009

[32] Andrew Kusiak, Zhe Song, and Haiyang Zheng, "Anticipatory Control of Wind Turbine with Data- Driven Predictive Models*," IEEE Transactions on Energy Conversion*, vol. 24, no. 3, September 2009

[33] Lulian Munteanu, Antoneta Bratcu, Seddik Bacha, Daniel Roye, and Joel Guiraud, "Hardware-in the- Loop-based Simulator for a Class of Variable-speed Wind Energy Conversion Systems: Design and Performance Assessment," *IEEE Transactions on Energy Conversion*, vol. 25, no. 2, June 2010

[34] Lingling Fan, Subbaraya Yuvarajan, and Rajesh Kavasseri," Harmonic Analysis of a DFIG for a Wind Energy Conversion System," *IEEE Transactions on Energy Conversion*, vol. 25, no. 1, March 2010

[35] Seyed Dehghan, Mustafa Mohamadian, and Ali Varjani, "A New Variable-Speed Wind Energy Conversion System Using Permanent-Magnet Synchronous Generator and Z-Source Inverter," *IEEE Transactions on Energy Conversion*, vol. 24, no. 3, September 2009

[36] Nitin Joshi, and Ned Mohan, " A Novel Scheme to Connect Wind Turbines to the Power Grid*," IEEE Transactions on Energy Conversion*, vol. 24, no. 2, June 2009

[37] P.M. Jesus, Edgardo Castronuovo , and M. T. Leao, "Reactive Power Response of Wind Generation under an Incremental Network-Loss Allocation Approach," *IEEE Transactions on Energy Conversion*, vol. 23, no. 2, June 2008

[38] Miguel Montilla-DJesus, David Santos-Martin, Santiago Arnaltes, and Edgardo Castronuovo, "Optimal Operation of Offshore Wind Farms with Line-Commutated HDVC Link Connection," *IEEE Transactions on Energy Conversion*, vol. 25, no. 2, June 2010

[39] S.M. Muyeen, Rion Takahashi, Toshiaki Murata, and Junji Tamura, "Integration of an Energy Capacitor System with a Variable-Speed Wind Generator," *IEEE Transactions on Energy Conversion*, vol. 24, no. 3, September 2009

[40] Luis Ochoa, Antonio Padilha-Feltrin, and Gareth P. Harrison, "Time-Series – Based Maximization of Distributed Wind Power Generation Integration," *IEEE Transactions on Energy Conversion*, vol. 23, no. 3, September 2008

[41] Diwakar Joshi, and Suresh Jangamshetti," A Novel Method to Estimate the O & M Costs for the Financial Planning of the Wind Power Projects Based on Wind Speed - A Case Study," *IEEE Transactions on Energy Conversion*, vol. 25, no. 1, March 2010

[42] David McMillan, and Graham Ault, "Techno-Economic Comparison of Operational Aspects for Direct Drive and Gearbox-Driven Wind Turbines," *IEEE Transactions on Energy Conversion*, vol. 25, no. 1, March 2010

[43] Nayeen Rhmat Ullah, Kankar Bhattacharya, and Torbjom Thrininger, "Wind Farms as a Reactive Power Ancillary Service Providers – Technical and Economic Issues," *IEEE Transactions on Energy Conversion*, vol. 24, no. 3, June 2009

[44] Renewable Energy World, "EC&R Completes 780-MW Roscoe Wind Farm," October 2 2009. [Online]. Available: http://www.renewableenergyworld.com

[45] J. Conroy and R. Watson, "Aggregate modeling of wind farms containing full-converter wind turbine generators with permanent magnet synchronous machines: Transient stability studies," *IET Renewable Power Generation*, vol. 3, no. 1, pp. 39-52, 2009

[46] A. Perdana, S. Uski-Joutsenvou, O. Carlson, and B. Lemstrom, "Comparison of an aggregated model of a wind farm consisting of fixed-speed wind turbines with field measurement," *Wind Energy*, vol. 11, no. 1, pp. 13-27, 2008

[47] V. Akhmatov, "An aggregated model of a large wind farm with variable speed wind turbines equipped with doubly-fed induction generators," *Wind Engineering*, vol. 28, no. 4, pp. 479-486, 2004

[48] Zhou, H. Q., Song, Z. P., Wang, J. P., Xue, Y., "A Review on Dynamic Equivalent Methods for Large Scale Wind Farms," *Power and Energy Engineering Conference (APPEEC), Asia-Pacific* , pp.1,7, 25-28, March 2011, IEEE Conference Publisher 2011

[49] Yang Yongbo, Jiang Bo, Yang Huayun, Ai Bing; Zha Xiaoming, "Aggregating DFIGS in power system online analysis," *Power Engineering and Automation Conference (PEAM), 2011 IEEE* , vol.2, no., pp.63,67, 8-9 Sept. 2011

[50] Yongbo Yang; Xiaoming Zha, "Aggregating wind farm with DFIG in power system online analysis," *Power Electronics and Motion Control Conference, 2009. IPEMC '09. IEEE 6th International* , pp.2233,2237, 17-20 May 2009

[51] L.M. Fernández, C.A. García, J.R. Saenz, F. Jurado, "Equivalent models of wind farms by using aggregated wind turbines and equivalent winds," *Energy Conversion and Management*, vol. 50, Issue 3, March 2009, pp. 691–704

[52] Xu ZhenHua, Li Xinran, Hu LongHui, Li JinXin, "Aggregation of doubly-fed induction generator based wind farm considering storage device and coordinated control strategy," *Advanced Power System Automation and Protection (APAP), 2011 International Conference on* , vol.2, no., pp.1013,1018, 16-20 Oct. 2011

[53] Shu-Chen Wang, Pei-Hwa Huang, "Fuzzy c-means clustering for power system coherency," *Systems, Man and Cybernetics, 2005 IEEE International Conference on* , vol.3, no., pp.2850,2855 Vol. 3, 10-12 Oct. 2005

[54] Daye Yang, Liangeng Ban, Zutao Xiang, Ning Du, Bin Zheng; Zipng Wu, "An aggregation method of wind farm model for electromagnetic transient simulation analysis," *Power Electronics and Machines in Wind Applications (PEMWA), 2012 IEEE* , vol. 1, no. 5, pp. 16-18, July 2012

[55] Li Lin, Kui Ding, Juan Tan, Ningbo Wang, Yanhong Ma, "Coherency-based dynamic equivalence method for power system centralized large scale wind power," *Power System Technology (POWERCON), 2012 IEEE International Conference on*, pp.1-6, Oct. 30 2012-Nov. 2 2012

[56] Ben Kilani, K., Elleuch, M., "Simplified modelling of wind farms for voltage dip transients," *Systems, Signals and Devices (SSD), 2012 9th International Multi-Conference on*, pp.1-6, March 20-23, 2012

[57] Meng, Z. J., Xue, F., "Applications of the Equivalent Wind Method for the Aggregation of DFIG Wind Turbines," *Power and Energy Engineering Conference (APPEEC), 2011 Asia-Pacific*, pp.1-4, March 25-28, 2011

[58] S. Fan, J. R. Liao, R. Yokoyama, L. Chen, and Wei-Jen L, " Forecast the wind generation using a two-stage network based on metrological information," *IEEE Transactions on Energy Conversion*, vol. 24, no. 2, June 2009

[59] A European team work, Kariniotakis, G., et al, "Next generation forecasting tools for the optimal management of wind generation," *Peer reviewed, 2006 PMAPS Conference IEEE, 'Probabilistic Methods Applied to Power Systems'*, Stockholm, Sweden, June 2006

[60] C. Dica, Camelia-loana Dica, Deniela Vasiliu, Gh. Comanescu, and Monica Ungureanu, "Wind power short-term forecasting system," *IEEE Bucharest Power Tech Conference*, June 28th – July 2nd, Bucharest, Romania, 2009

[61] R. Cardenas, R. Pena, G. Asher, and J. Clare, "Power smoothing in wind generation systems using a sensorless vector controlled induction machine driving a flywheel," *IEEE Trans. Energy Convers*, vol. 19, no. 1, pp. 206–216, Mar. 200

[62] L. Ran, J. R. Bumby, and P. J. Tavner, "Use of turbine inertia for power smoothing of wind turbines with a DFIG," *in Proc. 11th Int. Conf. Harmonics Quality Power*, Sep. 2004, pp. 106–111

[63] Changling Luo, Hadi Banakar, Baike Shen, and Boon-Teck Ooi, "Strategies to Smooth Wind Power Fluctuations of Wind Turbine Generator," *IEEE Transactions On Energy Conversion*, vol. 22, no. 2, June 2007, pp. 341-350

[64] Pao, Lucy Y.; Johnson, K.E., "A tutorial on the dynamics and control of wind turbines and wind farms," *American Control Conference, 2009. ACC '09*, pp.2076-2089, June 10-12, 2009

[65] Bottu, M., Crow, M.L., Elmore, A.C., "Design of a Conditioner for smoothing wind turbine output power," *North American Power Symposium (NAPS)*, pp 26-28, Sept. 2010

[66] Sheikh, M. R I, Muyeen, S. M., Takahashi, R., Tamura, J., "Smoothing control of wind generator output fluctuations by using superconducting Magnetic Energy Storage unit," *Electrical Machines and Systems, 2009. ICEMS 2009. International Conference on*,pp.1-6, Nov. 15-18, 2009

[67] Esmaili, A, Nasiri, A," Energy storage of short-term and long-term wind energy support," *IECON 2010 - 36th Annual Conference on IEEE Industrial Electronics Society*, pp. 3281 – 3286 , 2010

[68] Ogimi, K, et al, "A study on optimum capacity of battery energy storage system for wind farm operation with wind power forecast," *IEEE 15th International Conference on Harmonics and Quality of Power (ICHQP)*, pp. 118 – 123, 2012

[69] Yoshimoto, K., Nanahara, T., and Koshimizu, G.," New control model for regulation state-of-charge of a battery in hybrid wind power/battery energy storage system," *IEEE PES Power Systems Conference and Exposition, PSCE '06*, pp. 1244 – 1251, 2006

[70] N. A. Janssens, G. Lambin, and N. Bragard, "Active Power Control Strategies of DFIG Wind Turbines, " *IEEE Power Tech 2007, Lausanne (Switzerland)*, 1-5 July 2007

[71] Kaiser R.," Optimized battery-management system to improve storage lifetime in renewable energy systems," *Journal of Power Sources, 168 (1 SPEC. ISS.)*, pp. 58-65, 2007

[72] M. H. Ali, Bin Wu, and R. A. Dougal, "An Overview of SMES Applications in Power and Energy Systems, " *IEEE Transactions On Sustainable Energy*, vol. 1, no. 1, pp. 38-48, April 2010

[73] Cesar A. S. Monry, "Operation of Energy Storage in Power Systems with High Wind Penetration, " *PhD dissertation, University of Washington*, USA, 2011

[74] K. E. Johnson, L. Y. Pao, M. J. Balas, and L. J. Fingersh, "Control of variable-speed wind turbines: Standard and adaptive techniques for maximizing energy capture," *IEEE Control Syst. Mag*., vol. 26, no. 3, pp. 70–81, Jun. 2006

[75] L. Zhang, H. Li, C. E, J. Li, and H. Xu, "Pitch control of large scale wind turbine based on fuzzy-PD method," *in Proc. Int. Conf. Electric Utility Deregulation Restructuring Power Technol*., Nanjing, China, 2008, pp. 2447–2452

[76] H. Geng and G. Yang, "Robust pitch controller for output power leveling of variable-speed variable-pitch wind turbine generator systems," *IET Renewable Power Generation*, vol. 3, no. 2, pp. 168–179, Jun. 2009

[77] Pan, T., Ji, Z., Jiang, Z., " Maximum power point tracking of wind energy conversion systems based on sliding mode extremum seeking control.," *In Proceedings of IEEE Energy 2030*, Atlanta, GA, USA, 17–18 November 2008, pp. 1–5

[78] De Almeida, R.G., Peas Lopes, J.A., "Participation of Doubly Fed Induction Wind Generators in System Frequency Regulation," *Power Systems, IEEE Transactions on* , vol.22, no.3, pp.944,950, Aug. 2007

[79] " Interim report- System Disturbance on 4 November 2006," *Union for the Co-ordination of Transmission of Electricity*, Brussels, Belgium, 2006

[80] S. Heier, " Grid Integration of Wind Energy Conversion Systems*," 2nd Edition, Wiley*, England,2006

[81] Fadhil T. Aula and Samuel C. Lee, "Power fluctuation reduction methodology for the grid-connected renewable power systems," *Proc. SPIE 8688, Active and Passive Smart Structures and Integrated Systems 2013, 86881W* ,April 10, 2013

[82] Hatta, T., "Applications of sodium-sulfur batteries," *Transmission and Distribution Conference and Exposition (T&D), 2012 IEEE PES*, pp. 1-3, 2012

[83] Boyle, G., "Renewable energy: Power for a sustainable future," *Third Ed., Oxford University Press*, USA, 2012

[84] J.P. Deane, B.P. Ó Gallachóir, E.J. McKeogh, "Techno-economic review of existing and new pumped hydro energy storage plant," *Renewable and Sustainable Energy Reviews,* vol. 14, Issue 4, May 2010, pp. 1293-1302

[85] Guzman, Humberto A. R., "Value of Pumped-Storage Hydro for Wind Power Integration in the British Columbia Hydroelectric System," *MScE Thesis, University of British Columbia*, 2010

[86] John S. Anagnostopoulos, Dimitris E. Papantonis, "Study of pumped storage schemes to support high RES penetration in the electric power system of Greece," *Energy*, vol. 45, Issue 1, September 2012, pp. 416-423

[87] Dimitris Al. Katsaprakakis, Dimitris G. Christakis, Arthouros Zervos, Dimitris Papantonis, Spiros Voutsinas, " Pumped storage systems introduction in isolated power production systems," *Renewable Energy*, vol. 33, Issue 3, March 2008, pp. 467-490

[88] M. Ali, I. Ilie, J. V. Milanović, and G. Chicco," Wind Farm Model Aggregation Using Probabilistic Clustering," *IEEE Transactions ON Power Systems*, vol. 28, no. 1, pp. 309-316, February 2013

[89] Jenkins, G. M. and Box, G. E. P, "Time Series Analysis: Forecasting and control, "*Prentice Hall,* New Jersey, 1970

[90] Qingle, P. and Min, Z. ," Very Short-Term Load Forecasting Based on Neural Network and Rough Set," *2010 International Conference on Intelligent Computation Technology and Automation*, vol. 3 , 2010

[91] Bakirtzis, A. G et al, "A Neural Network Short-Term Load Forecasting Model for the Greek Power System." *IEEE Transactions on Power Systems*, 11:858 – 863, 1996

[92] Papalexopoulos, A. D., Hao, S., and Peng, T. M., "An Implementation of a Neural Network Based Load Forecasting Model for the EMS. " *IEEE Transactions on Power Systems,* 9:1956 –1962, 1994

[93] Khotanzad, A. et al, "ANNSTLF-A Neural Network-Based Electric Load Forecasting System. " *IEEE Transactions on Neural Networks,* 8:835 –846, 1997

[94] Chen, H., Canizares, C. A., and Singh, A.,"ANN Based Short-Term Load Forecasting in Electricity Markets." *Proceedings of the IEEE Power*

Engineering Society Transmission and Distribution Conference, 2:411 –415, 2001

[95] Baharudin, Z., Jamaluddin, M. F., and Saad, N., "Fuzzy Logic Technique for Short Term Load Forecasting," *BICET Brunei Darussalam*, 2005

[96] Baharudin, Z., Saad, N., and Ibrahim, R., "A Fuzzy Logic Technique for Short Term Load forecasting." *2nd ICAIET Sabah Malaysia*, 2003

[97] PJM Interconnection LLC, www.pjm.com

[98] National Renewable Energy Laboratory, U.S. Department of Energy, U.S. Energy Information Administration (EIA), March 2012, Available online at: http://www1.eere.energy.gov/wind/wind_how.html http://www.eia.gov/energyexplained/index.cfm?page=wind_electricity_generation

[99] Fadhil T. Aula and Samuel C. Lee, "Weather Adaptive Renewable Energy Based Self Correctional Dynamic Power System for 2020 and Beyond," *21st International Conference on Systems Engineering, ICSEng 2011*, Las Vegas, Nevada, USA, 2011

[100] L. E. Kean, "Microcontroller to Intel® architecture conversion: programmable logic controller using Intel® Atom ™ Processor," *Intel Corporation*, 2010

[101] Embedded Intel Solution, winter 2011, Available online at: http://www.embeddedintel.com/

[102] Intel® Atom™ Processor N270 for Embedded Computing, Intel in Embedded and Communication, 2008: Intel.com/go/embedded

[103] G. Deyoung, "Erotech's low power Intel® Atom ™ based catalyst module design: The industry's lowest power Intel® Atom ™ based modules," Whitepaper, Eurotech, 2012

[104] Fadhil T. Aula and Samuel C. Lee, "Grid Power Optimization Based on Adapting Load Forecasting and Weather Forecasting for System Which Involves Wind Power Systems," *Smart Grid and Renewable Energy, Scientific Research*, vol.3, no. 2, pp. 112-118, May 2012

[105] United States Department of Energy, "Smart Grid", available at: www.oe.energy.gov/smartgrid.htm

[106] L. Freris and D. Infield, "Renewable Energy in Power Systems," *John Wily and Sons, Ltd,* 2008

[107] M. Espinoza, J. Suykens, R. Belmans, and B. De Moor, "Electric Load Forecasting Using Kernel-Based Modeling," *IEEE Control Systems*, vol. 27, Issues 5, 2007

[108] H.L. Willis, "Spatial Electric Load Forecasting," *Marcel Dekker*, New York, 1996

[109] G. E. P Box and G. M. Jenkins, "Time Series Analysis: Forecasting and control," *Prentice Hall*, New Jersey, 1970

[110] P. Qingle and Z. Min ," Very Short-Term Load Forecasting Based on Neural Network and Rough Set," *2010 In-ternational Conference on Intelligent Computation Tech-nology and Automation*, vol. 3, 2010

[111] A. G. Bakirtzis, V. Petridis, S J. Kiartzis, M. C. Alexiadis, and A. H. Maissis, "A Neural Network Short-Term Load Forecasting Model for the Greek Power System," *IEEE Transactions on Power Systems*, 11:858 –863, 1996

[112] D. Papalexopoulos, S. Hao, and T. M. Peng , "An Imple-mentation of a Neural Network Based Load Forecasting Model for the EMS," *IEEE Transactions on Power Systems*, vol. 9:1956 –1962, 1994

[113] Khotanzad, R. A. Rohani, T. L. Lu, A. Abaye, M. Davis, and D. J. Maratukulam, "ANNSTLF-A Neural Net-work-Based Electric Load Forecasting System*," IEEE Transactions on Neural Networks*, 8:835 –846, 1997

[114] H. Chen, C. A. Canizares, and A. Singh, "ANN Based Short-Term Load Forecasting in Electricity Markets," *Proceedings of the IEEE Power Engineering Society Transmission and Distribution Conference*, 2:411 –415, 2001

[115] Z. Baharudin, M. F. Jamaluddin, and N. Saad, "Fuzzy Logic Technique for Short Term Load Forecasting," *BICET Brunei Darussalam*, Aug 2005

[116] Z. Baharudin, N. Saad, and R. Ibrahim, "A Fuzzy Logic Technique for Short Term Load forecasting," *2nd ICAIET Sabah Malaysia*, 2003

[117] Fadhil T. Aula and Samuel C. Lee, "An operational power management method for the grid containing renewable power systems utilizing short-term weather and load forecasting data," *Proc. SPIE 8692, Sensors and Smart Structures Technologies for Civil, Mechanical, and Aerospace Systems 2013*, 86924O, April 19, 2013

Appendix A: Wind Forecasting Data

Weatherford Wind Energy Center
Weatherford, OK 73096

Location	Latitude: 35.5261633	
	Longitude: -98.7075744	
Recording Date	12/4/2011	Forecasting one day ahead
Time (hour)	Wind (mph)	Wind (m/s)
0	12	10.73
1	10	8.94
2	12	10.73
3	15	13.41
4	13.5	12.07
5	13.5	12.07
6	15	13.41
7	18	16.09
8	21	18.78
9	21.5	19.22
10	21.5	19.22
11	21.5	19.22
12	21	18.78
13	20.5	18.33
14	19.5	17.43
15	19	16.99
16	17	15.20
17	15	13.41
18	15	13.41
19	15	13.41
20	15	13.41
21	16	14.31
22	17	15.20
23	17	15.20

Appendix B: Wind Actual Data

Weatherford Wind Energy Center
Weatherford, OK 73096

Location	Latitude:	35.5261633
	Longitude:	-98.7075744
Recording Date	12/5/2011	

Time (hour)	Wind (mph)	Wind (m/s)
0:15	11.6	5.19
0:35	13.8	6.17
0:55	11.6	5.19
1:15	20.8	9.30
1:35	24.2	10.82
1:55	25.4	11.35
2:15	26.5	11.85
2:35	20.8	9.30
2:55	20.8	9.30
3:15	20.8	9.30
3:35	17.3	7.73
3:55	15	6.71
4:15	16.2	7.24
4:35	20.8	9.30
4:55	24.2	10.82
5:15	23	10.28
5:35	19.6	8.76
5:55	26.5	11.85
6:15	26.5	11.85
6:35	28.8	12.87
6:55	36.8	16.45
7:15	38	16.99
7:35	39.1	17.48
7:55	27.7	12.38
8:15	35.7	15.96
8:35	40.3	18.02
8:55	41.5	18.55
9:15	44.9	20.07
9:35	41.4	18.51
9:55	34.6	15.47
10:15	47.2	21.10
10:35	46	20.56
10:55	42.6	19.04

11:15	42.6	19.04
11:35	51.8	23.16
11:55	48.4	21.64
12:15	38	16.99
12:35	40.3	18.02
12:55	35.7	15.96
13:15	33.4	14.93
13:35	41.5	18.55
13:55	36.9	16.50
14:15	39.2	17.52
14:35	41.4	18.51
14:55	33.4	14.93
15:15	34.6	15.47
15:35	38	16.99
15:55	31.1	13.90
16:15	40.3	18.02
16:35	38	16.99
16:55	41.4	18.51
17:15	38	16.99
17:35	33.4	14.93
17:55	42.6	19.04
18:15	35.7	15.96
18:35	40.3	18.02
18:55	42.6	19.04
19:15	25.8	11.53
19:35	43.8	19.58
19:55	36.2	16.18
20:15	38	16.99
20:35	35.7	15.96
20:55	39.2	17.52
21:15	35.7	15.96
21:35	40.3	18.02
21:55	34.5	15.42
22:15	32.2	14.39
22:35	27.7	12.38
22:55	26.5	11.85
23:15	26.5	11.85
23:35	24.2	10.82
23:55	24.2	10.82

Appendix C: Characteristics of 1 MW NaS Battery Energy Storage System

Term	Specifications
Rated Discharge Power	AC 1 MW (DC 1.05 MW)
Rated Charge Power	AC 1 MW (DC 0.95 MW)
Nominal DC Voltage	640 V
Stored Electric Energy	AC 6 MWh (DC 6.32 MWh)
Charging hours	6-8 hours at rated load
Discharge hours	6-8 hours at rated load